
Faculty of Science

Faculty Publications

Measurement of flow harmonics correlations with mean transverse momentum in lead–lead and proton–lead collisions at $\sqrt{s_{NN}}=5.02$ TeV with the ATLAS detector

Aad, G., Abbott, B., Abbott, D. C., Abed Abud, A., Abeling, K., Abhayasinghe, D. K., ... Zwalinski, L.

2019.

© 2019 Aad, G., Abbott, B., Abbott, D. C., Abed Abud, A., Abeling, K., Abhayasinghe, D. K., ... Zwalinski, L. *This article is an open access article distributed under the terms and conditions of the Creative Commons Attribution (CC BY) license.* <http://creativecommons.org/licenses/by/4.0/>

This article was originally published at:
<https://doi.org/10.1140/epjc/s10052-019-7489-6>

Citation for this paper:

Aad, G., Abbott, B., Abbott, D. C., Abed Abud, A., Abeling, K., Abhayasinghe, D. K., ... Zwalinski, L. (2019). Measurement of flow harmonics correlations with mean transverse momentum in lead–lead and proton–lead collisions at $\sqrt{s_{NN}}=5.02$ TeV with the ATLAS detector. *The European Physical Journal C*, 79(12). <https://doi.org/10.1140/epjc/s10052-019-7489-6>



Measurement of flow harmonics correlations with mean transverse momentum in lead–lead and proton–lead collisions at $\sqrt{s_{NN}} = 5.02$ TeV with the ATLAS detector

ATLAS Collaboration*

CERN, 1211 Geneva 23, Switzerland

Received: 12 July 2019 / Accepted: 13 November 2019 / Published online: 3 December 2019
© CERN for the benefit of the ATLAS collaboration 2019

Abstract To assess the properties of the quark–gluon plasma formed in ultrarelativistic ion collisions, the ATLAS experiment at the LHC measures a correlation between the mean transverse momentum and the flow harmonics. The analysis uses data samples of lead–lead and proton–lead collisions obtained at the centre-of-mass energy per nucleon pair of 5.02 TeV, corresponding to total integrated luminosities of $22 \mu\text{b}^{-1}$ and 28nb^{-1} , respectively. The measurement is performed using a modified Pearson correlation coefficient with the charged-particle tracks on an event-by-event basis. The modified Pearson correlation coefficients for the 2nd-, 3rd-, and 4th-order flow harmonics are measured in the lead–lead collisions as a function of event centrality quantified as the number of charged particles or the number of nucleons participating in the collision. The measurements are performed for several intervals of the charged-particle transverse momentum. The correlation coefficients for all studied harmonics exhibit a strong centrality evolution, which only weakly depends on the charged-particle momentum range. In the proton–lead collisions, the modified Pearson correlation coefficient measured for the 2nd-order flow harmonics shows only weak centrality dependence. The lead-lead data is qualitatively described by the predictions based on the hydrodynamical model.

1 Introduction

The large azimuthal anisotropy observed for particles produced in heavy-ion collisions at RHIC [1–4] and the LHC [5–8] is one of the main signatures of the formation of strongly interacting matter called quark–gluon plasma (QGP). A standard picture of an ultrarelativistic heavy-ion collision is that the initial, asymmetric ‘almond’ shape of the colliding nuclei’s overlap region leads to the formation of pressure gradients in the QGP. These pressure gradients transform the

initial shape into an azimuthal anisotropy of the final-state particle distributions through a nearly ideal hydrodynamic evolution and subsequent QGP hadronisation process [9]. The azimuthal anisotropy is customarily decomposed into Fourier components with the amplitude of the n th term denoted by v_n and known as a flow harmonic [10]. Theoretical hydrodynamical models successfully describe observed flow phenomena at low particle transverse momenta [11]. The properties of QGP were recently studied with measurements of correlations between flow harmonics of different order [12–16] as well as with analyses of event shapes [16–20]. It is expected that in lead–lead (Pb+Pb) collisions the magnitudes of the azimuthal flow harmonics [6,7] should be correlated with the mean transverse momentum [p_T] of the particles on an event-by-event basis [21]. In this paper, that correlation is called the v_n –[p_T] correlation. In proton–lead (p +Pb) collisions, the measurements of multi-particle correlations [22] show evidence of collective phenomena. The spectra of identified particles in p +Pb collisions are consistent with a presence of the radial flow [23] while the nuclear modification factor at high p_T approaches unity [24]. Despite intensive studies, the mechanism responsible for the collective behaviour in small collision systems still remains unknown [9]. In p +Pb collisions the v_n –[p_T] correlation could provide constraints on the initial geometry of the particle source, thereby reducing the overall modelling uncertainty. According to the hydrodynamical model predictions [25], in p +Pb collisions the v_n –[p_T] correlation is sensitive to the distribution of energy deposition in the first stage of the collision. For a larger source a positive v_2 –[p_T] correlation is expected while for a compact source the negative correlation is obtained. Simultaneous measurements of v_n –[p_T] correlations in small and large systems may help disentangle the role of initial conditions and subsequent dynamical QGP evolution in final-state particle distributions.

* e-mail: atlas.publications@cern.ch

To measure the strength of the v_n – $[p_T]$ correlation, the Pearson correlation coefficient (PCC) R [25] is used where

$$R = \frac{\text{cov}(v_n\{2\}^2, [p_T])}{\sqrt{\text{Var}(v_n\{2\}^2)}\sqrt{\text{Var}([p_T])}}. \quad (1)$$

The term $v_n\{2\}^2$ is the square of the n th-order flow harmonic obtained using the two-particle correlation method [26], $\text{cov}(v_n\{2\}^2, [p_T])$ is the covariance between $v_n\{2\}^2$ and $[p_T]$, and $\text{Var}(v_n\{2\}^2)$ and $\text{Var}([p_T])$ are the variances of the $v_n\{2\}^2$ and $[p_T]$ distributions, respectively. Experimentally, however, the finite event-by-event charged-particle track multiplicity results in an additional broadening of the $v_n\{2\}^2$ and $[p_T]$ distributions due to statistical fluctuations. Thus, the values of the respective variances are increased, especially for $[p_T]$. The magnitude of this broadening depends on the choice of kinematic region and on detector performance, making direct comparisons between experimental results and with theoretical calculations difficult. To overcome this problem, a modified correlation coefficient ρ , less sensitive to the charged-particle multiplicity than R , was suggested in Ref. [25]. To reduce the auto-correlation effects and those due to the finite charged-particle multiplicity in an event, the variances of the $v_n\{2\}^2$ and $[p_T]$ distributions are replaced by corresponding *dynamical* variables, which are more sensitive to intrinsic initial-state fluctuations. The variance of $v_n\{2\}^2$ is replaced by its dynamical counterpart [27]

$$\begin{aligned} \text{Var}(v_n\{2\}^2)_{\text{dyn}} &= v_n\{2\}^4 - v_n\{4\}^4 \\ &= \langle \text{corr}_n\{4\} \rangle - \langle \text{corr}_n\{2\} \rangle^2, \end{aligned} \quad (2)$$

where $\text{corr}_n\{2\}$ and $\text{corr}_n\{4\}$ are the two- and four-particle correlations [26] and where angular brackets denote that they are averaged over events. These correlations are described in detail in Sect. 4.

The variance of $[p_T]$ is replaced by the dynamical p_T fluctuation magnitude [28,29] c_k defined as

$$c_k = \left\langle \frac{1}{N_{\text{pair}}} \sum_i \sum_{j \neq i} (p_{T,i} - \langle [p_T] \rangle)(p_{T,j} - \langle [p_T] \rangle) \right\rangle \quad (3)$$

where $\langle [p_T] \rangle$ is the average $[p_T]$ over the all analysed events. The modified PCC ρ is thus defined as

$$\rho = \frac{\text{cov}(v_n\{2\}^2, [p_T])}{\sqrt{\text{Var}(v_n\{2\}^2)_{\text{dyn}}}\sqrt{c_k}}. \quad (4)$$

It was demonstrated in Ref. [25] that the ρ coefficient calculated using realistic and finite multiplicities provides a reliable estimate of the true value of R found in the limit of infinite multiplicity, whereas the coefficient R , calculated using Eq. (1) for finite multiplicity underestimates the true value.

The ALICE experiment measured [20] that the charged-particle p_T spectrum is correlated with the magnitude of the elliptic flow. It is measured to be harder in collisions with the higher second flow harmonics and softer in collisions where the elliptic flow is smaller. The magnitude of spectra modification is observed to increase with p_T , starting to be significant at around 1 GeV and reaching a few percent at around 5 GeV. The modification is found to be most significant in the mid-central collisions, decreasing in the most central ones. The ALICE results suggest that the value of the correlation coefficient should be significant in mid-central and central collisions and that its magnitude and centrality dependence should be sensitive to the scale of intrinsic fluctuations of v_2 and p_T . Including particles of higher p_T in the measurement is expected to result in increased values of the $\rho(v_2\{2\}^2, [p_T])$. The $[p_T]$ correlations with v_2 in peripheral Pb+Pb collisions, v_3 and v_4 in wide centrality range as well as for the v_2 in high multiplicity p +Pb are unexplored by measurements.

This paper reports on the first measurement of the ρ coefficient with the ATLAS detector in Pb+Pb and p +Pb collisions at a centre-of-mass energy per nucleon pair of 5.02 TeV. The Pb+Pb data sample with a total integrated luminosity of $22 \mu\text{b}^{-1}$ was collected in 2015, and the p +Pb sample with 28nb^{-1} in 2013.

This paper is organised as follows. Section 2 gives a brief description of the ATLAS detector. Details of the event selection and charged-particle reconstruction are provided in Sect. 3. Section 4 describes the analysis procedure for calculating the ρ coefficient. Systematic uncertainties are described in Sect. 5 and Appendix A. Results are presented in Sect. 6, followed by a summary in Sect. 7.

2 Experimental setup

The ATLAS experiment [30] at the LHC is a multipurpose particle detector with a forward–backward symmetric cylindrical geometry and a near 4π solid angle coverage. The inner detector (ID) covers the pseudorapidity¹ range $|\eta| < 2.5$ and is surrounded by a thin superconducting solenoid providing a 2 T axial magnetic field. The ID consists of silicon pixel, silicon microstrip (SCT), and straw tube tracking detectors. After the 2013 p +Pb run, an additional pixel silicon layer, the insertable B-layer [31,31,32], was installed prior to the 5.02 TeV Pb+Pb data-taking to attain more precise track-

¹ ATLAS uses a right-handed coordinate system with its origin at the nominal interaction point (IP) in the centre of the detector and the z -axis along the beam pipe. The x -axis points from the IP to the centre of the LHC ring, and the y -axis points upward. Cylindrical coordinates (r , ϕ) are used in the transverse plane, ϕ being the azimuthal angle around the z -axis. The pseudorapidity is defined in terms of the polar angle θ as $\eta = -\ln \tan(\theta/2)$.

ing. Lead/liquid-argon (LAr) sampling calorimeters provide electromagnetic (EM) energy measurements with high granularity. A steel/scintillator tile hadronic calorimeter covers the central pseudorapidity range ($|\eta| < 1.7$). The endcap and forward regions are instrumented with LAr calorimeters for EM and hadronic energy measurements up to $|\eta| = 4.9$. The forward calorimeter (FCal) covers $3.2 < |\eta| < 4.9$ and is used for centrality estimation [10]. The minimum-bias trigger scintillators (MBTS) are located on each side of the detector at $z = \pm 3.6$ m and detect charged particles with $2.07 < |\eta| < 3.86$. The zero-degree calorimeter (ZDC), located in the LHC tunnel and covering $|\eta| > 8.3$, is used for triggering on collision events and pile-up event rejection. It is calibrated to resolve an individual neutron originating from the collision spectators.

A two-level trigger system selects events [33,34]. The level-1 trigger is implemented in hardware and preselects up to 10^5 events per second for further decisions by the high-level trigger (HLT). The software-based HLT tuned for Pb+Pb collision data selects up to 1000 events per second for recording. This analysis primarily uses charged-particle tracks in the ID, but information from the central calorimeters and the ZDC is also used for triggering, event selection, and analysis.

3 Event and track selection

The Pb+Pb data in this analysis were selected using two mutually exclusive minimum-bias triggers. Events with semi-central and central collisions were selected if the scalar sum of transverse energy in the entire ATLAS calorimeter system exceeded 50 GeV. Peripheral events, i.e. those with large impact parameter of the colliding Pb nuclei, fail the 50 GeV selection and were instead selected by requiring a deposition in the ZDC corresponding to at least one neutron and by requiring at least one track reconstructed in the HLT. Data in this analysis are required to come from periods when the entire detector was functioning normally. The events are required to have a reconstructed vertex within 100 mm of the nominal interaction point. The contribution from events containing more than one inelastic interaction (pile-up) is studied by exploiting correlations between the transverse energy measured in the FCal (ΣE_T^{FCal}) with the estimated number of neutrons in the ZDC, and with the number of tracks associated with a primary vertex [27,35]. The distribution of ΣE_T^{FCal} and the distribution of the number of neutrons in events with more than one collision are broader than the corresponding distributions in events with only one collision. Pile-up events are suppressed by rejecting events with abnormally large values of either ΣE_T^{FCal} or the number of neutrons in the ZDC compared with the charged-particle

multiplicity in the event. Approximately 0.2% of the events are rejected by these requirements.

The p +Pb data in this analysis were selected using minimum-bias triggers and high-multiplicity triggers (HMT). The minimum-bias trigger required signals in both sides of the MBTS system with a timing difference of less than 10 ns to eliminate non-collision backgrounds. The HMT required the total transverse energy in the calorimeter at level-one and the number of ID track candidates reconstructed in the HLT to be above predefined thresholds. Six combinations of thresholds were used to optimise data-taking during periods with different luminosities. Samples of events collected by these triggers are combined by applying event weights to reproduce the charged-particle multiplicity distribution of the minimum-bias trigger. Further details of the data selection are given in Refs. [22,36]. The average pile-up probability in the p +Pb dataset is approximately 3% but can be significantly larger in high-multiplicity events. Events with more than one reconstructed vertex are removed from the sample. Similarly to the Pb+Pb dataset, to remove events where the two interaction vertices are too close to resolve as independent ones, the ZDC signal on the Pb fragmentation side is used. The distribution of the number of neutrons, which is broader in events with pile-up than that for the events without pile-up is exploited for that purpose [36]. The fraction of rejected events varies with the event activity and reaches a maximum of 10% for events with the highest multiplicities.

The analysis for both collision systems is performed in narrow bins of event activity defined by the charged-particle multiplicity N_{ch} (described in Sect. 4), which estimates the collision centrality. In addition, the Pb+Pb results are presented as a function of collision centrality expressed by the average number of nucleons participating in the collision, N_{part} , to allow comparison with theoretical predictions [37]. The centrality is estimated from the ΣE_T^{FCal} distribution [6,10] using the Glauber model [38]. The number of events passing the selection requirements is 1.3×10^8 for Pb+Pb within the 0–80% centrality interval. For the p +Pb system, about 0.64×10^8 events enter the analysis.

The charged-particle tracks reconstructed in the ID are required to satisfy selection criteria in order to suppress the contribution of incorrectly reconstructed tracks and secondary products of particle decays. The selection criteria include the requirement that the number of hits in the pixel and SCT detectors should be greater than two and eight, respectively, for the Pb+Pb data and greater than one and six for the p +Pb data. The track impact parameters relative to the collision vertex in the transverse direction, $|d_0|$, and longitudinal direction, $|z_0 \sin \theta|$, are required to be less than 1 mm for tracks in the Pb+Pb data sample and less than 1.5 mm in the p +Pb sample. In addition, in p +Pb collisions, the track impact parameter significances must satisfy $|d_0/\sigma_{d_0}| < 3$ and $|z_0 \sin \theta/\sigma_z| < 3$, where σ_{d_0} and σ_z are the uncertainties

in d_0 and $z_0 \sin \theta$ determined from the covariance matrix of the track fit. The different selection criteria for Pb+Pb and p +Pb optimise the performance of the track reconstruction in differing running conditions.

Corrections needed due to track reconstruction effects are evaluated using 4×10^6 Pb+Pb and 10^7 p +Pb minimum-bias Monte Carlo (MC) events generated by the HIJING v1.38b [39] event generator. After the generation, an azimuthal flow is implemented using the afterburner technique [40], and the p_T spectrum is reweighted to match the data. Generated events were simulated in the detector by the GEANT 4-based [41] ATLAS detector simulation programs [42] and reconstructed using the same procedures and detector conditions as the data. Track reconstruction corrections are applied to each selected track using weights to account for the tracking efficiency ϵ and the fake-track fraction f . The efficiency is defined as the fraction of primary MC charged particles that are matched to reconstructed tracks, and f is the fraction of tracks that are not matched to primary MC particles or are produced from random combinations of hits in the ID. A similar analysis procedure is described in Refs. [10, 16]. The fake-track fraction and tracking efficiency are determined as functions of the track p_T and η and of the track multiplicity in the event. Tracks included in the analysis are weighted with the factor $(1 - f)/\epsilon$. An additional multiplicative weight evaluated from data is applied to the data to correct for detector non-uniformity in the azimuthal angle. These weights are obtained by requiring the tracks to be distributed uniformly in azimuth in all pseudorapidity slices of width 0.1.

In the Pb+Pb data, the contribution of fake tracks is largest in central collisions at the lowest analysed track p_T of 0.5 GeV and at the largest $|\eta|$, reaching up to 20%. The fake-track rate is below 1% for tracks with p_T above 2 GeV and $|\eta| < 1.5$. The tracking efficiency depends weakly on centrality, and in the most central events it is about 3% less than in more peripheral events. The efficiency increases with the track p_T from about 50% at the lowest analysed p_T to 70% above 2 GeV. It is highest at mid-rapidity and drops by about 15% for $|\eta| > 1$. For p +Pb collisions, with p_T increasing from 0.3 to 1 GeV the efficiency increases from about 75% (60%) to 83% (70%) at $\eta \approx 0$ ($|\eta| > 2$). The p +Pb tracking efficiency is independent of the event's multiplicity for $N_{ch} \geq 10$, i.e. in the multiplicity range used in the analysis. The fake rate in p +Pb collisions is very low, below 1% (3%) at $\eta \approx 0$ ($|\eta| > 2$).

4 Correlation coefficient ρ

In each event, charged-particle tracks are grouped into three regions of subevents based on their pseudorapidity: region A with $-2.5 < \eta < -0.75$, central region B with $|\eta| < 0.5$ and region C with $0.75 < \eta < 2.5$. The v_n^2 for the

$n = 2-4$ harmonics are calculated by correlating charged-particle tracks from subevents A and C, which are separated in pseudorapidity to suppress non-flow contributions. Tracks in central region B are used to obtain the mean value of the charged-particle transverse momentum in the event, $[p_T]$, defined as

$$[p_T] = \frac{1}{\sum_b w_b} \sum_b w_b p_{Tb}$$

where the summation is over tracks in region B, labelled by index b . The variable c_k (Eq. (3)) is also calculated using tracks from region B. Here, and in following formulas, the weights w include the fake-track fraction, efficiency, and azimuthal non-uniformity corrections, as discussed in Sect. 3.

The covariance term from the numerator of Eq. (4) is defined as

$$\begin{aligned} & \text{cov}(v_n\{2\}^2, [p_T]) \\ &= \text{Re} \left(\left\langle \frac{1}{\sum_{a,c} w_a w_c} \sum_{a,c} w_a w_c e^{in\phi_a - in\phi_c} ([p_T] - \langle [p_T] \rangle) \right\rangle \right), \end{aligned} \tag{5}$$

where ϕ is the azimuthal angle and indices a and c span the tracks in regions A and C, respectively.

The two- and four-particle correlations used to define the dynamical variance in Eq. (2), which enters the denominator of Eq. (4), are calculated as in Ref. [26]

$$\begin{aligned} \langle \text{corr}_n\{2\} \rangle &= \text{Re} \left(\left\langle \frac{1}{\sum_{a,c} w_a w_c} \sum_{a,c} w_a w_c e^{in\phi_a - in\phi_c} \right\rangle \right) \\ &= \text{Re} (\langle q_{n,a} q_{n,c}^* \rangle) \end{aligned} \tag{6}$$

where the q_a and q_c are the complex flow vectors of subevent A and subevent C, respectively, and the asterisk denotes the complex conjugate. The flow vectors are

$$q_{n,a} = \frac{1}{\sum_a w_a} \sum_a w_a e^{in\phi_a} \quad \text{and} \quad q_{n,c} = \frac{1}{\sum_c w_c} \sum_c w_c e^{in\phi_c}.$$

The four-particle correlation is obtained from the expression

$$\langle \text{corr}_n\{4\} \rangle = \text{Re} \left(\left\langle \frac{(Q_{n,a}^2 - Q_{2n,a})(Q_{n,c}^2 - Q_{2n,c})^*}{S_a S_c} \right\rangle \right), \tag{7}$$

where for subevent A

$$\begin{aligned} Q_{n,a} &= \sum_a w_a e^{in\phi_a}, & Q_{2n,a} &= \sum_a w_a^2 e^{i2n\phi_a}, \\ S_a &= \left(\sum_a w_a \right)^2 - \sum_a w_a^2, \end{aligned}$$

and similarly for subevent C. Equation (7) represents the sum $\sum e^{in(\phi_1^a + \phi_2^a - \phi_3^c - \phi_4^c)}$ over all particles from subevents A and C normalised by the number of quadruplets without auto-correlations in each subevent.

The second factor in the denominator of Eq. (4), the mean p_T fluctuation in the event class c_k , is defined by Eq. (3) and in this analysis it is calculated as

$$c_k = \left\langle \frac{1}{(\sum_b w_b)^2 - \sum_b w_b^2} \sum_b \sum_{b' \neq b} w_b w_{b'} (p_{T,b} - \langle [p_T] \rangle) w_{b'} (p_{T,b'} - \langle [p_T] \rangle) \right\rangle.$$

The summation indices b and b' run over all charged particles in region B.

The correlation coefficient expressed by Eq. (4) is evaluated for the range $0.5 < p_T < 2$ GeV in Pb+Pb collisions and $0.3 < p_T < 2$ GeV in p+Pb collisions. These intervals, called ‘main’, contain a large number of soft particles and constitute the main result of the analysis which can be compared with hydrodynamical models. For each system, two additional p_T ranges are considered: $0.5 < p_T < 5$ GeV and $1 < p_T < 2$ GeV in the analysis of Pb+Pb collisions, and $0.3 < p_T < 5$ GeV and $0.5 < p_T < 2$ GeV in p+Pb collisions. These ranges facilitate the study of the sensitivity of $\rho(v_n\{2\}^2, [p_T])$ to the high p_T part of the particle spectrum and to the lower charged-particle multiplicity from the higher minimum p_T value. The charged-particle p_T range $0.5 < p_T < 2$ GeV is common to both systems and can be used to compare the $\rho(v_2\{2\}^2, [p_T])$ results from Pb+Pb and p+Pb collisions.

The quantities of interest, i.e. $\text{cov}(v_n\{2\}^2, [p_T])$, $\text{Var}(v_n\{2\}^2)_{\text{dyn}}$, c_k , and $\rho(v_n\{2\}^2, [p_T])$, are determined in bins of reconstructed track multiplicity M_{AC} measured in the combination of regions A and C. This is done to avoid a negative correlation between the multiplicity in subevents A+C and B that occurs if the analysis is binned in multiplicity in the entire ID. Narrow M_{AC} bins are also chosen due to the sensitivity to multiplicity fluctuations of the multi-particle correlations that are used to obtain the $\text{Var}(v_n\{2\}^2)_{\text{dyn}}$ [27]. The events are grouped in fine bins with a width of ten in M_{AC} for $0.5 < p_T < 5$ GeV in the Pb+Pb analysis and $0.3 < p_T < 5$ GeV in the p+Pb analysis. It was cross-checked that the variables of interest obtained with a finer binning in M_{AC} are consistent with the measurement with the nominal binning.

To enable comparisons with the theoretical predictions and with future experimental results, measurements obtained in M_{AC} are presented as a function of the ATLAS ID multiplicity N_{ch} of $0.5 < p_T < 5$ GeV and $|\eta| < 2.5$. They are projected from the M_{AC} values taking into account tracking efficiency and fake-track production as described in the pre-

vious section. A similar analysis procedure is described in Ref. [22]. For the N_{part} dependencies in the Pb+Pb system, the results measured in M_{AC} multiplicity intervals are averaged, with weights equal to the probabilities to find any given M_{AC} value in the centrality intervals.

The formulation of the modified PCC $\rho(v_n\{2\}^2, [p_T])$ requires that there should be at least two tracks in each region (A, B, and C). Further, $\text{Var}(v_n\{2\}^2)_{\text{dyn}}$ calculated according to Eq. (6) can be negative at low multiplicities due to statistical fluctuations, which renders Eq. (4) invalid because of the $\sqrt{\text{Var}(v_n\{2\}^2)_{\text{dyn}}}$ term. For each M_{AC} bin, p_T interval, and harmonic, a criterion is applied that $\text{Var}(v_n\{2\}^2)_{\text{dyn}}$ needs to be positive at a level of at least one standard deviation of its statistical uncertainty. Results presented as a function of N_{ch} are produced only for those M_{AC} intervals. For the N_{part} dependencies in the Pb+Pb system, it is additionally required for each centrality interval that the fraction of rejected events due to this criterion does not exceed 1%.

5 Systematic uncertainties

The systematic uncertainty is estimated by varying individual aspects of the analysis. The systematic uncertainties for the main p_T interval are discussed for each collision system. Systematic uncertainties for the other p_T intervals behave consistently with the ones for the main p_T interval. Since the modified PCC $\rho(v_n\{2\}^2, [p_T])$ is a ratio of quantities which are calculated using tracks, many variations largely cancel out and the resulting systematic uncertainties are small. To suppress the statistical fluctuations and to get more robust estimation of systematic uncertainties, they are averaged over several, wide ranges of the charged-particle multiplicity. For each uncertainty source and for each measurement point, the maximum variation from the baseline measurement is used. The total resulting uncertainty is the sum of the individual contributions combined in quadrature. The following sources of systematic uncertainties are considered.

Track selection The tracking performance has a relatively small impact on $v_n\{2\}$, but it directly affects the $[p_T]$ and c_k via the admixture of the fake tracks, especially at low p_T . To assess the impact on $\rho(v_n\{2\}^2, [p_T])$, the measurement is repeated with tracks selected with looser and tighter track quality criteria, thus increasing and decreasing the fake-track rate, respectively. The weights used in the evaluation of measured quantities take the modified selection into account. The loose track selection in the Pb+Pb analysis relaxes requirements on the number of pixel and SCT hits to at least one and six, respectively. Additionally, the requirements on the transverse and longitudinal impact parameters of the track are relaxed to 1.5 mm. The tighter selection in the Pb+Pb analysis tightens the requirement on the transverse and lon-

itudinal impact parameters of the track to 0.5 mm. For the p +Pb analysis, the loose selection relaxes the requirements on the transverse and longitudinal impact parameters of the track to 2 mm and on the impact parameter significances to less than 4. In the tight selection, the impact parameter values and their significances must be less than 1 mm and 2, respectively. For each of the two track selections the absolute difference is calculated with respect to the baseline measurement: $|\rho(v_n\{2\}^2, [p_T])^{\text{base}} - \rho(v_n\{2\}^2, [p_T])^{\text{loose}}|$ or $|\rho(v_n\{2\}^2, [p_T])^{\text{base}} - \rho(v_n\{2\}^2, [p_T])^{\text{tight}}|$. The largest difference is taken as a systematic uncertainty.

Detector material Since the tracks that are used in the calculation of $\rho(v_n\{2\}^2, [p_T])$ are weighted by the inverse of the tracking efficiency, a bias in its estimation due to inaccurate modelling of the material in the detector may change the balance between low- and high- p_T tracks in the sums. Based on simulations, the estimated uncertainty in the detector description is obtained [43,44]. The resulting p_T - and η -dependent uncertainties in the track efficiency of up to 4% are used to determine the systematic uncertainty.

Tracking azimuthal uniformity In this analysis, the weighting factors w correct for any non-uniformity in the azimuthal angle distribution of reconstructed tracks. The weights are obtained from the data by requiring azimuthal uniformity over the two-dimensional distribution of reconstructed tracks in the η - ϕ plane. The effect of that correction on the result is conservatively estimated by comparing the baseline measurement and the measurement obtained without applying this weight. The uncertainty is small, and it envelopes potential effects of imperfections in the weighting factors determination, including their dependence on the transverse momentum, collision centrality, run-by-run differences, on dead module maps or the vertex position.

Residual pile-up events The selection criteria discussed in Sect. 3 suppress the fraction of pile-up events accepted for analysis to almost zero in central Pb+Pb collisions. To estimate the systematic uncertainty related to pile-up, the measurement is conservatively repeated without this event rejection, resulting in at most a 1% difference in the most central Pb+Pb events for the $\rho(v_2\{2\}^2, [p_T])$ coefficient. The p +Pb data were taken with higher pile-up than the Pb+Pb data. To estimate the impact of contamination by residual pile-up events, p +Pb results were obtained with only the vertex criteria applied. The variation covers the estimated residual pile-up fraction in events of the highest track multiplicity [36].

Centrality selection The minimum-bias trigger is fully efficient for the 0–85% centrality interval. However, the total fraction of inelastic Pb+Pb events selected is known only to 1% accuracy due to trigger inefficiency and possible sample contamination in more peripheral interactions. The centrality is estimated using the ΣE_T^{FCal} distribution [6,10] and the

Glauber model [38] to obtain the mapping from the observed ΣE_T^{FCal} to the number of nucleons participating in the collision, N_{part} . The modified PCC uncertainty is evaluated by repeating the analysis with the altered centrality selections on the ΣE_T^{FCal} distribution, which results in $\pm 1\%$ uncertainty in the total fraction of inelastic Pb+Pb events. The centrality selection contributes mainly to uncertainties for peripheral collisions.

Figure 1 shows the magnitude of the systematic uncertainties $\delta\rho(v_n\{2\}^2, [p_T])$ for $n = 2 - 4$ in Pb+Pb collisions as a function of N_{ch} . In Pb+Pb collisions, the systematic uncertainty of the measured correlation coefficients across different order harmonics and centralities is not dominated by a single source. One of the largest uncertainties comes from restoring the azimuthal uniformity, and dominates for the second order harmonic in the most central collisions and for the third and fourth order harmonics almost over the full centrality range. A sizeable contribution to the uncertainty for all three harmonics is due to the track selection. The impact of the detector material is rather small except for a significant contribution for the fourth order harmonic in the most central events. The residual pile-up in Pb+Pb collisions gives a negligible contribution. Figure 1d shows systematic uncertainties for $\rho(v_2\{2\}^2, [p_T])$ coefficients in p +Pb collisions for the main interval of $0.3 < p_T < 2$ GeV as a function of event activity. In p +Pb interactions the largest uncertainty in the most active collisions ($N_{\text{ch}} > 150$) originates from pile-up. The track selection is a source of sizeable uncertainty for this collision system, while the azimuthal uniformity correction procedure and the detector material have a small impact.

Details on the contributions to systematic uncertainties from different sources of c_k , $\text{Var}(v_n\{2\}^2)_{\text{dyn}}$ and $\text{cov}(v_n\{2\}^2, [p_T])$ are included in the Appendix.

6 Results

6.1 The constituents of the modified PCC

The constituents of the modified PCC, c_k , $\text{Var}(v_n\{2\}^2)_{\text{dyn}}$ and $\text{cov}(v_n\{2\}^2, [p_T])$ and are combined, using Eq. (4), to obtain ρ . Figure 2 shows the dynamical p_T fluctuation coefficient c_k as a function of charged-particle multiplicity in Pb+Pb and p +Pb collision systems for tracks in three different p_T intervals. A strong decrease of c_k with increasing N_{ch} is observed in all measured results. A similar decrease was seen for c_k in Au+Au and Pb+Pb data at lower centre-of-mass energies [28,29], evaluated for lower p_T range, $0.15 < p_T < 2$ GeV, not accessible with the ATLAS detector. For the same N_{ch} , the c_k values differ by an order of magnitude for different p_T ranges of tracks used in the analysis. For the intervals with the same lower p_T limit, the c_k

Fig. 1 The systematic uncertainty of $\rho(v_n\{2\}^2, [p_T])$ as a function of N_{ch} measured with tracks from main p_T intervals for each collision system for the **a** second, **b** third, and **c** fourth harmonics in Pb+Pb collisions, and for **d** $\rho(v_2\{2\}^2, [p_T])$ in p+Pb collisions. The total uncertainty is also shown

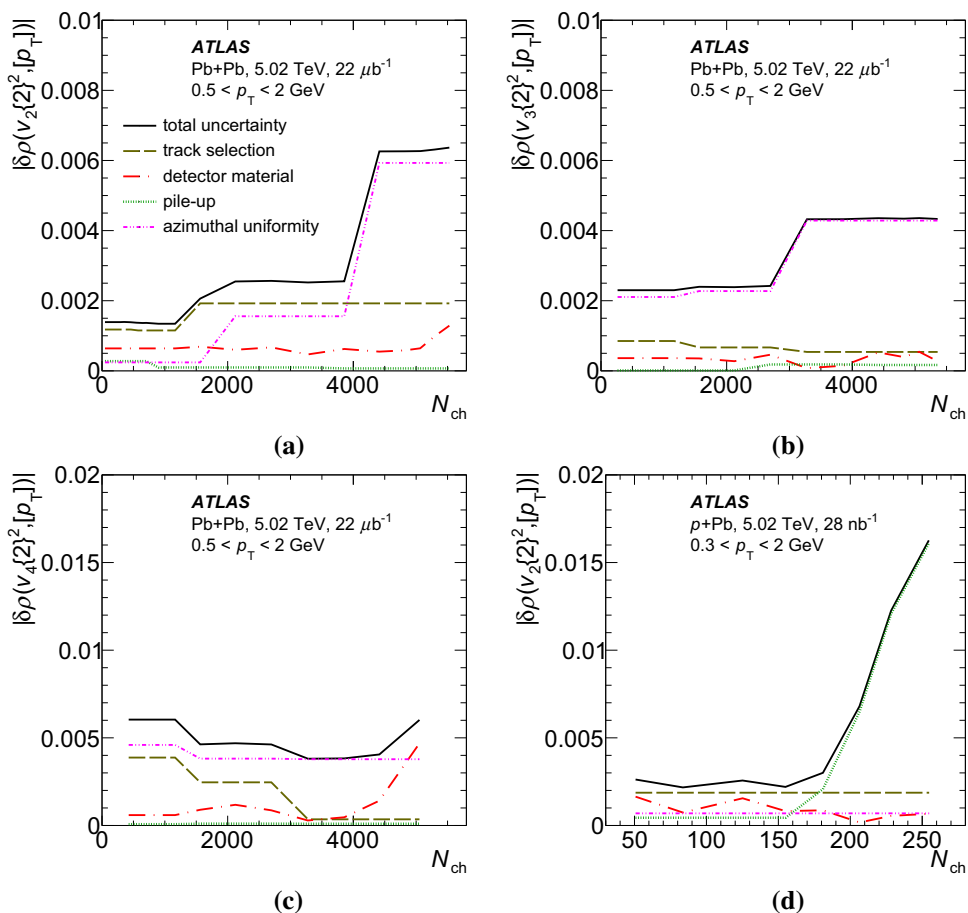
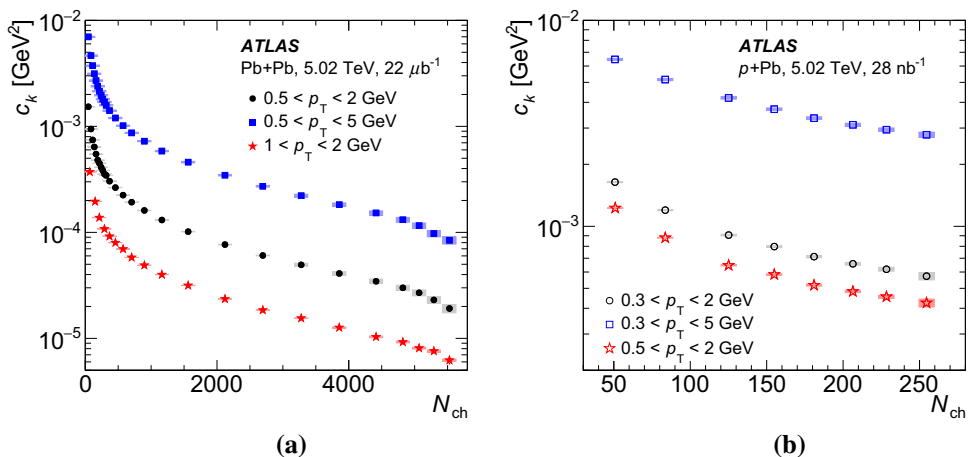


Fig. 2 The variable c_k for three p_T ranges as a function of the charged-particle multiplicity N_{ch} of **a** Pb+Pb and **b** p+Pb collisions. The statistical and systematic uncertainties are shown as vertical error bars (smaller than symbols) and boxes, respectively

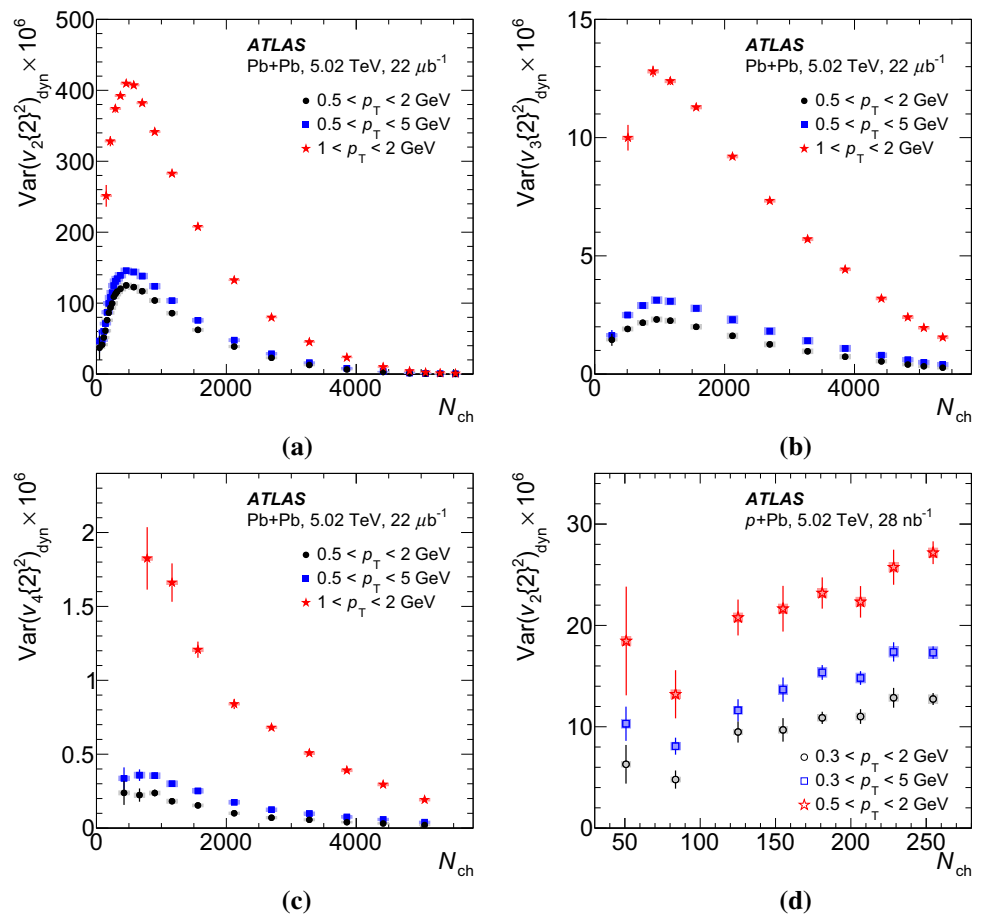


values are higher for the interval with the larger upper p_T limit.

Figure 3 shows $\text{Var}(v_n\{2\}^2)_{\text{dyn}}$ for $n = 2 - 4$ as function of N_{ch} for Pb+Pb collisions. For low multiplicities, $\text{Var}(v_n\{2\}^2)_{\text{dyn}}$ increases with increasing N_{ch} , reaching a maximum at N_{ch} of approximately 500 (1000) for $n = 2$ ($n = 3$), respectively. At higher N_{ch} values the variances decrease with multiplicity. The dynamical variance for $n = 4$, measured for $N_{ch} \gtrsim 500$, decreases with increas-

ing N_{ch} . The ordering $\text{Var}(v_2\{2\}^2)_{\text{dyn}} > \text{Var}(v_3\{2\}^2)_{\text{dyn}} > \text{Var}(v_4\{2\}^2)_{\text{dyn}}$ and the multiplicity dependence of $\text{Var}(v_n\{2\}^2)_{\text{dyn}}$ are similar to the ordering and centrality dependence of $v_n\{2\}$ measured by ATLAS [10]. Also shown in Fig. 3 is $\text{Var}(v_2\{2\}^2)_{\text{dyn}}$ for p+Pb collisions as a function of N_{ch} . The dependence is monotonic, similarly to $v_2\{2\}$ [45]. In both collision systems and for all harmonics, the same ordering of $\text{Var}(v_n\{2\}^2)_{\text{dyn}}$ depending on the p_T interval is

Fig. 3 The variance $\text{Var}(v_n\{2\}^2)_{\text{dyn}}$ for $n = 2 - 4$ for **a-c** Pb+Pb collisions and $\text{Var}(v_2\{2\}^2)_{\text{dyn}}$ for **d** p +Pb collisions for the three p_T intervals as a function of charged-particle multiplicity N_{ch} . The statistical and systematic uncertainties are shown as vertical error bars and boxes, respectively



observed. The largest variances are observed for the p_T intervals with an increased lower limit. This is expected as the $v_n\{2\}$ value increases strongly with p_T below 3 GeV [10]. Additionally, the interval in which the upper limit on p_T is set to 5 GeV integrates the region with the highest values of $v_n\{2\}$ (which occur around 3 GeV) and thus the values of the variance are expected to be larger than that for the main p_T range.

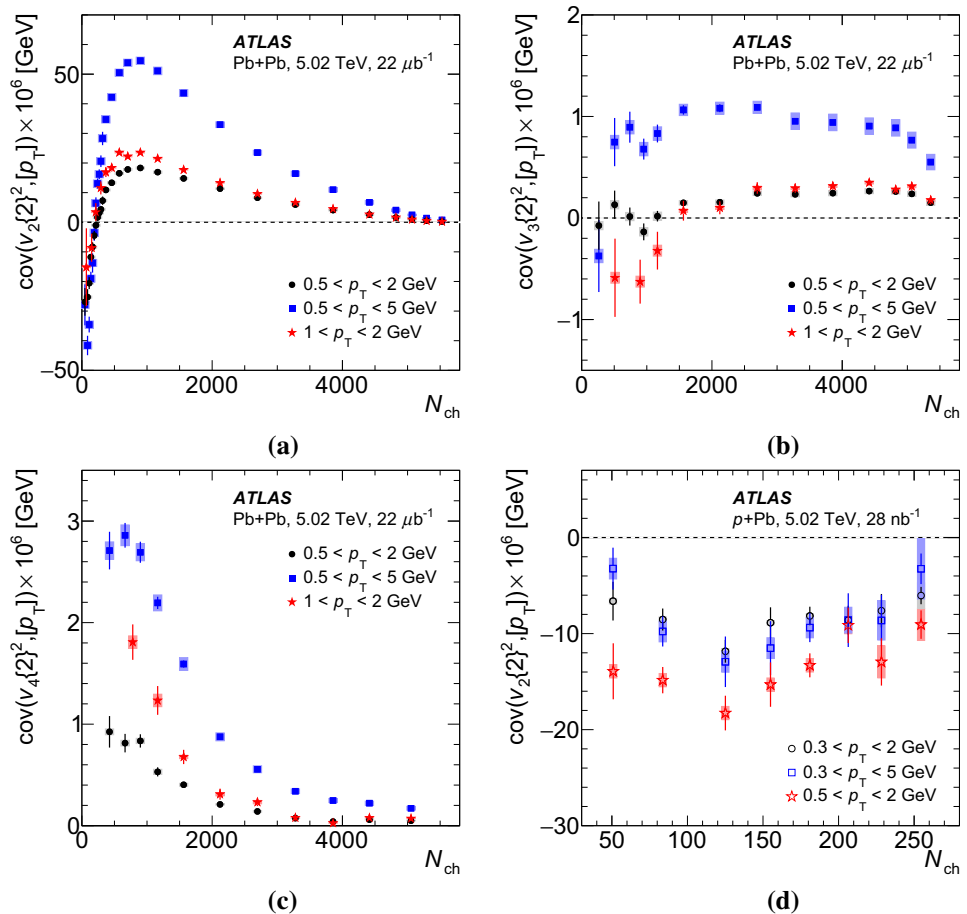
In Fig. 4, the covariances $\text{cov}(v_n\{2\}^2, [p_T])$ are shown for the 2nd-, 3rd-, and 4th-order harmonics in Pb+Pb collisions and for the second-order harmonics in p +Pb collisions. They are presented as a function of N_{ch} for three p_T intervals. Significant positive correlations between $v_n\{2\}$ and $[p_T]$ are observed in the Pb+Pb events. The measured covariances depend on the charged-particle multiplicity and the p_T range of the charged particles. In Pb+Pb collisions, a strong dependence on the multiplicity is observed for $n = 2$ and 4. The $\text{cov}(v_3\{2\}^2, [p_T])$ depends only weakly on N_{ch} . A negative $\text{cov}(v_2\{2\}^2, [p_T])$ is measured at multiplicities $N_{\text{ch}} < 200$ and a negative $\text{cov}(v_3\{2\}^2, [p_T])$ for $1 < p_T < 2$ GeV below $N_{\text{ch}} < 1800$. The covariances $\text{cov}(v_2\{2\}^2, [p_T])$ in p +Pb events are negative in the entire measured N_{ch} range and show weak N_{ch} dependence. Unlike in Pb+Pb events, the

$\text{cov}(v_2\{2\}^2, [p_T])$ in p +Pb events have similar magnitudes for different p_T intervals.

6.2 The modified PCC

The modified PCC $\rho(v_n\{2\}^2, [p_T])$ for $n = 2 - 4$ in Pb+Pb collisions and for $n = 2$ in p +Pb collisions is shown in Fig. 5. In Pb+Pb collisions, the behaviour of $\rho(v_2\{2\}^2, [p_T])$ is similar for all p_T intervals. It starts at negative values for $N_{\text{ch}} < 200$ and rapidly increases with multiplicity up to ~ 1500 particles where the increase slows down and reaches the maximum at $N_{\text{ch}} \approx 4500$ of 0.24–0.3, depending on the p_T interval. At even higher N_{ch} , the $\rho(v_2\{2\}^2, [p_T])$ value decreases rapidly. The significant correlation observed for mid-central events suggests a connection between anisotropic and radial [46] flows which might be attributed to stronger hydrodynamic response (larger pressure gradients) to the large initial-state eccentricities [47]. The modified PCC multiplicity dependence could reflect a balance between stronger radial flow observed in central collision and the larger initial eccentricity seen in peripheral interactions. The decrease observed in central collisions, for $N_{\text{ch}} \gtrsim 5000$, might be related to the increased role of

Fig. 4 The covariance $\text{cov}(v_n\{2\}^2, [p_T])$ for $n = 2 - 4$ in **a-c** Pb+Pb collisions and $\text{cov}(v_2\{2\}^2, [p_T])$ in **d** p +Pb collisions for three p_T ranges as a function of the charged-particle multiplicity N_{ch} . The statistical and systematic uncertainties are shown as vertical error bars and boxes, respectively

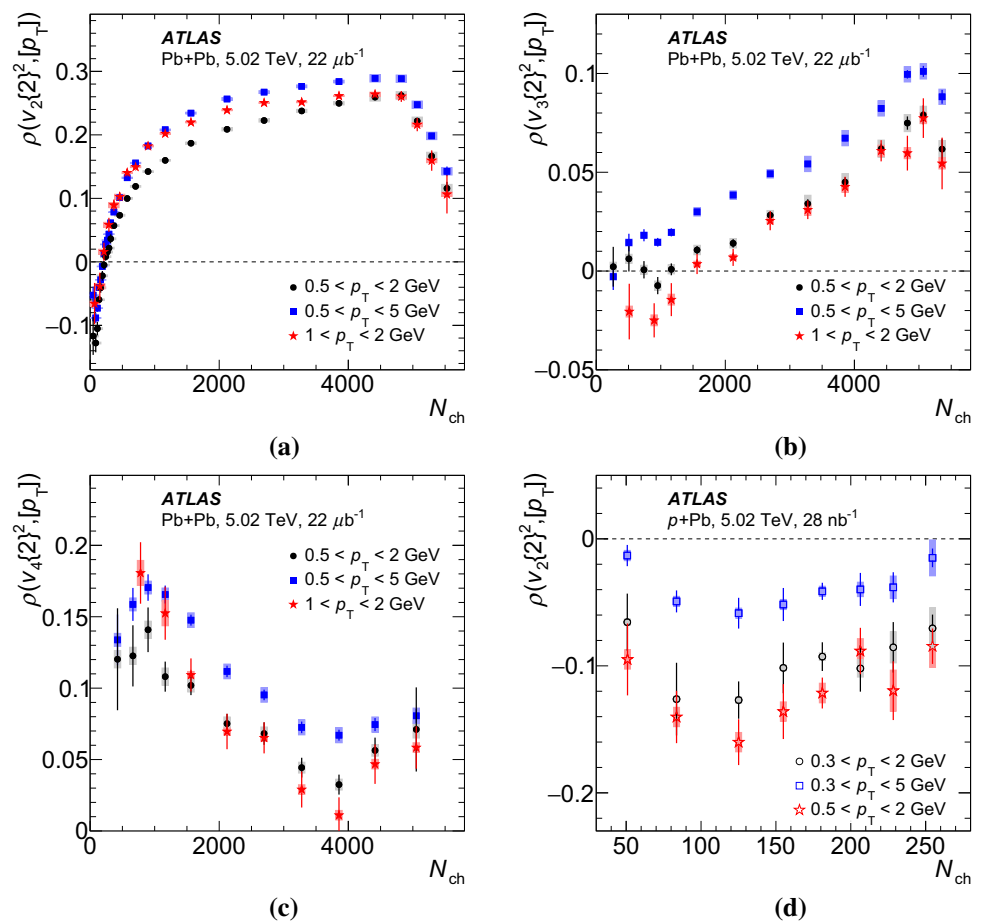


initial-state fluctuations in anisotropic flow [27]. However, a complete understanding of this effect would require a more precise modelling of heavy ion collisions. The correlation coefficients calculated with the upper p_T limit of 2 GeV are 10–20% smaller than the values obtained with a p_T limit of 5 GeV. The correlation coefficient $\rho(v_3\{2\}^2, [p_T])$ is evaluated in Pb+Pb collisions for the same three p_T ranges. The magnitudes measured for $\rho(v_3\{2\}^2, [p_T])$ are significantly smaller than those measured for $\rho(v_2\{2\}^2, [p_T])$ and similar to the magnitudes of $\rho(v_4\{2\}^2, [p_T])$. All three curves increase with N_{ch} in the range of $1000 < N_{\text{ch}} < 5000$. At low values of N_{ch} , a flattening of the trend can be noticed. In the most central collisions, a breakdown of the rise is seen, similarly to the $\rho(v_2\{2\}^2, [p_T])$. Above $N_{\text{ch}} \sim 1500$, the curves for the two intervals with the same maximum p_T are consistent with each other and are below the curve for the interval which uses tracks with p_T up to 5 GeV. The largest values of $\rho(v_4\{2\}^2, [p_T])$ are observed at $N_{\text{ch}} \approx 1000$. For high N_{ch} , $\rho(v_4\{2\}^2, [p_T])$ decreases with N_{ch} up to about $N_{\text{ch}} \approx 4000$ and rises slowly at higher values. The trends obtained for p_T intervals with the same minimum value are consistent above $N_{\text{ch}} \sim 1500$ as is the case for $\rho(v_3\{2\}^2, [p_T])$. The decrease for $N_{\text{ch}} < 4000$ might be due to a contribution to v_4 from

a non-linear term containing v_2^2 , decreasing with increasing centrality [13]. However, a theoretical modelling of the initial state and its subsequent evolution would be required to support this interpretation. Similarly to the $\rho(v_3\{2\}^2, [p_T])$, the $\rho(v_4\{2\}^2, [p_T])$ correlations measured with the larger upper p_T limit show the sensitivity of the $\rho(v_n\{2\}^2, [p_T])$ coefficients to the high p_T part of the particle spectrum contaminated with non-flow correlations from jets. On the other hand, the correlations measured for the intervals with fixed upper p_T limit (2 GeV) and varied lower p_T limits are similar, demonstrating insensitivity of the modified PCC coefficients to a significant change of the event charged-particle multiplicity as expected [25]. The fourth-order correlations are weaker than those for the second-order flow harmonic and for $N_{\text{ch}} > 4000$ are comparable to $\rho(v_3\{2\}^2, [p_T])$. The results for all harmonics indicate a change in the trend in events with high N_{ch} around 4500, which suggests a change in the nature of the correlations in those events [47].

In p +Pb collisions, $\rho(v_2\{2\}^2, [p_T])$ exhibits much weaker N_{ch} dependence than that in Pb+Pb collisions. For the main p_T interval, the modified PCC assumes a negative value of approximately -0.1 and is almost constant within uncertain-

Fig. 5 The PCC $\rho(v_n\{2\}^2, [p_T])$ for $n = 2 - 4$ in **a-c** Pb+Pb collisions and **d** p +Pb collisions as a function of the charged-particle multiplicity N_{ch} for three p_T ranges. The statistical and systematic uncertainties are shown as vertical error bars and boxes, respectively



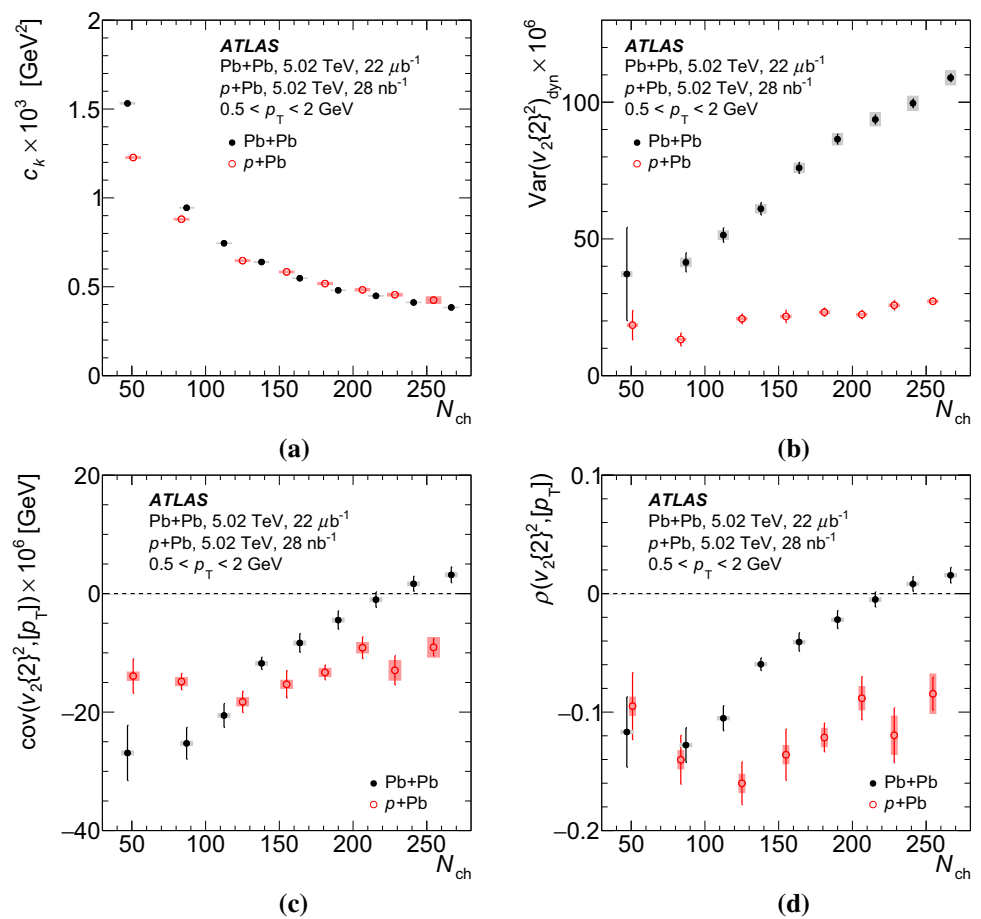
ties. Values for different lower p_T limits are similar, and the $\rho(v_2\{2\}^2, [p_T])$ magnitudes for the larger upper p_T limit are smaller. The magnitude (and sign) of the modified PCC in p +Pb collisions is expected to be related to the distribution of the energy deposition in the initial state, as predicted by the hydrodynamic model [25]. In hydrodynamics, in p +Pb collision, for small sources a higher initial pressure gradients and smaller eccentricities are expected to be generated. This mechanism could lead to the negative correlation of the final state observables, this is the mean transverse momentum and higher order flow harmonics. Thus, the negative value of the modified PCC for $v_2\{2\}$ in p +Pb and peripheral Pb+Pb that is measured should provide valuable constraints for models describing the collectivity in small systems.

6.3 Comparison of p +Pb and Pb+Pb results

Figure 6 shows a comparison of p +Pb and Pb+Pb results shown in Figs. 2, 3, 4, 5 for the common p_T interval of $0.5 < p_T < 2$ GeV. The values of the c_k (Fig. 6a) are similar for p +Pb and Pb+Pb collisions in this p_T interval, while the behaviour of the dynamical variance $\text{Var}(v_2\{2\}^2)_{\text{dyn}}$ (Fig. 6b) is very different due to the different initial eccentricities in the

overlap regions in Pb+Pb and p +Pb collisions. Only a small rise with the multiplicity is observed for p +Pb collisions, which is in agreement with a slow increase of $v_2\{2\}$ with growing event activity [22, 36, 45]. For $N_{ch} \approx 50$, the dynamical variances are comparable between Pb+Pb and p +Pb collisions. The N_{ch} dependence of $\text{cov}(v_2\{2\}^2, [p_T])$ is significantly different for Pb+Pb and p +Pb collisions. A steady rise from negative to positive values with N_{ch} is observed for peripheral Pb+Pb collisions, and approximately constant values are obtained for p +Pb collisions. The N_{ch} dependence of $\rho(v_2\{2\}^2, [p_T])$ is different for the two collision systems. Much weaker N_{ch} dependence of modified PCC is observed in p +Pb collisions compared to Pb+Pb collisions. For $N_{ch} < 100$ the values of $\rho(v_2\{2\}^2, [p_T])$ are consistent between Pb+Pb and p +Pb collisions. The negative $\rho(v_2\{2\}^2, [p_T])$ coefficients for the small systems in p +Pb and Pb+Pb collisions may suggest a more compact source model [25]. The comparison of the systems underlines the importance of the initial stage in the correlations described by the $\rho(v_2\{2\}^2, [p_T])$ coefficient. The theoretical predictions for midcentral and central Pb+Pb collisions suggests that for a large system an increase of the mean transverse momentum indicates a stronger transverse flow and a stronger collective

Fig. 6 Comparison of **a** c_k , **b** $\text{Var}(v_2\{2\}^2)_{\text{dyn}}$, **c** $\text{cov}(v_2\{2\}^2, [p_T])$, and the **d** $\rho(v_2\{2\}^2, [p_T])$ for the range $0.5 < p_T < 2$ GeV as a function of the charged-particle multiplicity N_{ch} . The statistical and systematic uncertainties are shown as vertical error bars and boxes, respectively



response to the initial geometry of the source, characterized by the positive value of the modified PCC.

6.4 Comparison to theoretical predictions

To compare the Pb+Pb results with a theoretical prediction in Ref. [25], the $\rho(v_n\{2\}^2, [p_T])$ coefficients for $0.5 < p_T < 2$ GeV are obtained as a function of centrality intervals expressed by N_{part} using the procedure described in Sect. 4. Figure 7 shows the N_{part} dependence of $\rho(v_n\{2\}^2, [p_T])$ for $n = 2 - 4$ in Pb+Pb collisions. It resembles the trends observed in Fig. 5, which show the modified PCC as a function of N_{ch} , a measure of event activity. The theoretical predictions of the $\rho(v_n\{2\}^2, [p_T])$ coefficient are based on a model in which the initial conditions were generated with nucleon positions by a MC Glauber model [48]. These initial conditions are then evolved using the pressure-driven 3+1D hydrodynamical simulations with viscous effects followed by the statistical particle emission to match multiplicities observed experimentally [37]. The modified Pearson correlation coefficient is then extracted from the final-state particles. The predictions for all harmonics are consistent with the

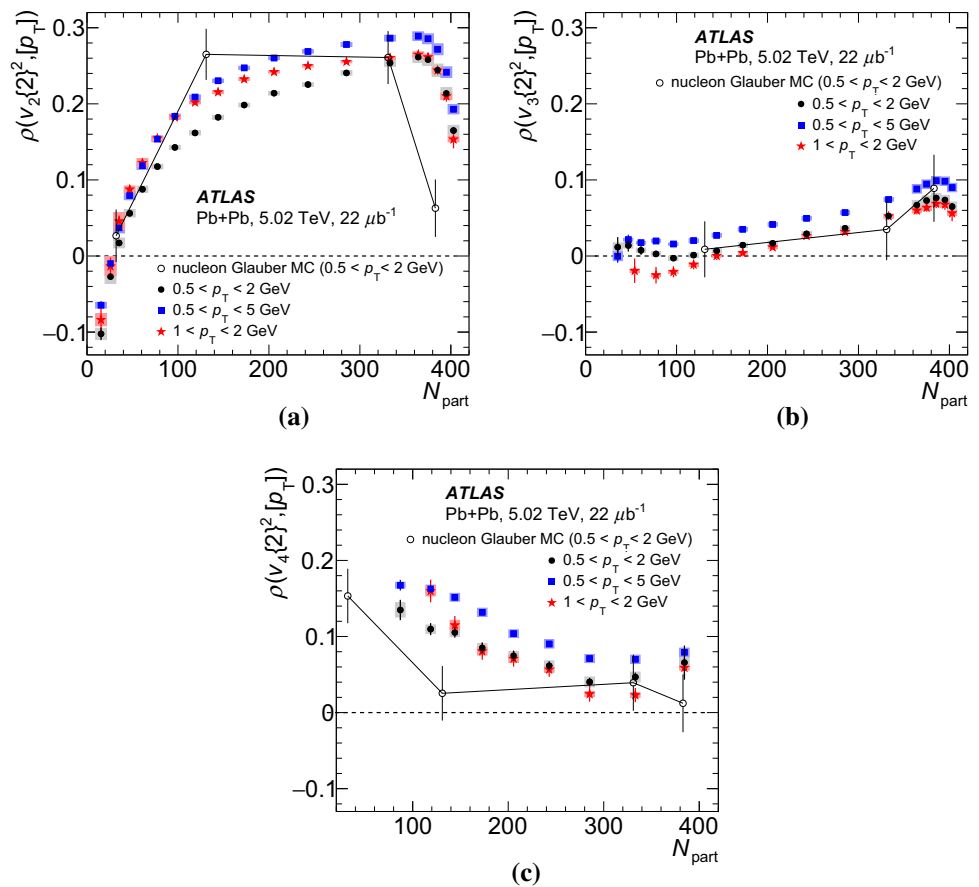
data within the large model uncertainties except for the most central collisions where the predictions underestimate the measured $\rho(v_2\{2\}^2, [p_T])$ and for the semi-peripheral collisions, for $N_{\text{part}} \sim 130$, where the predictions overestimate the $\rho(v_2\{2\}^2, [p_T])$ and underestimate $\rho(v_4\{2\}^2, [p_T])$.

7 Summary

The first measurement of the modified PCC $\rho(v_n\{2\}^2, [p_T])$, which quantifies the correlation between the flow harmonics and the mean transverse momentum, is performed by ATLAS experiment at the LHC. The measurement uses $22 \mu\text{b}^{-1}$ of Pb+Pb data and 28nb^{-1} of p+Pb data at the same centre-of-mass energy per nucleon pair of 5.02 TeV.

The correlation coefficient for several charged-particle p_T ranges is measured as a function of the number of charged particles N_{ch} and, in Pb+Pb collisions, the average number of nucleons participating in the collision, N_{part} . For the 2nd-, 3rd-, and 4th-order harmonics, the measured quantities exhibit a dependence on the choice of charged-particle p_T range. Measurements with an upper limit of 5 GeV on p_T indicate a stronger correlation than those with an upper limit

Fig. 7 The PCC $\rho(v_n\{2\}^2, [p_T])$ for **a** $n = 2$, **b** $n = 3$, and **c** $n = 4$ in Pb+Pb collisions as a function of N_{part} for three p_T ranges. The statistical and systematic uncertainties are shown as vertical error bars and boxes, respectively. A comparison with model predictions [37] is also shown with a line added to guide the eye



of 2 GeV. For mid-central and central collisions, when varying the lower p_T limit, consistent values of $\rho(v_3\{2\}^2, [p_T])$ and $\rho(v_4\{2\}^2, [p_T])$ coefficients are obtained, whereas for the $\rho(v_2\{2\}^2, [p_T])$ coefficient a difference of 10–20% is seen. As a function of event activity, for Pb+Pb collisions, a strong positive correlation $\rho(v_2\{2\}^2, [p_T])$ is observed in mid-central and central collisions while negative values are measured for peripheral events. The correlation $\rho(v_3\{2\}^2, [p_T])$ is found to be weaker, yet non-zero. The values of $\rho(v_4\{2\}^2, [p_T])$ are also positive in the studied centrality range. Non-monotonic behaviour is observed in central Pb+Pb collisions. That trend observed for $\rho(v_2\{2\}^2, [p_T])$ in Pb+Pb collisions is in line with expectations drawn from the ALICE results [20]. In p +Pb collisions, the value of $\rho(v_2\{2\}^2, [p_T])$ is negative and approximately independent of N_{ch} .

The modified PCC is a valuable tool for studying the dynamics of heavy-ion collisions. It provides a reliable estimate of the magnitude of correlations calculated using finite multiplicities. In comparison with existing results, it allows quantitative comparisons between the experimental data and theoretical models. The precise measurements of this observable, presented in this paper, provide useful insights into the interplay of the azimuthal anisotropies (azimuthal flow)

and the mean event p_T (radial flow), providing input for a better understanding of QGP dynamics and for constraining the theoretical models. The obtained $\rho(v_n\{2\}^2, [p_T])$ coefficients for $0.5 < p_T < 2$ GeV were compared with a theoretical prediction based on the pressure-driven 3+1D hydrodynamical simulations with viscous effects. The predictions for all harmonics are consistent with the data within the large model uncertainties. The only exception are the most central collisions, where the predictions underestimate the measured $\rho(v_2\{2\}^2, [p_T])$ and the semi-peripheral collisions, where the predictions overestimate the $\rho(v_2\{2\}^2, [p_T])$ and underestimate $\rho(v_4\{2\}^2, [p_T])$. Sizeable positive correlations observed for non-peripheral Pb+Pb collisions support a qualitatively expected scenario in which the azimuthal flow originates from the pressure gradients.

In small system collisions the magnitude of the transverse flow is expected to be very sensitive to the size of the initial source in the hydrodynamic model. In particular, in the compact source scenario in p +Pb collisions, the smaller source sizes are expected to yield larger transverse flow and smaller initial eccentricities. The negative sign of the modified PCC measured in p +Pb collisions seems to support the compact source scenario, and indicates the role of the initial conditions in these systems.

Acknowledgements We thank CERN for the very successful operation of the LHC, as well as the support staff from our institutions without whom ATLAS could not be operated efficiently. We acknowledge the support of ANPCyT, Argentina; YerPhI, Armenia; ARC, Australia; BMWFW and FWF, Austria; ANAS, Azerbaijan; SSTC, Belarus; CNPq and FAPESP, Brazil; NSERC, NRC and CFI, Canada; CERN; CONICYT, Chile; CAS, MOST and NSFC, China; COLCIENCIAS, Colombia; MSMT CR, MPO CR and VSC CR, Czech Republic; DNRF and DNSRC, Denmark; IN2P3-CNRS, CEA-DRF/IRFU, France; SRNSFG, Georgia; BMBF, HGF, and MPG, Germany; GSRT, Greece; RGC, Hong Kong SAR, China; ISF and Benozio Center, Israel; INFN, Italy; MEXT and JSPS, Japan; CNRST, Morocco; NWO, Netherlands; RCN, Norway; MNiSW and NCN, Poland; FCT, Portugal; MNE/IFA, Romania; MES of Russia and NRC KI, Russian Federation; JINR; MESTD, Serbia; MSSR, Slovakia; ARRS and MIZŠ, Slovenia; DST/NRF, South Africa; MINECO, Spain; SRC and Wallenberg Foundation, Sweden; SERI, SNSF and Cantons of Bern and Geneva, Switzerland; MOST, Taiwan; TAEK, Turkey; STFC, United Kingdom; DOE and NSF, United States of America. In addition, individual groups and members have received support from BCKDF, CANARIE, CRC and Compute Canada, Canada; COST, ERC, ERDF, Horizon 2020, and Marie Skłodowska-Curie Actions, European Union; Investissements d’Avenir Labex and Idex, ANR, France; DFG and AvH Foundation, Germany; Herakleitos, Thales and Aristeia programmes co-financed by EU-ESF and the Greek NSRF, Greece; BSF-NSF and GIF, Israel; CERCA Programme Generalitat de Catalunya, Spain; The Royal Society and Leverhulme Trust, United Kingdom. The crucial computing support from all WLCG partners is acknowledged gratefully, in particular from CERN, the ATLAS Tier-1 facilities at TRIUMF (Canada), NDGF (Denmark, Norway, Sweden), CC-IN2P3 (France), KIT/GridKA (Germany), INFN-CNAF (Italy), NL-T1 (Netherlands), PIC (Spain), ASGC (Taiwan), RAL (UK) and BNL (USA), the Tier-2 facilities worldwide and large non-WLCG resource providers. Major contributors of computing resources are listed in Ref. [49].

Data Availability Statement This manuscript has no associated data or the data will not be deposited. [Authors’ comment: “All ATLAS scientific output is published in journals, and preliminary results are made available in Conference Notes. All are openly available, without restriction on use by external parties beyond copyright law and the standard conditions agreed by CERN. Data associated with journal publications are also made available: tables and data from plots (e.g. cross section values, likelihood profiles, selection efficiencies, cross section limits, ...) are stored in appropriate repositories such as HEPDATA (<http://hepdata.cedar.ac.uk/>). ATLAS also strives to make additional material

related to the paper available that allows a reinterpretation of the data in the context of new theoretical models. For example, an extended encapsulation of the analysis is often provided for measurements in the framework of RIVET (<http://rivet.hepforge.org/>).” This information is taken from the ATLAS Data Access Policy, which is a public document that can be downloaded from <http://opendata.cern.ch/record/413>.]

Open Access This article is distributed under the terms of the Creative Commons Attribution 4.0 International License (<http://creativecommons.org/licenses/by/4.0/>), which permits unrestricted use, distribution, and reproduction in any medium, provided you give appropriate credit to the original author(s) and the source, provide a link to the Creative Commons license, and indicate if changes were made. Funded by SCOAP³.

Appendix

A Systematic uncertainty of c_k , $\text{Var}(v_n\{2\}^2)_{\text{dyn}}$ and $\text{cov}(v_n\{2\}^2, [p_T])$

This section presents the systematic uncertainties of c_k , $\text{Var}(v_n\{2\}^2)_{\text{dyn}}$ and $\text{cov}(v_n\{2\}^2, [p_T])$ for the Pb+Pb and p +Pb collisions at 5.02 TeV as a function of N_{ch} . Each figure shows individual contributions to the total uncertainty from sources described in Sect. 5, i.e. track selection, detector material, tracking azimuthal non-uniformity and residual pile-up events. Figure 8 shows contributions to the systematic uncertainty of c_k measured with tracks from the main p_T intervals in Pb+Pb and p +Pb collisions. The contributions to the systematic uncertainty of $\text{Var}(v_n\{2\}^2)_{\text{dyn}}$ as a function of N_{ch} for each collision system for the second, third, and fourth order harmonics in Pb+Pb collisions, and for $\text{Var}(v_2\{2\}^2)_{\text{dyn}}$ in p +Pb collisions are shown in Fig. 9. Figure 10 presents the corresponding systematic uncertainty of $\text{cov}(v_n\{2\}^2, [p_T])$ for the second, third, and fourth order harmonics in Pb+Pb collisions, and for $\text{cov}(v_2\{2\}^2, [p_T])$ in p +Pb collisions.

Fig. 8 The systematic uncertainty of c_k as a function of N_{ch} measured with tracks from main p_T intervals in **a** Pb+Pb collisions and in **b** p +Pb collisions. The total uncertainty is also shown

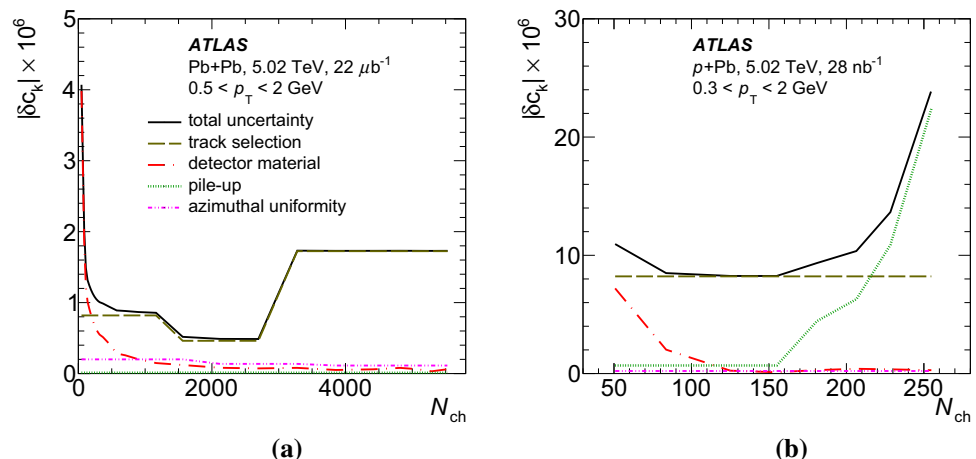


Fig. 9 The systematic uncertainty of $\text{Var}(v_n\{2\}^2)_{\text{dyn}}$ as a function of N_{ch} measured with tracks from main p_T intervals for each collision system for the **a** second, **b** third, and **c** fourth order harmonics in Pb+Pb collisions, and for **d** $\text{Var}(v_2\{2\}^2)_{\text{dyn}}$ in p+Pb collisions. The total uncertainty is also shown

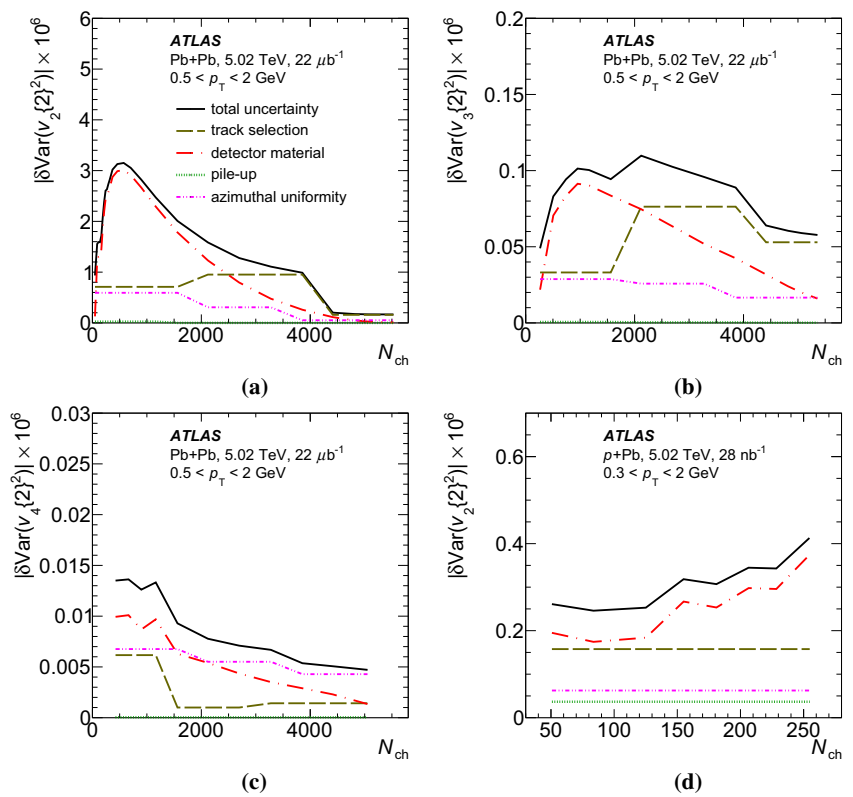
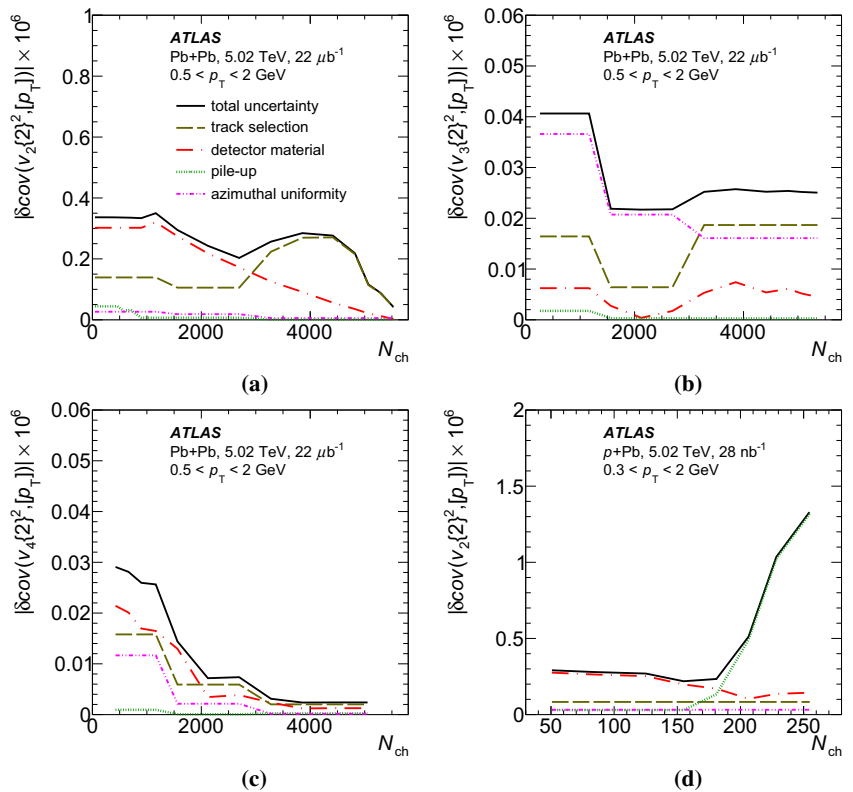


Fig. 10 The systematic uncertainty of $\text{cov}(v_n\{2\}^2, [p_T])$ as a function of N_{ch} measured with tracks from main p_T intervals for each collision system for the **a** second, **b** third, and **c** fourth order harmonics in Pb+Pb collisions, and for **d** $\text{cov}(v_2\{2\}^2, [p_T])$ in p+Pb collisions. The total uncertainty is also shown



References

1. PHOBOS Collaboration, The PHOBOS perspective on discoveries at RHIC. Nucl. Phys. A **757**, 28 (2005). [arXiv:nucl-ex/0410022](#)
2. STAR Collaboration, Experimental and theoretical challenges in the search for the quark gluon plasma: The STAR Collaboration's critical assessment of the evidence from RHIC collisions. Nucl. Phys. A **757**, 102 (2005). [arXiv:nucl-ex/0501009](#)
3. BRAHMS Collaboration, Quark gluon plasma and color glass condensate at RHIC? The Perspective from the BRAHMS experiment. Nucl. Phys. A **757**, 1 (2005). [arXiv:nucl-ex/0410020](#)
4. PHENIX Collaboration, Formation of dense partonic matter in relativistic nucleus-nucleus collisions at RHIC: Experimental evaluation by the PHENIX collaboration. Nucl. Phys. A **757**, 184 (2005). [arXiv:nucl-ex/0410003](#)
5. ALICE Collaboration, Elliptic flow of charged particles in Pb–Pb collisions at $\sqrt{s_{NN}} = 2.76$ TeV. Phys. Rev. Lett. **105**, 252302 (2010). [arXiv:1011.3914](#) [nucl-ex]
6. ATLAS Collaboration, Measurement of the pseudorapidity and transverse momentum dependence of the elliptic flow of charged particles in lead–lead collisions at $\sqrt{s_{NN}} = 2.76$ TeV with the ATLAS detector. Phys. Lett. B **707**, 330 (2012). [arXiv:1108.6018](#) [hep-ex]
7. ATLAS Collaboration, Measurement of the azimuthal anisotropy for charged particle production in $\sqrt{s_{NN}} = 2.76$ TeV lead–lead collisions with the ATLAS detector. Phys. Rev. C **86**, 014907 (2012). [arXiv:1203.3087](#) [hep-ex]
8. CMS Collaboration, Measurement of the elliptic anisotropy of charged particles produced in PbPb collisions at $\sqrt{s_{NN}} = 2.76$ TeV. Phys. Rev. C **87**, 014902 (2013). [arXiv:1204.1409](#) [hep-ex]
9. J. Schukraft, QM2017: status and key open questions in ultra-relativistic heavy-ion physics. Nucl. Phys. C **967**, 1 (2017). [arXiv:1705.02646](#) [nucl-ex]
10. ATLAS Collaboration, Measurement of the azimuthal anisotropy of charged particles produced in $\sqrt{s_{NN}} = 5.02$ TeV Pb+Pb collisions with the ATLAS detector. Eur. Phys. J. C **78**, 997 (2018). [arXiv:1808.03951](#) [nucl-ex]
11. S. Ryu et al., Importance of the bulk viscosity of QCD in ultrarelativistic heavy-ion collisions. Phys. Rev. Lett. **115**, 132301 (2015). [arXiv:1502.01675](#) [nucl-th]
12. Z. Qiu, U. Heinz, Hydrodynamic event-plane correlations in Pb + Pb collisions at $\sqrt{s} = 2.76$ ATeV. Phys. Lett. B **717**, 261 (2012). [arXiv:1208.1200](#) [nucl-th]
13. ATLAS Collaboration, Measurement of the correlation between flow harmonics of different order in lead–lead collisions at $\sqrt{s_{NN}} = 2.76$ TeV with the ATLAS detector. Phys. Rev. C **92**, 034903 (2015). [arXiv:1504.01289](#) [hep-ex]
14. D. Teaney, L. Yan, Triangularity and dipole dsymmetry in relativistic heavy ion collisions. Phys. Rev. C **83**, 064904 (2011). [arXiv:1010.1876](#) [nucl-th]
15. R.S. Bhalerao, J.-Y. Ollitrault, S. Pal, Characterizing flow fluctuations with moments. Phys. Lett. B **742**, 94 (2015). [arXiv:1411.5160](#) [nucl-th]
16. ATLAS Collaboration, Measurement of the distributions of event-by-event flow harmonics in lead–lead collisions at $\sqrt{s_{NN}} = 2.76$ TeV with the ATLAS detector at the LHC. JHEP **11** 183 (2013). [arXiv:1305.2942](#) [hep-ex]
17. PHENIX Collaboration, Multiparticle azimuthal correlations for extracting event-by-event elliptic and triangular flow in Au + Au collisions at $\sqrt{s_{NN}} = 200$ GeV. Phys. Rev. C **99**, 024903 (2019). [arXiv:1804.10024](#) [nucl-ex]
18. PHOBOS Collaboration, Non-flow correlations and elliptic flow fluctuations in Au + Au collisions at $\sqrt{s_{NN}} = 200$ GeV. Phys. Rev. C **81**, 034915 (2010). [arXiv:1002.0534](#) [nucl-ex]
19. J. Schukraft, A. Timmins, S. Voloshin, Ultra-relativistic nuclear collisions: event shape engineering. Phys. Lett. B **719**, 394 (2013). [arXiv:1208.4563](#) [nucl-ex]
20. ALICE Collaboration, Event-shape engineering for inclusive spectra and elliptic flow in Pb–Pb collisions at $\sqrt{s_{NN}} = 2.76$ TeV. Phys. Rev. C **93**, 034916 (2016). [arXiv:1507.06194](#) [hep-ex]
21. U. Heinz, R. Snellings, Collective flow and viscosity in relativistic heavy-ion collisions. Annu. Rev. Nucl. Part. Sci. **63**, 123 (2013). [arXiv:1301.2826](#) [nucl-th]
22. ATLAS Collaboration, Measurement of multi-particle azimuthal correlations in pp , $p + Pb$ and low-multiplicity Pb + Pb collisions with the ATLAS detector. Eur. Phys. J. C **77**, 428 (2017). [arXiv:1705.04176](#) [hep-ex]
23. ALICE Collaboration, Multiplicity dependence of pion, kaon, proton and lambda production in p–Pb collisions at $\sqrt{s_{NN}} = 5.02$ TeV. Phys. Lett. B **728**, 25 (2014). [arXiv:1307.6796](#) [nucl-th]
24. ALICE Collaboration, Transverse momentum spectra and nuclear modification factors of charged particles in pp, p–Pb and Pb–Pb collisions at the LHC. JHEP **11**, 013 (2018). [arXiv:1802.09145](#) [nucl-ex]
25. P. Bozek, Transverse-momentum-flow correlations in relativistic heavy-ion collisions. Phys. Rev. C **93**, 044908 (2016). [arXiv:1601.04513](#) [nucl-th]
26. J. Jia, M. Zhou, A. Trzupek, Revealing long-range multiparticle collectivity in small collision systems via subevent cumulants. Phys. Rev. C **96**, 034906 (2017). [arXiv:1701.03830](#) [nucl-ex]
27. ATLAS Collaboration, Measurement of flow harmonics with multiparticle cumulants in Pb+Pb collisions at $\sqrt{s_{NN}} = 2.76$ TeV with the ATLAS detector. Eur. Phys. J. C **74**, 3157 (2014). [arXiv:1408.4342](#) [hep-ex]
28. STAR Collaboration, Incident energy dependence of p_t correlations at relativistic energies. Phys. Rev. C **72**, 044902 (2005). [arXiv:nucl-ex/0504031](#) [nucl-ex]
29. ALICE Collaboration, Event-by-event mean p_T fluctuations in pp and Pb–Pb collisions at the LHC. Eur. Phys. J. C **74**, 3077 (2014). [arXiv:1407.5530](#) [nucl-ex]
30. ATLAS Collaboration, The ATLAS experiment at the CERN large hadron collider. JINST **3**, S08003 (2008)
31. ATLAS Collaboration, ATLAS Insertable B-Layer Technical Design Report, ATLAS-TDR-19, 2010. <https://cds.cern.ch/record/1291633> (Addendum: ATLAS-TDR-19-ADD-1, 2012, <https://cds.cern.ch/record/1451888>)
32. B. Abbott et al., Production and integration of the ATLAS Insertable B-Layer. JINST **13**, T05008 (2018). [arXiv:1803.00844](#) [physics.ins-det]
33. ATLAS Collaboration, Performance of the ATLAS Trigger System in 2010. Eur. Phys. J. C **72**, 1849 (2012). [arXiv:1110.1530](#) [hep-ex]
34. ATLAS Collaboration, Performance of the ATLAS trigger system in 2015. Eur. Phys. J. C **77**, 317 (2017). [arXiv:1611.09661](#) [hep-ex]
35. ATLAS Collaboration, Fluctuations of anisotropic flow in Pb+Pb collisions at $\sqrt{s_{NN}} = 5.02$ TeV with the ATLAS detector (2019). [arXiv:1904.04808](#) [nucl-ex]
36. ATLAS Collaboration, Measurement of long-range pseudorapidity correlations and azimuthal harmonics in $\sqrt{s_{NN}} = 5.02$ TeV proton–lead collisions with the ATLAS detector. Phys. Rev. C **90**, 044906 (2014). [arXiv:1409.1792](#) [hep-ex]
37. P. Bozek, W. Broniowski, M. Rybczynski, Wounded quarks in A + A, p + A, and p + p collisions. Phys. Rev. C **94**, 014902 (2016). [arXiv:1604.07697](#) [nucl-th]
38. B. Alver, M. Baker, C. Loizides, P. Steinberg, The PHOBOS Glauber Monte Carlo (2008). [arXiv:0805.4411v1](#)
39. X.-N. Wang, M. Gyulassy, Hijing: a Monte Carlo model for multiple jet production in pp, pA, and AA collisions. Phys. Rev. D **44**, 3501 (1991)

40. J. Jia, S. Mohapatra, Disentangling flow and nonflow correlations via Bayesian unfolding of the event-by-event distributions of harmonic coefficients in ultrarelativistic heavy-ion collisions. *Phys. Rev. C* **88**, 014907 (2013). [arXiv:1304.1471](#) [nucl-ex]
41. S. Agostinelli et al., Geant4—a simulation toolkit. *Nucl. Instrum. Methods A* **506**, 250 (2003)
42. ATLAS Collaboration, The ATLAS simulation infrastructure. *Eur. Phys. J. C* **70**, 823 (2010). [arXiv:1005.4568](#) [physics.ins-det]
43. ATLAS Collaboration, Study of the material of the ATLAS inner detector for Run 2 of the LHC. *JINST* **12**, P12009 (2017). [arXiv:1707.02826](#) [hep-ex]
44. ATLAS Collaboration, Charged-particle distributions in $\sqrt{s} = 13$ TeV pp interactions measured with the ATLAS detector at the LHC. *Phys. Lett. B* **758**, 67 (2016). [arXiv:1602.01633](#) [hep-ex]
45. ATLAS Collaboration, Measurement of long-range multiparticle azimuthal correlations with the subevent cumulant method in pp and $p + Pb$ collisions with the ATLAS detector at the CERN Large Hadron Collider. *Phys. Rev. C* **97**, 024904 (2018). [arXiv:1708.03559](#) [hep-ex]
46. S. Voloshin, A.M. Poskanzer, R. Snellings, Collective phenomena in non-central nuclear collisions (2008). [arXiv:0809.2949](#) [nucl-ex]
47. A. Mazeliauskas, D. Teaney, Fluctuations of harmonic and radial flow in heavy ion collisions with principal components. *Phys. Rev. C* **93**, 024913 (2016). [arXiv:1509.07492](#) [nucl-th]
48. C. Loizides, Glauber modeling of high-energy nuclear collisions at the subnucleon level. *Phys. Rev. C* **94**, 024914 (2016). [arXiv:1603.07375](#) [nucl-ex]
49. ATLAS Collaboration, ATLAS Computing Acknowledgements, ATL-GEN-PUB-2016-002. <https://cds.cern.ch/record/2202407>

ATLAS Collaboration

G. Aad¹⁰¹, B. Abbott¹²⁸, D. C. Abbott¹⁰², A. Abed Abud^{70a,70b}, K. Abeling⁵³, D. K. Abhayasinghe⁹³, S. H. Abidi¹⁶⁷, O. S. AbouZeid⁴⁰, N. L. Abraham¹⁵⁶, H. Abramowicz¹⁶¹, H. Abreu¹⁶⁰, Y. Abulaiti⁶, B. S. Acharya^{66a,66b,o}, B. Achkar⁵³, S. Adachi¹⁶³, L. Adam⁹⁹, C. Adam Bourdarios⁵, L. Adamczyk^{83a}, L. Adamek¹⁶⁷, J. Adelman¹²¹, M. Adersberger¹¹⁴, A. Adiguzel^{12c.ak}, S. Adorni⁵⁴, T. Adye¹⁴⁴, A. A. Affolder¹⁴⁶, Y. Afik¹⁶⁰, C. Agapopoulou¹³², M. N. Agaras³⁸, A. Aggarwal¹¹⁹, C. Agheorghiesei^{27c}, J. A. Aguilar-Saavedra^{140a,140f.aj}, F. Ahmadov⁷⁹, W. S. Ahmed¹⁰³, X. Ai¹⁸, G. Aielli^{73a,73b}, S. Akatsuka⁸⁵, T. P. A. Åkesson⁹⁶, E. Akilli⁵⁴, A. V. Akimov¹¹⁰, K. Al Khoury¹³², G. L. Alberghi^{23a,23b}, J. Albert¹⁷⁶, M. J. Alconada Verzini¹⁶¹, S. Alderweireldt³⁶, M. Aleksa³⁶, I. N. Aleksandrov⁷⁹, C. Alexa^{27b}, D. Alexandre¹⁹, T. Alexopoulos¹⁰, A. Alfonsi¹²⁰, F. Alfonsi^{23a,23b}, M. Alhroob¹²⁸, B. Ali¹⁴², G. Alimonti^{68a}, J. Alison³⁷, S. P. Alkire¹⁴⁸, C. Allaire¹³², B. M. M. Allbrooke¹⁵⁶, B. W. Allen¹³¹, P. P. Allport²¹, A. Aloisio^{69a,69b}, A. Alonso⁴⁰, F. Alonso⁸⁸, C. Alpigiani¹⁴⁸, A. A. Alshehri⁵⁷, M. Alvarez Estevez⁹⁸, D. Álvarez Piqueras¹⁷⁴, M. G. Alvigi^{69a,69b}, Y. Amaral Coutinho^{80b}, A. Ambler¹⁰³, L. Ambroz¹³⁵, C. Amelung²⁶, D. Amidei¹⁰⁵, S. P. Amor Dos Santos^{140a}, S. Amoroso⁴⁶, C. S. Amrouche⁵⁴, F. An⁷⁸, C. Anastopoulos¹⁴⁹, N. Andari¹⁴⁵, T. Andeen¹¹, C. F. Anders^{61b}, J. K. Anders²⁰, A. Andreazza^{68a,68b}, V. Andrei^{61a}, C. R. Anelli¹⁷⁶, S. Angelidakis³⁸, A. Angerami³⁹, A. V. Anisenkov^{122a,122b}, A. Annovi^{71a}, C. Antel^{61a}, M. T. Anthony¹⁴⁹, M. Antonelli⁵¹, D. J. A. Antrim¹⁷¹, F. Anulli^{72a}, M. Aoki⁸¹, J. A. Aparisi Pozo¹⁷⁴, L. Aperio Bella^{15a}, G. Arabidze¹⁰⁶, J. P. Araque^{140a}, V. Araujo Ferraz^{80b}, R. Araujo Pereira^{80b}, C. Arcangeletti⁵¹, A. T. H. Arce⁴⁹, F. A. Arduh⁸⁸, J.-F. Arguin¹⁰⁹, S. Argyropoulos⁷⁷, J.-H. Arling⁴⁶, A. J. Armbruster³⁶, A. Armstrong¹⁷¹, O. Arnaez¹⁶⁷, H. Arnold¹²⁰, A. Artamonov^{111.*}, G. Artoni¹³⁵, S. Artz⁹⁹, S. Asai¹⁶³, N. Asbah⁵⁹, E. M. Asimakopoulou¹⁷², L. Asquith¹⁵⁶, J. Assahsah^{35d}, K. Assamagan²⁹, R. Astalos^{28a}, R. J. Atkin^{33a}, M. Atkinson¹⁷³, N. B. Atlay¹⁹, H. Atmani¹³², K. Augsten¹⁴², G. Avolio³⁶, R. Avramidou^{60a}, M. K. Ayoub^{15a}, A. M. Azoulay^{168b}, G. Azeulos^{109.az}, H. Bachacou¹⁴⁵, K. Bachas^{67a,67b}, M. Backes¹³⁵, F. Backman^{45a,45b}, P. Bagnaia^{72a,72b}, M. Bahmani⁸⁴, H. Bahrasemani¹⁵², A. J. Bailey¹⁷⁴, V. R. Bailey¹⁷³, J. T. Baines¹⁴⁴, M. Bajic⁴⁰, C. Bakalis¹⁰, O. K. Baker¹⁸³, P. J. Bakker¹²⁰, D. Bakshi Gupta⁸, S. Balaji¹⁵⁷, E. M. Baldin^{122a,122b}, P. Balek¹⁸⁰, F. Balli¹⁴⁵, W. K. Balunas¹³⁵, J. Balz⁹⁹, E. Banas⁸⁴, A. Bandyopadhyay²⁴, Sw. Banerjee^{181.j}, A. A. E. Bannoura¹⁸², L. Barak¹⁶¹, W. M. Barbe³⁸, E. L. Barberio¹⁰⁴, D. Barberis^{55a,55b}, M. Barbero¹⁰¹, G. Barbour⁹⁴, T. Barillari¹¹⁵, M.-S. Barisits³⁶, J. Barkeloo¹³¹, T. Barklow¹⁵³, R. Barnea¹⁶⁰, S. L. Barnes^{60c}, B. M. Barnett¹⁴⁴, R. M. Barnett¹⁸, Z. Barnovska-Blenesny^{60a}, A. Baroncelli^{60a}, G. Barone²⁹, A. J. Barr¹³⁵, L. Barranco Navarro^{45a,45b}, F. Barreiro⁹⁸, J. Barreiro Guimarães da Costa^{15a}, S. Barsov¹³⁸, R. Bartoldus¹⁵³, G. Bartolini¹⁰¹, A. E. Barton⁸⁹, P. Bartos^{28a}, A. Basalae⁴⁶, A. Bassalat^{132.as}, M. J. Basso¹⁶⁷, R. L. Bates⁵⁷, S. Batlamous^{35e}, J. R. Batley³², B. Batool¹⁵¹, M. Battaglia¹⁴⁶, M. Baue^{72a,72b}, F. Bauer¹⁴⁵, K. T. Bauer¹⁷¹, H. S. Bawa^{31.m}, J. B. Beacham⁴⁹, T. Beau¹³⁶, P. H. Beauchemin¹⁷⁰, F. Becherer⁵², P. Bechtel²⁴, H. C. Beck⁵³, H. P. Beck^{20.s}, K. Becker⁵², M. Becker⁹⁹, C. Becot⁴⁶, A. Beddall^{12d}, A. J. Beddall^{12a}, V. A. Bednyakov⁷⁹, M. Bedognetti¹²⁰, C. P. Bee¹⁵⁵, T. A. Beermann⁷⁶, M. Begalli^{80b}, M. Begel²⁹, A. Behera¹⁵⁵, J. K. Behr⁴⁶, F. Beisiegel²⁴, A. S. Bell⁹⁴, G. Bella¹⁶¹, L. Bellagamba^{23b}, A. Bellerive³⁴, P. Bellos⁹, K. Beloborodov^{122a,122b}, K. Belotskiy¹¹², N. L. Belyaev¹¹², D. Benchechroun^{35a}, N. Benekos¹⁰, Y. Benhammou¹⁶¹, D. P. Benjamin⁶, M. Benoit⁵⁴, J. R. Bensinger²⁶, S. Bentvelsen¹²⁰, L. Beresford¹³⁵, M. Beretta⁵¹, D. Berge⁴⁶, E. Bergeaas Kuutmann¹⁷², N. Berger⁵, B. Bergmann¹⁴², L. J. Bergsten²⁶, J. Beringer¹⁸, S. Berlendis⁷, N. R. Bernard¹⁰², G. Bernardi¹³⁶, C. Bernius¹⁵³, T. Berry⁹³, P. Berta⁹⁹, C. Bertella^{15a}, I. A. Bertram⁸⁹, O. Bessidskaia Bylund¹⁸², N. Besson¹⁴⁵, A. Bethani¹⁰⁰, S. Bethke¹¹⁵, A. Betti²⁴, A. J. Bevan⁹², J. Beyer¹¹⁵

D. S. Bhattacharya¹⁷⁷, R. Bi¹³⁹, R. M. Bianchi¹³⁹, O. Biebel¹¹⁴, D. Biedermann¹⁹, R. Bielski³⁶, K. Bierwagen⁹⁹, N. V. Biesuz^{71a,71b}, M. Biglietti^{74a}, T. R. V. Billoud¹⁰⁹, M. Bindi⁵³, A. Bingul^{12d}, C. Bini^{72a,72b}, S. Biondi^{23a,23b}, M. Birman¹⁸⁰, T. Bisanz⁵³, J. P. Biswal¹⁶¹, D. Biswas^{181j}, A. Bitadze¹⁰⁰, C. Bittrich⁴⁸, K. Bjørke¹³⁴, K. M. Black²⁵, T. Blazek^{28a}, I. Bloch⁴⁶, C. Blocker²⁶, A. Blue⁵⁷, U. Blumenschein⁹², G. J. Bobbink¹²⁰, V. S. Bobrovnikov^{122a,122b}, S. S. Bocchetta⁹⁶, A. Bocci⁴⁹, D. Boerner⁴⁶, D. Bogavac¹⁴, A. G. Bogdanchikov^{122a,122b}, C. Boehm^{45a}, V. Boisvert⁹³, P. Bokan^{53,172}, T. Bold^{83a}, A. S. Boldyrev¹¹³, A. E. Bolz^{61b}, M. Bomben¹³⁶, M. Bona⁹², J. S. Bonilla¹³¹, M. Boonekamp¹⁴⁵, H. M. Borecka-Bielska⁹⁰, A. Borisov¹²³, G. Borissov⁸⁹, J. Bortfeldt³⁶, D. Bortoletto¹³⁵, D. Boscherini^{23b}, M. Bosman¹⁴, J. D. Bossio Sola¹⁰³, K. Bouaouda^{35a}, J. Boudreau¹³⁹, E. V. Bouhova-Thacker⁸⁹, D. Boumediene³⁸, S. K. Boutle⁵⁷, A. Boveia¹²⁶, J. Boyd³⁶, D. Boye^{33b,at}, I. R. Boyko⁷⁹, A. J. Bozson⁹³, J. Bracinik²¹, N. Brahimy¹⁰¹, G. Brandt¹⁸², O. Brandt³², F. Braren⁴⁶, B. Brau¹⁰², J. E. Brau¹³¹, W. D. Breaden Madden⁵⁷, K. Brendlinger⁴⁶, L. Brenner⁴⁶, R. Brenner¹⁷², S. Bressler¹⁸⁰, B. Brickwedde⁹⁹, D. L. Briglin²¹, D. Britton⁵⁷, D. Britzger¹¹⁵, I. Brock²⁴, R. Brock¹⁰⁶, G. Brooijmans³⁹, W. K. Brooks^{147b}, E. Brost¹²¹, J. H. Broughton²¹, P. A. Bruckman de Renstrom⁸⁴, D. Bruncko^{28b}, A. Bruni^{23b}, G. Bruni^{23b}, L. S. Bruni¹²⁰, S. Bruno^{73a,73b}, B. H. Brunt³², M. Bruschi^{23b}, N. Brusino¹³⁹, P. Bryant³⁷, L. Bryngemark⁹⁶, T. Buanes¹⁷, Q. Buat³⁶, P. Buchholz¹⁵¹, A. G. Buckley⁵⁷, I. A. Budagov⁷⁹, M. K. Bugge¹³⁴, F. Bühner⁵², O. Bulekov¹¹², T. J. Burch¹²¹, S. Burdin⁹⁰, C. D. Burgard¹²⁰, A. M. Burger¹²⁹, B. Burghgrave⁸, K. Burka^{83a}, J. T. P. Burr⁴⁶, C. D. Burton¹¹, J. C. Burzynski¹⁰², V. Büscher⁹⁹, E. Buschmann⁵³, P. J. Bussey⁵⁷, J. M. Butler²⁵, C. M. Buttar⁵⁷, J. M. Butterworth⁹⁴, P. Butti³⁶, W. Buttinger³⁶, A. Buzatu¹⁵⁸, A. R. Buzykaev^{122a,122b}, G. Cabras^{23a,23b}, S. Cabrera Urbán¹⁷⁴, D. Caforio⁵⁶, H. Cai¹⁷³, V. M. M. Cairo¹⁵³, O. Cakir^{4a}, N. Calace³⁶, P. Calafiura¹⁸, A. Calandri¹⁰¹, G. Calderini¹³⁶, P. Calfayan⁶⁵, G. Callea⁵⁷, L. P. Caloba^{80b}, S. Calvente Lopez⁹⁸, D. Calvet³⁸, S. Calvet³⁸, T. P. Calvet¹⁵⁵, M. Calvetti^{71a,71b}, R. Camacho Toro¹³⁶, S. Camarda³⁶, D. Camarero Munoz⁹⁸, P. Camarri^{73a,73b}, D. Cameron¹³⁴, R. Caminal Armadans¹⁰², C. Camincher³⁶, S. Campana³⁶, M. Campanelli⁹⁴, A. Camplani⁴⁰, A. Campoverde¹⁵¹, V. Canale^{69a,69b}, A. Canesse¹⁰³, M. Cano Bret^{60c}, J. Cantero¹²⁹, T. Cao¹⁶¹, Y. Cao¹⁷³, M. D. M. Capeans Garrido³⁶, M. Capua^{41a,41b}, R. Cardarelli^{73a}, F. Cardillo¹⁴⁹, G. Carducci^{41a,41b}, I. Carli¹⁴³, T. Carli³⁶, G. Carlino^{69a}, B. T. Carlson¹³⁹, L. Carminati^{68a,68b}, R. M. D. Carney^{45a,45b}, S. Caron¹¹⁹, E. Carquin^{147b}, S. Carrá⁴⁶, J. W. S. Carter¹⁶⁷, M. P. Casado^{14,e}, A. F. Casha¹⁶⁷, D. W. Casper¹⁷¹, R. Castelijns¹²⁰, F. L. Castillo¹⁷⁴, V. Castillo Gimenez¹⁷⁴, N. F. Castro^{140a,140e}, A. Catinaccio³⁶, J. R. Catmore¹³⁴, A. Cattai³⁶, J. Caudron²⁴, V. Cavaliere²⁹, E. Cavallaro¹⁴, M. Cavalli-Sforza¹⁴, V. Cavasinni^{71a,71b}, E. Celebi^{12b}, F. Ceradini^{74a,74b}, L. Cerda Alberich¹⁷⁴, K. Cerny¹³⁰, A. S. Cerqueira^{80a}, A. Cerri¹⁵⁶, L. Cerrito^{73a,73b}, F. Cerutti¹⁸, A. Cervelli^{23a,23b}, S. A. Cetin^{12b}, Z. Chadi^{35a}, D. Chakraborty¹²¹, S. K. Chan⁵⁹, W. S. Chan¹²⁰, W. Y. Chan⁹⁰, J. D. Chapman³², B. Chargeishvili^{159b}, D. G. Charlton²¹, T. P. Charman⁹², C. C. Chau³⁴, S. Che¹²⁶, S. Chekanov⁶, S. V. Chekulaev^{168a}, G. A. Chelkov^{79,ay}, M. A. Chelstowska³⁶, B. Chen⁷⁸, C. Chen^{60a}, C. H. Chen⁷⁸, H. Chen²⁹, J. Chen^{60a}, J. Chen³⁹, S. Chen¹³⁷, S. J. Chen^{15c}, X. Chen^{15b,ax}, Y. Chen⁸², Y.-H. Chen⁴⁶, H. C. Cheng^{63a}, H. J. Cheng^{15a,15d}, A. Cheplakov⁷⁹, E. Cheremushkina¹²³, R. Cherkaoui El Moursli^{35e}, E. Cheu⁷, K. Cheung⁶⁴, T. J. A. Chevalérias¹⁴⁵, L. Chevalier¹⁴⁵, V. Chiarella⁵¹, G. Chiarelli^{71a}, G. Chiodini^{67a}, A. S. Chisholm²¹, A. Chitan^{27b}, I. Chiu¹⁶³, Y. H. Chiu¹⁷⁶, M. V. Chizhov⁷⁹, K. Choi⁶⁵, A. R. Chomont^{72a,72b}, S. Chouridou¹⁶², Y. S. Chow¹²⁰, M. C. Chu^{63a}, X. Chu^{15a}, J. Chudoba¹⁴¹, A. J. Chuinard¹⁰³, J. J. Chwastowski⁸⁴, L. Chytka¹³⁰, D. Cieri¹¹⁵, K. M. Ciesla⁸⁴, D. Cinca⁴⁷, V. Cindro⁹¹, I. A. Cioară^{27b}, A. Ciocio¹⁸, F. Ciroto^{69a,69b}, Z. H. Citron^{180,k}, M. Citterio^{68a}, D. A. Ciubotaru^{27b}, B. M. Ciungu¹⁶⁷, A. Clark⁵⁴, M. R. Clark³⁹, P. J. Clark⁵⁰, C. Clement^{45a,45b}, Y. Coadou¹⁰¹, M. Cobal^{66a,66c}, A. Coccaro^{55b}, J. Cochran⁷⁸, H. Cohen¹⁶¹, A. E. C. Coimbra³⁶, L. Colasurdo¹¹⁹, B. Cole³⁹, A. P. Colijn¹²⁰, J. Collot⁵⁸, P. Conde Muñino^{140a,f}, E. Coniavitis⁵², S. H. Connell^{33b}, I. A. Connelly⁵⁷, S. Constantinescu^{27b}, F. Conventi^{69a,aaa}, A. M. Cooper-Sarkar¹³⁵, F. Cormier¹⁷⁵, K. J. R. Cormier¹⁶⁷, L. D. Corpe⁹⁴, M. Corradi^{72a,72b}, E. E. Corrigan⁹⁶, F. Corriveau^{103,af}, A. Cortes-Gonzalez³⁶, M. J. Costa¹⁷⁴, F. Costanza⁵, D. Costanzo¹⁴⁹, G. Cowan⁹³, J. W. Cowley³², J. Crane¹⁰⁰, K. Cranmer¹²⁴, S. J. Crawley⁵⁷, R. A. Creager¹³⁷, S. Crépe-Renaudin⁵⁸, F. Crescioli¹³⁶, M. Cristinziani²⁴, V. Croft¹²⁰, G. Crosetti^{41a,41b}, A. Cueto⁵, T. Cuhadar Donszelmann¹⁴⁹, A. R. Cukierman¹⁵³, S. Czekierda⁸⁴, P. Czodrowski³⁶, M. J. Da Cunha Sargedas De Sousa^{60b}, J. V. Da Fonseca Pinto^{80b}, C. Da Via¹⁰⁰, W. Dabrowski^{83a}, T. Dado^{28a}, S. Dahbi^{35e}, T. Dai¹⁰⁵, C. Dallapiccola¹⁰², M. Dam⁴⁰, G. D'amen²⁹, V. D'Amico^{74a,74b}, J. Damp⁹⁹, J. R. Dandoy¹³⁷, M. F. Daneri³⁰, N. P. Dang^{181,j}, N. S. Dann¹⁰⁰, M. Danninger¹⁷⁵, V. Dao³⁶, G. Darbo^{55b}, O. Dartsis⁵, A. Dattagupta¹³¹, T. Daubney⁴⁶, S. D'Auria^{68a,68b}, W. Davey²⁴, C. David⁴⁶, T. Davidek¹⁴³, D. R. Davis⁴⁹, I. Dawson¹⁴⁹, K. De⁸, R. De Asmundis^{69a}, M. De Beurs¹²⁰, S. De Castro^{23a,23b}, S. De Cecco^{72a,72b}, N. De Groot¹¹⁹, P. de Jong¹²⁰, H. De la Torre¹⁰⁶, A. De Maria^{15c}, D. De Pedis^{72a}, A. De Salvo^{72a}, U. De Sanctis^{73a,73b}, M. De Santis^{73a,73b}, A. De Santo¹⁵⁶, K. De Vasconcelos Corga¹⁰¹, J. B. De Vivie De Regie¹³², C. Debenedetti¹⁴⁶, D. V. Dedovich⁷⁹, A. M. Deiana⁴², M. Del Gaudio^{41a,41b}, J. Del Peso⁹⁸, Y. Delabat Diaz⁴⁶, D. Delgove¹³², F. Deliot^{145,r}, C. M. Delitzsch⁷, M. Della Pietra^{69a,69b}, D. Della Volpe⁵⁴, A. Dell'Acqua³⁶, L. Dell'Asta^{73a,73b}, M. Delmastro⁵, C. Delporte¹³², P. A. Delsart⁵⁸, D. A. DeMarco¹⁶⁷, S. Demers¹⁸³, M. Demichev⁷⁹, G. Demontigny¹⁰⁹, S. P. Denisov¹²³, D. Denysiuk¹²⁰,

L. D'Eramo¹³⁶, D. Derendarz⁸⁴, J. E. Derkaoui^{35d}, F. Derue¹³⁶, P. Dervan⁹⁰, K. Desch²⁴, C. Deterre⁴⁶, K. Dette¹⁶⁷, C. Deutsch²⁴, M. R. Devesa³⁰, P. O. Deviveiros³⁶, A. Dewhurst¹⁴⁴, F. A. Di Bello⁵⁴, A. Di Ciaccio^{73a,73b}, L. Di Ciaccio⁵, W. K. Di Clemente¹³⁷, C. Di Donato^{69a,69b}, A. Di Girolamo³⁶, G. Di Gregorio^{71a,71b}, B. Di Micco^{74a,74b}, R. Di Nardo¹⁰², K. F. Di Petrillo⁵⁹, R. Di Sipio¹⁶⁷, D. Di Valentino³⁴, C. Diaconu¹⁰¹, F. A. Dias⁴⁰, T. Dias Do Vale^{140a}, M. A. Diaz^{147a}, J. Dickinson¹⁸, E. B. Diehl¹⁰⁵, J. Dietrich¹⁹, S. Díez Cornell⁴⁶, A. Dimitrievska¹⁸, W. Ding^{15b}, J. Dingfelder²⁴, F. Dittus³⁶, F. Djama¹⁰¹, T. Djobava^{159b}, J. I. Djuvsland¹⁷, M. A. B. Do Vale^{80c}, M. Dobre^{27b}, D. Dodsworth²⁶, C. Dogliani⁹⁶, J. Dolejsi¹⁴³, Z. Dolezal¹⁴³, M. Donadelli^{80d}, B. Dong^{60c}, J. Donini³⁸, A. D'Onofrio⁹², M. D'Onofrio⁹⁰, J. Dopke¹⁴⁴, A. Doria^{69a}, M. T. Dova⁸⁸, A. T. Doyle⁵⁷, E. Drechsler¹⁵², E. Dreyer¹⁵², T. Dreyer⁵³, A. S. Drobac¹⁷⁰, Y. Duan^{60b}, F. Dubinin¹¹⁰, M. Dubovsky^{28a}, A. Dubreuil⁵⁴, E. Duchovni¹⁸⁰, G. Duckeck¹¹⁴, A. Ducourthial¹³⁶, O. A. Ducu¹⁰⁹, D. Duda¹¹⁵, A. Dudarev³⁶, A. C. Dudder⁹⁹, E. M. Duffield¹⁸, L. Dufflot¹³², M. Dührssen³⁶, C. Dülsen¹⁸², M. Dumancic¹⁸⁰, A. E. Dumitriu^{27b}, A. K. Duncan⁵⁷, M. Dunford^{61a}, A. Duperrin¹⁰¹, H. Duran Yildiz^{4a}, M. Düren⁵⁶, A. Durglishvili^{159b}, D. Duschinger⁴⁸, B. Dutta⁴⁶, D. Duvnjak¹, G. I. Dyckes¹³⁷, M. Dyndal³⁶, S. Dysch¹⁰⁰, B. S. Dzedzic⁸⁴, K. M. Ecker¹¹⁵, R. C. Edgar¹⁰⁵, M. G. Eggleston⁴⁹, T. Eifert³⁶, G. Eigen¹⁷, K. Einsweiler¹⁸, T. Ekelof¹⁷², H. El Jarrari^{35e}, M. El Kacimi^{35c}, R. El Kosseifi¹⁰¹, V. Ellajosyula¹⁷², M. Ellert¹⁷², F. Ellinghaus¹⁸², A. A. Elliot⁹², N. Ellis³⁶, J. Elmsheuser²⁹, M. Elsing³⁶, D. Emeliyanov¹⁴⁴, A. Emerman³⁹, Y. Enari¹⁶³, M. B. Epland⁴⁹, J. Erdmann⁴⁷, A. Ereditato²⁰, M. Errenst³⁶, M. Escalier¹³², C. Escobar¹⁷⁴, O. Estrada Pastor¹⁷⁴, E. Etzion¹⁶¹, H. Evans⁶⁵, A. Ezhilov¹³⁸, F. Fabbri⁵⁷, L. Fabbri^{23a,23b}, V. Fabiani¹¹⁹, G. Facini⁹⁴, R. M. Faisca Rodrigues Pereira^{140a}, R. M. Fakhruddinov¹²³, S. Falciano^{72a}, P. J. Falke⁵, S. Falke⁵, J. Faltova¹⁴³, Y. Fang^{15a}, Y. Fang^{15a}, G. Fanourakis⁴⁴, M. Fanti^{68a,68b}, M. Faraj^{66a,66c,v}, A. Farbin⁸, A. Farilla^{74a}, E. M. Farina^{70a,70b}, T. Farooque¹⁰⁶, S. Farrell¹⁸, S. M. Farrington⁵⁰, P. Farthouat³⁶, F. Fassi^{35e}, P. Fassnacht³⁶, D. Fassouliotis⁹, M. Fauci Giannelli⁵⁰, W. J. Fawcett³², L. Fayard¹³², O. L. Fedin^{138,p}, W. Fedorko¹⁷⁵, M. Feickert⁴², L. Felgioni¹⁰¹, A. Fell¹⁴⁹, C. Feng^{60b}, E. J. Feng³⁶, M. Feng⁴⁹, M. J. Fenton⁵⁷, A. B. Fenyuk¹²³, J. Ferrando⁴⁶, A. Ferrante¹⁷³, A. Ferrari¹⁷², P. Ferrari¹²⁰, R. Ferrari^{70a}, D. E. Ferreira de Lima^{61b}, A. Ferrer¹⁷⁴, D. Ferrere⁵⁴, C. Ferretti¹⁰⁵, F. Fiedler⁹⁹, A. Filipčić⁹¹, F. Filthaut¹¹⁹, K. D. Finelli²⁵, M. C. N. Fiolhais^{140a,140c,a}, L. Fiorini¹⁷⁴, F. Fischer¹¹⁴, W. C. Fisher¹⁰⁶, I. Fleck¹⁵¹, P. Fleischmann¹⁰⁵, R. R. M. Fletcher¹³⁷, T. Flick¹⁸², B. M. Flierl¹¹⁴, L. Flores¹³⁷, L. R. Flores Castillo^{63a}, F. M. Follega^{75a,75b}, N. Fomin¹⁷, J. H. Foo¹⁶⁷, G. T. Forcolin^{75a,75b}, A. Formica¹⁴⁵, F. A. Förster¹⁴, A. C. Forti¹⁰⁰, A. G. Foster²¹, M. G. Foti¹³⁵, D. Fournier¹³², H. Fox⁸⁹, P. Francavilla^{71a,71b}, S. Francescato^{72a,72b}, M. Franchini^{23a,23b}, S. Franchino^{61a}, D. Francis³⁶, L. Franconi²⁰, M. Franklin⁵⁹, A. N. Fray⁹², P. M. Freeman²¹, B. Freund¹⁰⁹, W. S. Freund^{80b}, E. M. Freundlich⁴⁷, D. C. Frizzell¹²⁸, D. Froidevaux³⁶, J. A. Frost¹³⁵, C. Fukunaga¹⁶⁴, E. Fullana Torregrosa¹⁷⁴, E. Fumagalli^{55a,55b}, T. Fusayasu¹¹⁶, J. Fuster¹⁷⁴, A. Gabrielli^{23a,23b}, A. Gabrielli¹⁸, G. P. Gach^{83a}, S. Gadatsch⁵⁴, P. Gadow¹¹⁵, G. Gagliardi^{55a,55b}, L. G. Gagnon¹⁰⁹, C. Galea^{27b}, B. Galhardo^{140a}, G. E. Gallardo¹³⁵, E. J. Gallas¹³⁵, B. J. Gallop¹⁴⁴, G. Galster⁴⁰, R. Gamboa Goni⁹², K. K. Gan¹²⁶, S. Ganguly¹⁸⁰, J. Gao^{60a}, Y. Gao⁵⁰, Y. S. Gao^{31,m}, C. García¹⁷⁴, J. E. García Navarro¹⁷⁴, J. A. García Pascual^{15a}, C. Garcia-Argos⁵², M. Garcia-Sciveres¹⁸, R. W. Gardner³⁷, N. Garelli¹⁵³, S. Gargiulo⁵², V. Garonne¹³⁴, A. Gaudiello^{55a,55b}, G. Gaudio^{70a}, I. L. Gavrilenko¹¹⁰, A. Gavrilyuk¹¹¹, C. Gay¹⁷⁵, G. Gaycken⁴⁶, E. N. Gazis¹⁰, A. A. Geanta^{27b}, C. M. Gee¹⁴⁶, C. N. P. Gee¹⁴⁴, J. Geisen⁵³, M. Geisen⁹⁹, M. P. Geisler^{61a}, C. Gemme^{55b}, M. H. Genest⁵⁸, C. Geng¹⁰⁵, S. Gentile^{72a,72b}, S. George⁹³, T. Geralis⁴⁴, L. O. Gerlach⁵³, P. Gessinger-Befurt⁹⁹, G. Gessner⁴⁷, S. Ghasemi¹⁵¹, M. Ghasemi Bostanabad¹⁷⁶, A. Ghosh¹³², A. Ghosh⁷⁷, B. Giacobbe^{23b}, S. Giagu^{72a,72b}, N. Giangiacomi^{23a,23b}, P. Giannetti^{71a}, A. Giannini^{69a,69b}, G. Giannini¹⁴, S. M. Gibson⁹³, M. Gignac¹⁴⁶, D. Gillberg³⁴, G. Gilles¹⁸², D. M. Gingrich^{3,az}, M. P. Giordani^{66a,66c}, F. M. Giorgi^{23b}, P. F. Giraud¹⁴⁵, G. Giugliarelli^{66a,66c}, D. Giugni^{68a}, F. Giuli^{73a,73b}, S. Gkaitatzis¹⁶², I. Gkialas^{9,h}, E. L. Gkoukousis¹⁴, P. Gkoutoumis¹⁰, L. K. Gladilin¹¹³, C. Glasman⁹⁸, J. Glatzer¹⁴, P. C. F. Glaysheer⁴⁶, A. Glazov⁴⁶, G. R. Gledhill¹³¹, M. Goblirsch-Kolb²⁶, D. Godin¹⁰⁹, S. Goldfarb¹⁰⁴, T. Golling⁵⁴, D. Golubkov¹²³, A. Gomes^{140a,140b}, R. Goncalves Gama⁵³, R. Gonçalves^{140a,140b}, G. Gonella⁵², L. Gonella²¹, A. Gongadze⁷⁹, F. Gonnella²¹, J. L. Gonski⁵⁹, S. González de la Hoz¹⁷⁴, S. Gonzalez-Sevilla⁵⁴, G. R. Gonzalvo Rodriguez¹⁷⁴, L. Goossens³⁶, P. A. Gorbounov¹¹¹, H. A. Gordon²⁹, B. Gorini³⁶, E. Gorini^{67a,67b}, A. Gorišek⁹¹, A. T. Goshaw⁴⁹, M. I. Gostkin⁷⁹, C. A. Gottardo¹¹⁹, M. Gouighri^{35b}, D. Goujdami^{35c}, A. G. Goussiou¹⁴⁸, N. Govender^{33b}, C. Goy⁵, E. Gozani¹⁶⁰, I. Grabowska-Bold^{83a}, E. C. Graham⁹⁰, J. Gramling¹⁷¹, E. Gramstad¹³⁴, S. Grancagnolo¹⁹, M. Grandi¹⁵⁶, V. Gratchev¹³⁸, P. M. Gravila^{27f}, F. G. Gravili^{67a,67b}, C. Gray⁵⁷, H. M. Gray¹⁸, C. Grefe²⁴, K. Gregersen⁹⁶, I. M. Gregor⁴⁶, P. Grenier¹⁵³, K. Grevtsov⁴⁶, C. Grieco¹⁴, N. A. Grieser¹²⁸, J. Griffiths⁸, A. A. Grillo¹⁴⁶, K. Grimm^{31,l}, S. Grinstein^{14,aa}, J.-F. Grivaz¹³², S. Groh⁹⁹, E. Gross¹⁸⁰, J. Grosse-Knetter⁵³, Z. J. Grout⁹⁴, C. Grud¹⁰⁵, A. Grummer¹¹⁸, L. Guan¹⁰⁵, W. Guan¹⁸¹, J. Guenther³⁶, A. Guerguichon¹³², J. G. R. Guerrero Rojas¹⁷⁴, F. Guescini¹¹⁵, D. Guest¹⁷¹, R. Gugel⁵², T. Guillemain⁵, S. Guindon³⁶, U. Gul⁵⁷, J. Guo^{60c}, W. Guo¹⁰⁵, Y. Guo^{60a,t}, Z. Guo¹⁰¹, R. Gupta⁴⁶, S. Gurbuz^{12c}, G. Gustavino¹²⁸, M. Guth⁵², P. Gutierrez¹²⁸, C. Gutsche⁹⁴, C. Guyot¹⁴⁵, C. Gwenlan¹³⁵, C. B. Gwilliam⁹⁰, A. Haas¹²⁴, C. Haber¹⁸, H. K. Hadavand⁸, N. Haddad^{35e}, A. Hadeef^{60a}, S. Hageböck³⁶, M. Haleem¹⁷⁷, J. Haley¹²⁹, G. Halladjian¹⁰⁶, G. D. Hallewell¹⁰¹, K. Hamacher¹⁸², P. Hamal¹³⁰, K. Hamano¹⁷⁶, H. Hamdaoui^{35e}, G. N. Hamity¹⁴⁹,

K. Han^{60a,am}, L. Han^{60a}, S. Han^{15a,15d}, Y. F. Han¹⁶⁷, K. Hanagaki^{81,y}, M. Hance¹⁴⁶, D. M. Handl¹¹⁴, B. Haney¹³⁷, R. Hankache¹³⁶, E. Hansen⁹⁶, J. B. Hansen⁴⁰, J. D. Hansen⁴⁰, M. C. Hansen²⁴, P. H. Hansen⁴⁰, E. C. Hanson¹⁰⁰, K. Hara¹⁶⁹, T. Harenberg¹⁸², S. Harkusha¹⁰⁷, P. F. Harrison¹⁷⁸, N. M. Hartmann¹¹⁴, Y. Hasegawa¹⁵⁰, A. Hasib⁵⁰, S. Hassani¹⁴⁵, S. Haug²⁰, R. Hauser¹⁰⁶, L. B. Havener³⁹, M. Havranek¹⁴², C. M. Hawkes²¹, R. J. Hawkings³⁶, D. Hayden¹⁰⁶, C. Hayes¹⁵⁵, R. L. Hayes¹⁷⁵, C. P. Hays¹³⁵, J. M. Hays⁹², H. S. Hayward⁹⁰, S. J. Haywood¹⁴⁴, F. He^{60a}, M. P. Heath⁵⁰, V. Hedberg⁹⁶, L. Heelan⁸, S. Heer²⁴, K. K. Heidegger⁵², W. D. Heidorn⁷⁸, J. Heilman³⁴, S. Heim⁴⁶, T. Heim¹⁸, B. Heinemann^{46,au}, J. J. Heinrich¹³¹, L. Heinrich³⁶, C. Heinz⁵⁶, J. Hejbal¹⁴¹, L. Helary^{61b}, A. Held¹⁷⁵, S. Hellesund¹³⁴, C. M. Helling¹⁴⁶, S. Hellman^{45a,45b}, C. Helsen³⁶, R. C. W. Henderson⁸⁹, Y. Heng¹⁸¹, S. Henkelmann¹⁷⁵, A. M. Henriques Correia³⁶, G. H. Herbert¹⁹, H. Herde²⁶, V. Herget¹⁷⁷, Y. Hernández Jiménez^{33c}, H. Herr⁹⁹, M. G. Herrmann¹¹⁴, T. Herrmann⁴⁸, G. Herten⁵², R. Hertenberger¹¹⁴, L. Hervas³⁶, T. C. Herwig¹³⁷, G. G. Hesketh⁹⁴, N. P. Hessey^{168a}, A. Higashida¹⁶³, S. Higashino⁸¹, E. Higón-Rodríguez¹⁷⁴, K. Hildebrand³⁷, E. Hill¹⁷⁶, J. C. Hill³², K. K. Hill²⁹, K. H. Hiller⁴⁶, S. J. Hillier²¹, M. Hils⁴⁸, I. Hinchliffe¹⁸, F. Hinterkeuser²⁴, M. Hirose¹³³, S. Hirose⁵², D. Hirschbuehl¹⁸², B. Hiti⁹¹, O. Hladik¹⁴¹, D. R. Hlaluku^{33c}, X. Hoad⁵⁰, J. Hobbs¹⁵⁵, N. Hod¹⁸⁰, M. C. Hodgkinson¹⁴⁹, A. Hoecker³⁶, F. Hoenic¹¹⁴, D. Hohn⁵², D. Hohov¹³², T. R. Holmes³⁷, M. Holzbock¹¹⁴, L. B. A. H. Hommels³², S. Honda¹⁶⁹, T. M. Hong¹³⁹, A. Hönl¹¹⁵, B. H. Hooberman¹⁷³, W. H. Hopkins⁶, Y. Horii¹¹⁷, P. Horn⁴⁸, L. A. Horyn³⁷, S. Hou¹⁵⁸, A. Houmada^{35a}, J. Howarth¹⁰⁰, J. Hoya⁸⁸, M. Hrabovsky¹³⁰, J. Hrdinka⁷⁶, I. Hristova¹⁹, J. Hrivnac¹³², A. Hrynevich¹⁰⁸, T. Hryn'ova⁵, P. J. Hsu⁶⁴, S.-C. Hsu¹⁴⁸, Q. Hu²⁹, S. Hu^{60c}, D. P. Huang⁹⁴, Y. Huang^{60a}, Y. Huang^{15a}, Z. Hubacek¹⁴², F. Hubaut¹⁰¹, M. Huebner²⁴, F. Huegging²⁴, T. B. Huffman¹³⁵, M. Huhtinen³⁶, R. F. H. Hunter³⁴, P. Huo¹⁵⁵, A. M. Hupe³⁴, N. Huseynov^{79,ah}, J. Huston¹⁰⁶, J. Huth⁵⁹, R. Hyneman¹⁰⁵, S. Hyrych^{28a}, G. Iacobucci⁵⁴, G. Iakovidis²⁹, I. Ibragimov¹⁵¹, L. Iconomidou-Fayard¹³², Z. Idrissi^{35e}, P. Iengo³⁶, R. Ignazzi⁴⁰, O. Igonkina^{120,ac,*}, R. Iguchi¹⁶³, T. Iizawa⁵⁴, Y. Ikegami⁸¹, M. Ikeno⁸¹, D. Iliadis¹⁶², N. Ilic^{119,u}, F. Iltzsche⁴⁸, G. Introzzi^{70a,70b}, M. Iodice^{74a}, K. Iordanidou^{168a}, V. Ippolito^{72a,72b}, M. F. Isacson¹⁷², M. Ishino¹⁶³, W. Islam¹²⁹, C. Issever¹³⁵, S. Istin¹⁶⁰, F. Ito¹⁶⁹, J. M. Iturbe Ponce^{63a}, R. Iuppa^{75a,75b}, A. Ivina¹⁸⁰, H. Iwasaki⁸¹, J. M. Izen⁴³, V. Izzo^{69a}, P. Jacka¹⁴¹, P. Jackson¹, R. M. Jacobs²⁴, B. P. Jaeger¹⁵², V. Jain², G. Jäkel¹⁸², K. B. Jakobi⁹⁹, K. Jakobs⁵², S. Jakobsen⁷⁶, T. Jakoubek¹⁴¹, J. Jamieson⁵⁷, K. W. Janas^{83a}, R. Jansky⁵⁴, J. Janssen²⁴, M. Janus⁵³, P. A. Janus^{83a}, G. Jarlskog⁹⁶, N. Javadov^{79,ah}, T. Javůrek³⁶, M. Javurkova⁵², F. Jeanneau¹⁴⁵, L. Jeanty¹³¹, J. Jejelava^{159a,ai}, A. Jelinskas¹⁷⁸, P. Jenni^{52,b}, J. Jeong⁴⁶, N. Jeong⁴⁶, S. Jézéquel⁵, H. Ji¹⁸¹, J. Jia¹⁵⁵, H. Jiang⁷⁸, Y. Jiang^{60a}, Z. Jiang^{153,q}, S. Jiggins⁵², F. A. Jimenez Morales³⁸, J. Jimenez Pena¹¹⁵, S. Jin^{15c}, A. Jinaru^{27b}, O. Jinnouchi¹⁶⁵, H. Jivan^{33c}, P. Johansson¹⁴⁹, K. A. Johns⁷, C. A. Johnson⁶⁵, K. Jon-And^{45a,45b}, R. W. L. Jones⁸⁹, S. D. Jones¹⁵⁶, S. Jones⁷, T. J. Jones⁹⁰, J. Jongmanns^{61a}, P. M. Jorge^{140a}, J. Jovicevic³⁶, X. Ju¹⁸, J. J. Junggeburth¹¹⁵, A. Juste Rozas^{14,aa}, A. Kaczmarska⁸⁴, M. Kado^{72a,72b}, H. Kagan¹²⁶, M. Kagan¹⁵³, C. Kahra⁹⁹, T. Kaji¹⁷⁹, E. Kajomovitz¹⁶⁰, C. W. Kalderon⁹⁶, A. Kaluza⁹⁹, A. Kamenshchikov¹²³, M. Kaneda¹⁶³, L. Kanjir⁹¹, Y. Kano¹⁶³, V. A. Kantserov¹¹², J. Kanzaki⁸¹, L. S. Kaplan¹⁸¹, D. Kar^{33c}, K. Karava¹³⁵, M. J. Kareem^{168b}, S. N. Karpov⁷⁹, Z. M. Karpova⁷⁹, V. Kartvelishvili⁸⁹, A. N. Karyukhin¹²³, L. Kashif¹⁸¹, R. D. Kass¹²⁶, A. Kastanas^{45a,45b}, C. Kato^{60c,60d}, J. Katzy⁴⁶, K. Kawade¹⁵⁰, K. Kawagoe⁸⁷, T. Kawaguchi¹¹⁷, T. Kawamoto¹⁶³, G. Kawamura⁵³, E. F. Kay¹⁷⁶, V. F. Kazanin^{122a,122b}, R. Keeler¹⁷⁶, R. Kehoe⁴², J. S. Keller³⁴, E. Kellermann⁹⁶, D. Kelsey¹⁵⁶, J. J. Kempster²¹, J. Kendrick²¹, O. Kepka¹⁴¹, S. Kersten¹⁸², B. P. Kerševan⁹¹, S. Ketabchi Haghighat¹⁶⁷, M. Khader¹⁷³, F. Khalil-Zada¹³, M. Khandoga¹⁴⁵, A. Khanov¹²⁹, A. G. Kharlamov^{122a,122b}, T. Kharlamova^{122a,122b}, E. E. Khoda¹⁷⁵, A. Khodinov¹⁶⁶, T. J. Khoo⁵⁴, E. Khramov⁷⁹, J. Khubua^{159b}, S. Kido⁸², M. Kiehn⁵⁴, C. R. Kilby⁹³, Y. K. Kim³⁷, N. Kimura⁹⁴, O. M. Kind¹⁹, B. T. King^{90,*}, D. Kirchmeier⁴⁸, J. Kirk¹⁴⁴, A. E. Kiryunin¹¹⁵, T. Kishimoto¹⁶³, D. P. Kisiuk¹⁶⁷, V. Kitali⁴⁶, O. Kivernyk⁵, T. Klapdor-Kleingrothaus⁵², M. Klassen^{61a}, M. H. Klein¹⁰⁵, M. Klein⁹⁰, U. Klein⁹⁰, K. Kleinknecht⁹⁹, P. Klimek¹²¹, A. Klimentov²⁹, T. Klingl²⁴, T. Klioutchnikova³⁶, F. F. Klitzner¹¹⁴, P. Kluit¹²⁰, S. Kluth¹¹⁵, E. Kneringer⁷⁶, E. B. F. G. Knoops¹⁰¹, A. Knue⁵², D. Kobayashi⁸⁷, T. Kobayashi¹⁶³, M. Kobel⁴⁸, M. Kocian¹⁵³, P. Kodys¹⁴³, P. T. Koenig²⁴, T. Koffas³⁴, N. M. Köhler³⁶, T. Koi¹⁵³, M. Kolb^{61b}, I. Koletsou⁵, T. Komarek¹³⁰, T. Kondo⁸¹, N. Kondrashova^{60c}, K. Köneke⁵², A. C. König¹¹⁹, T. Kono¹²⁵, R. Konoplich^{124,ap}, V. Konstantinides⁹⁴, N. Konstantinidis⁹⁴, B. Konya⁹⁶, R. Kopeliansky⁶⁵, S. Koperny^{83a}, K. Korcyl⁸⁴, K. Kordas¹⁶², G. Koren¹⁶¹, A. Korn⁹⁴, I. Korolkov¹⁴, E. V. Korolkova¹⁴⁹, N. Korotkova¹¹³, O. Kortner¹¹⁵, S. Kortner¹¹⁵, T. Kosek¹⁴³, V. V. Kostyukhin¹⁶⁶, A. Kotwal⁴⁹, A. Koulouris¹⁰, A. Kourkoumeli-Charalampidi^{70a,70b}, C. Kourkoumelis⁹, E. Kourlitis¹⁴⁹, V. Kouskoura²⁹, A. B. Kowalewska⁸⁴, R. Kowalewski¹⁷⁶, C. Kozakai¹⁶³, W. Kozanecki¹⁴⁵, A. S. Kozhin¹²³, V. A. Kramarenko¹¹³, G. Kramberger⁹¹, D. Krasnopevtsev^{60a}, M. W. Krasny¹³⁶, A. Krasznahorkay³⁶, D. Krauss¹¹⁵, J. A. Kremer^{83a}, J. Kretzschmar⁹⁰, P. Krieger¹⁶⁷, F. Krieter¹¹⁴, A. Krishnan^{61b}, K. Krizka¹⁸, K. Kroeninger⁴⁷, H. Kroha¹¹⁵, J. Kroll¹⁴¹, J. Kroll¹³⁷, J. Krstic¹⁶, U. Kruchonak⁷⁹, H. Krüger²⁴, N. Krumnack⁷⁸, M. C. Kruse⁴⁹, J. A. Krzysiak⁸⁴, T. Kubota¹⁰⁴, O. Kuchinskaja¹⁶⁶, S. Kuday^{4b}, J. T. Kuechler⁴⁶, S. Kuehn³⁶, A. Kugel^{61a}, T. Kuhl⁴⁶, V. Kukhtin⁷⁹, R. Kukla¹⁰¹, Y. Kulchitsky^{107,al}, S. Kuleshov^{147b}, Y. P. Kulinich¹⁷³, M. Kuna⁵⁸, T. Kunigo⁸⁵, A. Kupco¹⁴¹, T. Kupfer⁴⁷, O. Kuprash⁵²

H. Kurashige⁸², L. L. Kurchaninov^{168a}, Y. A. Kurochkin¹⁰⁷, A. Kurova¹¹², M. G. Kurth^{15a,15d}, E. S. Kuwertz³⁶, M. Kuze¹⁶⁵, A. K. Kvam¹⁴⁸, J. Kvita¹³⁰, T. Kwan¹⁰³, A. La Rosa¹¹⁵, L. La Rotonda^{41a,41b}, F. La Ruffa^{41a,41b}, C. Lacasta¹⁷⁴, F. Lacava^{72a,72b}, D. P. J. Lack¹⁰⁰, H. Lacker¹⁹, D. Lacour¹³⁶, E. Ladygin⁷⁹, R. Lafaye⁵, B. Laforge¹³⁶, T. Lagouri^{33c}, S. Lai⁵³, S. Lammers⁶⁵, W. Lampl⁷, C. Lampoudis¹⁶², E. Lançon²⁹, U. Landgraf⁵², M. P. J. Landon⁹², M. C. Lanfermann⁵⁴, V. S. Lang⁴⁶, J. C. Lange⁵³, R. J. Langenberg³⁶, A. J. Lankford¹⁷¹, F. Lanni²⁹, K. Lantsch²⁴, A. Lanza^{70a}, A. Lapertosa^{55a,55b}, S. Laplace¹³⁶, J. F. Laporte¹⁴⁵, T. Lari^{68a}, F. Lasagni Manghi^{23a,23b}, M. Lassnig³⁶, T. S. Lau^{63a}, A. Laudrain¹³², A. Laurier³⁴, M. Lavorgna^{69a,69b}, S. D. Lawlor⁹³, M. Lazzaroni^{68a,68b}, B. Le¹⁰⁴, E. Le Guirriec¹⁰¹, M. LeBlanc⁷, T. LeCompte⁶, F. Ledroit-Guillon⁵⁸, A. C. A. Lee⁹⁴, C. A. Lee²⁹, G. R. Lee¹⁷, L. Lee⁵⁹, S. C. Lee¹⁵⁸, S. J. Lee³⁴, B. Lefebvre^{168a}, M. Lefebvre¹⁷⁶, F. Legger¹¹⁴, C. Leggett¹⁸, K. Lehmann¹⁵², N. Lehmann¹⁸², G. Lehmann Miotto³⁶, W. A. Leight⁴⁶, A. Leisos^{162,z}, M. A. L. Leite^{80d}, C. E. Leitgeb¹¹⁴, R. Leitner¹⁴³, D. Lellouch^{180,*}, K. J. C. Leney⁴², T. Lenz²⁴, B. Lenzi³⁶, R. Leone⁷, S. Leone^{71a}, C. Leonidopoulos⁵⁰, A. Leopold¹³⁶, G. Lerner¹⁵⁶, C. Leroy¹⁰⁹, R. Les¹⁶⁷, C. G. Lester³², M. Levchenko¹³⁸, J. Levêque⁵, D. Levin¹⁰⁵, L. J. Levinson¹⁸⁰, D. J. Lewis²¹, B. Li^{15b}, B. Li¹⁰⁵, C.-Q. Li^{60a}, F. Li^{60c}, H. Li^{60a}, H. Li^{60b}, J. Li^{60c}, K. Li¹⁵³, L. Li^{60c}, M. Li^{15a}, Q. Li^{15a,15d}, Q. Y. Li^{60a}, S. Li^{60c,60d}, X. Li⁴⁶, Y. Li⁴⁶, Z. Li^{60b}, Z. Liang^{15a}, B. Liberti^{73a}, A. Liblong¹⁶⁷, K. Lie^{63c}, C. Y. Lin³², K. Lin¹⁰⁶, T. H. Lin⁹⁹, R. A. Linck⁶⁵, J. H. Lindon²¹, A. L. Lioni⁵⁴, E. Lipeles¹³⁷, A. Lipniacka¹⁷, M. Lisovsky^{61b}, T. M. Liss^{173,aw}, A. Lister¹⁷⁵, A. M. Litke¹⁴⁶, J. D. Little⁸, B. Liu⁷⁸, B. L. Liu⁶, H. B. Liu²⁹, H. Liu¹⁰⁵, J. B. Liu^{60a}, J. K. K. Liu¹³⁵, K. Liu¹³⁶, M. Liu^{60a}, P. Liu¹⁸, Y. Liu^{15a,15d}, Y. L. Liu¹⁰⁵, Y. W. Liu^{60a}, M. Livan^{70a,70b}, A. Lleres⁵⁸, J. Llorente Merino¹⁵², S. L. Lloyd⁹², C. Y. Lo^{63b}, F. Lo Sterzo⁴², E. M. Lobodzinska⁴⁶, P. Loch⁷, S. Loffredo^{73a,73b}, T. Lohse¹⁹, K. Lohwasser¹⁴⁹, M. Lokajicek¹⁴¹, J. D. Long¹⁷³, R. E. Long⁸⁹, L. Longo³⁶, K. A. Looper¹²⁶, J. A. Lopez^{147b}, I. Lopez Paz¹⁰⁰, A. Lopez Solis¹⁴⁹, J. Lorenz¹¹⁴, N. Lorenzo Martinez⁵, M. Losada²², P. J. Lösel¹¹⁴, A. Lösle⁵², X. Lou⁴⁶, X. Lou^{15a}, A. Lounis¹³², J. Love⁶, P. A. Love⁸⁹, J. J. Lozano Bahilo¹⁷⁴, M. Lu^{60a}, Y. J. Lu⁶⁴, H. J. Lubatti¹⁴⁸, C. Luci^{72a,72b}, A. Lucotte⁵⁸, C. Luedtke⁵², F. Luehring⁶⁵, I. Luise¹³⁶, L. Luminari^{72a}, B. Lund-Jensen¹⁵⁴, M. S. Lutz¹⁰², D. Lynn²⁹, R. Lysak¹⁴¹, E. Lytken⁹⁶, F. Lyu^{15a}, V. Lyubushkin⁷⁹, T. Lyubushkina⁷⁹, H. Ma²⁹, L. L. Ma^{60b}, Y. Ma^{60b}, G. Maccarrone⁵¹, A. Macchiolo¹¹⁵, C. M. Macdonald¹⁴⁹, J. Machado Miguens¹³⁷, D. Madaffari¹⁷⁴, R. Madar³⁸, W. F. Mader⁴⁸, N. Madysa⁴⁸, J. Maeda⁸², S. Maeland¹⁷, T. Maeno²⁹, M. Maerker⁴⁸, A. S. Maevskiy¹¹³, V. Magerl⁵², N. Magini⁷⁸, D. J. Mahon³⁹, C. Maidantchik^{80b}, T. Maier¹¹⁴, A. Maio^{140a,140b,140d}, O. Majersky^{28a}, S. Majewski¹³¹, Y. Makida⁸¹, N. Makovec¹³², B. Malaescu¹³⁶, Pa. Malecki⁸⁴, V. P. Maleev¹³⁸, F. Malek⁵⁸, U. Mallik⁷⁷, D. Malon⁶, C. Malone³², S. Maltezos¹⁰, S. Malyukov⁷⁹, J. Mamuzic¹⁷⁴, G. Mancini⁵¹, I. Mandić⁹¹, L. Manhaes de Andrade Filho^{80a}, I. M. Maniatis¹⁶², J. Manjarres Ramos⁴⁸, K. H. Mankinen⁹⁶, A. Mann¹¹⁴, A. Manousos⁷⁶, B. Mansoulie¹⁴⁵, I. Mantos¹⁶², S. Manzoni¹²⁰, A. Marantis¹⁶², G. Marceca³⁰, L. Marchese¹³⁵, G. Marchiori¹³⁶, M. Marcisovsky¹⁴¹, C. Marcon⁹⁶, C. A. Marin Tobon³⁶, M. Marjanovic³⁸, Z. Marshall¹⁸, M. U. F. Martensson¹⁷², S. Marti-Garcia¹⁷⁴, C. B. Martin¹²⁶, T. A. Martin¹⁷⁸, V. J. Martin⁵⁰, B. Martin dit Latour¹⁷, L. Martinelli^{74a,74b}, M. Martinez^{14,aa}, V. I. Martinez Outschoorn¹⁰², S. Martin-Haugh¹⁴⁴, V. S. Martoiu^{27b}, A. C. Martyniuk⁹⁴, A. Marzin³⁶, S. R. Maschek¹¹⁵, L. Masetti⁹⁹, T. Mashimo¹⁶³, R. Mashinistov¹¹⁰, J. Masik¹⁰⁰, A. L. Maslennikov^{122a,122b}, L. Massa^{73a,73b}, P. Massarotti^{69a,69b}, P. Mastrandrea^{71a,71b}, A. Mastroberardino^{41a,41b}, T. Masubuchi¹⁶³, D. Matakias¹⁰, A. Matic¹¹⁴, P. Mättig²⁴, J. Maurer^{27b}, B. Maček⁹¹, D. A. Maximov^{122a,122b}, R. Mazini¹⁵⁸, I. Maznas¹⁶², S. M. Mazza¹⁴⁶, S. P. Mc Kee¹⁰⁵, T. G. McCarthy¹¹⁵, W. P. McCormack¹⁸, E. F. McDonald¹⁰⁴, J. A. McFayden³⁶, G. Mchedlidze^{159b}, M. A. McKay⁴², K. D. McLean¹⁷⁶, S. J. McMahan¹⁴⁴, P. C. McNamara¹⁰⁴, C. J. McNicol¹⁷⁸, R. A. McPherson^{176,af}, J. E. Mdhlluli^{33c}, Z. A. Meadows¹⁰², S. Meehan³⁶, T. Megy⁵², S. Mehlhase¹¹⁴, A. Mehta⁹⁰, T. Meideck⁵⁸, B. Meirose⁴³, D. Melini¹⁷⁴, B. R. Mellado Garcia^{33c}, J. D. Mellenthin⁵³, M. Melo^{28a}, F. Meloni⁴⁶, A. Melzer²⁴, S. B. Menary¹⁰⁰, E. D. Mendes Gouveia^{140a,140e}, L. Meng³⁶, X. T. Meng¹⁰⁵, S. Menke¹¹⁵, E. Meoni^{41a,41b}, S. Mergelmeyer¹⁹, S. A. M. Merkt¹³⁹, C. Merlassino²⁰, P. Mermod⁵⁴, L. Merola^{69a,69b}, C. Meroni^{68a}, O. Meshkov^{113,110}, J. K. R. Meshreki¹⁵¹, A. Messina^{72a,72b}, J. Metcalfe⁶, A. S. Mete¹⁷¹, C. Meyer⁶⁵, J. Meyer¹⁶⁰, J.-P. Meyer¹⁴⁵, H. Meyer Zu Theenhausen^{61a}, F. Miano¹⁵⁶, M. Michetti¹⁹, R. P. Middleton¹⁴⁴, L. Mijović⁵⁰, G. Mikenberg¹⁸⁰, M. Mikesikova¹⁴¹, M. Mikuž⁹¹, H. Mildner¹⁴⁹, M. Milesi¹⁰⁴, A. Milic¹⁶⁷, D. A. Millar⁹², D. W. Miller³⁷, A. Milov¹⁸⁰, D. A. Milstead^{45a,45b}, R. A. Mina^{153,q}, A. A. Minaenko¹²³, M. Miñano Moya¹⁷⁴, I. A. Minashvili^{159b}, A. I. Mincer¹²⁴, B. Mindur^{83a}, M. Mineev⁷⁹, Y. Minegishi¹⁶³, L. M. Mir¹⁴, A. Mirto^{67a,67b}, K. P. Mistry¹³⁷, T. Mitani¹⁷⁹, J. Mitrevski¹¹⁴, V. A. Mitsou¹⁷⁴, M. Mittal^{60c}, O. Miu¹⁶⁷, A. Miucci²⁰, P. S. Miyagawa¹⁴⁹, A. Mizukami⁸¹, J. U. Mjörnmark⁹⁶, T. Mkrtychyan¹⁸⁴, M. Mlynarikova¹⁴³, T. Moa^{45a,45b}, K. Mochizuki¹⁰⁹, P. Mogg⁵², S. Mohapatra³⁹, R. Moles-Valls²⁴, M. C. Mondragon¹⁰⁶, K. Mönig⁴⁶, J. Monk⁴⁰, E. Monnier¹⁰¹, A. Montalbano¹⁵², J. Montejo Berlingen³⁶, M. Montella⁹⁴, F. Monticelli⁸⁸, S. Monzani^{68a}, N. Morange¹³², D. Moreno²², M. Moreno Llácer³⁶, C. Moreno Martinez¹⁴, P. Morettini^{55b}, M. Morgenstern¹²⁰, S. Morgenstern⁴⁸, D. Mori¹⁵², M. Morii⁵⁹, M. Morinaga¹⁷⁹, V. Morisbak¹³⁴, A. K. Morley³⁶, G. Mornacchi³⁶, A. P. Morris⁹⁴, L. Morvaj¹⁵⁵, P. Moschovakos³⁶, B. Moser¹²⁰, M. Mosidze^{159b}, T. Moskalets¹⁴⁵, H. J. Moss¹⁴⁹, J. Moss^{31,n}, E. J. W. Moyses¹⁰², S. Muanza¹⁰¹, J. Mueller¹³⁹

R. S. P. Mueller¹¹⁴, D. Muenstermann⁸⁹, G. A. Mullier⁹⁶, J. L. Munoz Martinez¹⁴, F. J. Munoz Sanchez¹⁰⁰, P. Murin^{28b}, W. J. Murray^{144,178}, A. Murrone^{68a,68b}, M. Muškinja¹⁸, C. Mwewa^{33a}, A. G. Myagkov^{123,aq}, J. Myers¹³¹, M. Myska¹⁴², B. P. Nachman¹⁸, O. Nackenhorst⁴⁷, A. Nag Nag⁴⁸, K. Nagai¹³⁵, K. Nagano⁸¹, Y. Nagasaka⁶², M. Nagel⁵², J. L. Nagle²⁹, E. Nagy¹⁰¹, A. M. Nairz³⁶, Y. Nakahama¹¹⁷, K. Nakamura⁸¹, T. Nakamura¹⁶³, I. Nakano¹²⁷, H. Nanjo¹³³, F. Napolitano^{61a}, R. F. Naranjo Garcia⁴⁶, R. Narayan⁴², I. Naryshkin¹³⁸, T. Naumann⁴⁶, G. Navarro²², H. A. Neal^{105,*}, P. Y. Nechaeva¹¹⁰, F. Nechansky⁴⁶, T. J. Neep²¹, A. Negri^{70a,70b}, M. Negrini^{23b}, C. Nellist⁵³, M. E. Nelson¹³⁵, S. Nemecek¹⁴¹, P. Nemethy¹²⁴, M. Nessi^{36,d}, M. S. Neubauer¹⁷³, M. Neumann¹⁸², P. R. Newman²¹, Y. S. Ng¹⁹, Y. W. Y. Ng¹⁷¹, B. Ngair^{35c}, H. D. N. Nguyen¹⁰¹, T. Nguyen Manh¹⁰⁹, E. Nibigira³⁸, R. B. Nickerson¹³⁵, R. Nicolaidou¹⁴⁵, D. S. Nielsen⁴⁰, J. Nielsen¹⁴⁶, N. Nikiforou¹¹, V. Nikolaenko^{123,aq}, I. Nikolic-Audit¹³⁶, K. Nikolopoulos²¹, P. Nilsson²⁹, H. R. Nindhito⁵⁴, Y. Ninomiya⁸¹, A. Nisati^{72a}, N. Nishu^{60c}, R. Nisius¹¹⁵, I. Nitsche⁴⁷, T. Nitta¹⁷⁹, T. Nobe¹⁶³, Y. Noguchi⁸⁵, I. Nomidis¹³⁶, M. A. Nomura²⁹, M. Nordberg³⁶, N. Norjoharuddeen¹³⁵, T. Novak⁹¹, O. Novgorodova⁴⁸, R. Novotny¹⁴², L. Nozka¹³⁰, K. Ntekas¹⁷¹, E. Nurse⁹⁴, F. G. Oakham^{34,az}, H. Oberlack¹¹⁵, J. Ocariz¹³⁶, A. Ochi⁸², I. Ochoa³⁹, J. P. Ochoa-Ricoux^{147a}, K. O'Connor²⁶, S. Oda⁸⁷, S. Odaka⁸¹, S. Oerdek⁵³, A. Ogrodnik^{83a}, A. Oh¹⁰⁰, S. H. Oh⁴⁹, C. C. Ohm¹⁵⁴, H. Oide¹⁶⁵, M. L. Ojeda¹⁶⁷, H. Okawa¹⁶⁹, Y. Okazaki⁸⁵, Y. Okumura¹⁶³, T. Okuyama⁸¹, A. Olariu^{27b}, L. F. Oleiro Seabra^{140a}, S. A. Olivares Pino^{147a}, D. Oliveira Damazio²⁹, J. L. Oliver¹, M. J. R. Olsson¹⁷¹, A. Olszewski⁸⁴, J. Olszowska⁸⁴, D. C. O'Neil¹⁵², A. P. O'Neill¹³⁵, A. Onofre^{140a,140e}, P. U. E. Onyisi¹¹, H. Oppen¹³⁴, M. J. Oreglia³⁷, G. E. Orellana⁸⁸, D. Orestano^{74a,74b}, N. Orlando¹⁴, R. S. Ori¹⁶⁷, V. O'Shea⁵⁷, R. Ospanov^{60a}, G. Otero y Garzon³⁰, H. Otono⁸⁷, P. S. Ott^{61a}, M. Ouchrif^{35d}, J. Ouellette²⁹, F. Ould-Saada¹³⁴, A. Ouraou¹⁴⁵, Q. Ouyang^{15a}, M. Owen⁵⁷, R. E. Owen²¹, V. E. Ozcan^{12c}, N. Ozturk⁸, J. Pacalt¹³⁰, H. A. Pacey³², K. Pachal⁴⁹, A. Pacheco Pages¹⁴, C. Padilla Aranda¹⁴, S. Pagan Griso¹⁸, M. Paganini¹⁸³, G. Palacino⁶⁵, S. Palazzo⁵⁰, S. Palestini³⁶, M. Palka^{83b}, D. Pallin³⁸, I. Panagoulas¹⁰, C. E. Pandini³⁶, J. G. Panduro Vazquez⁹³, P. Pani⁴⁶, G. Panizzo^{66a,66c}, L. Paolozzi⁵⁴, C. Papadatos¹⁰⁹, K. Papageorgiou^{9,h}, S. Parajuli⁴³, A. Paramonov⁶, D. Paredes Hernandez^{63b}, S. R. Paredes Saenz¹³⁵, B. Parida¹⁶⁶, T. H. Park¹⁶⁷, A. J. Parker³¹, M. A. Parker³², F. Parodi^{55a,55b}, E. W. P. Parrish¹²¹, J. A. Parsons³⁹, U. Parzefall⁵², L. Pascual Dominguez¹³⁶, V. R. Pascuzzi¹⁶⁷, J. M. P. Pasner¹⁴⁶, E. Pasqualucci^{72a}, S. Passaggio^{55b}, F. Pastore⁹³, P. Pasuwan^{45a,45b}, S. Pataria⁹⁹, J. R. Pater¹⁰⁰, A. Pathak^{181,j}, T. Pauly³⁶, B. Pearson¹¹⁵, M. Pedersen¹³⁴, L. Pedraza Diaz¹¹⁹, R. Pedro^{140a}, T. Peiffer⁵³, S. V. Peleganchuk^{122a,122b}, O. Penc¹⁴¹, H. Peng^{60a}, B. S. Peralva^{80a}, M. M. Perego¹³², A. P. Pereira Peixoto^{140a}, D. V. Perepelitsa²⁹, F. Peri¹⁹, L. Perini^{68a,68b}, H. Pernegger³⁶, S. Perrella^{69a,69b}, K. Peters⁴⁶, R. F. Y. Peters¹⁰⁰, B. A. Petersen³⁶, T. C. Petersen⁴⁰, E. Petit¹⁰¹, A. Petridis¹, C. Petridou¹⁶², P. Petroff¹³², M. Petrov¹³⁵, F. Petrucci^{74a,74b}, M. Pettee¹⁸³, N. E. Pettersson¹⁰², K. Petukhova¹⁴³, A. Peyaud¹⁴⁵, R. Pezoa^{147b}, L. Pezzotti^{70a,70b}, T. Pham¹⁰⁴, F. H. Phillips¹⁰⁶, P. W. Phillips¹⁴⁴, M. W. Phipps¹⁷³, G. Piacquadio¹⁵⁵, E. Pianori¹⁸, A. Picazio¹⁰², R. H. Pickles¹⁰⁰, R. Piegai³⁰, D. Pietreanu^{27b}, J. E. Pilcher³⁷, A. D. Pilkington¹⁰⁰, M. Pinamonti^{73a,73b}, J. L. Pinfold³, M. Pitt¹⁶¹, L. Pizzimento^{73a,73b}, M.-A. Pleier²⁹, V. Pleskot¹⁴³, E. Plotnikova⁷⁹, P. Podberezko^{122a,122b}, R. Poettgen⁹⁶, R. Poggi⁵⁴, L. Poggioli¹³², I. Pogrebnyak¹⁰⁶, D. Pohl²⁴, I. Pokharel⁵³, G. Polesello^{70a}, A. Poley¹⁸, A. Policicchio^{72a,72b}, R. Polifka¹⁴³, A. Polini^{23b}, C. S. Pollard⁴⁶, V. Polychronakos²⁹, D. Ponomarenko¹¹², L. Pontecorvo³⁶, S. Popa^{27a}, G. A. Popeneciu^{27d}, L. Portales⁵, D. M. Portillo Quintero⁵⁸, S. Pospisil¹⁴², K. Potamianos⁴⁶, I. N. Potrap⁷⁹, C. J. Potter³², H. Potti¹¹, T. Poulsen⁹⁶, J. Poveda³⁶, T. D. Powell¹⁴⁹, G. Pownall⁴⁶, M. E. Pozo Astigarraga³⁶, P. Pralavorio¹⁰¹, S. Prell⁷⁸, D. Price¹⁰⁰, M. Primavera^{67a}, S. Prince¹⁰³, M. L. Proffitt¹⁴⁸, N. Proklova¹¹², K. Prokofiev^{63c}, F. Prokoshin⁷⁹, S. Protopopescu²⁹, J. Proudfoot⁶, M. Przybycien^{83a}, D. Pudzha¹³⁸, A. Puri¹⁷³, P. Puzo¹³², J. Qian¹⁰⁵, Y. Qin¹⁰⁰, A. Quadt⁵³, M. Queitsch-Maitland⁴⁶, A. Qureshi¹, M. Racko^{28a}, P. Rados¹⁰⁴, F. Ragusa^{68a,68b}, G. Rahal⁹⁷, J. A. Raine⁵⁴, S. Rajagopalan²⁹, A. Ramirez Morales⁹², K. Ran^{15a,15d}, T. Rashid¹³², S. Raspopov⁵, D. M. Rauch⁴⁶, F. Rauscher¹¹⁴, S. Rave⁹⁹, B. Ravina¹⁴⁹, I. Ravinovich¹⁸⁰, J. H. Rawling¹⁰⁰, M. Raymond³⁶, A. L. Read¹³⁴, N. P. Readioff⁵⁸, M. Reale^{67a,67b}, D. M. Rebuffi^{70a,70b}, A. Redelbach¹⁷⁷, G. Redlinger²⁹, K. Reeves⁴³, L. Rehnisch¹⁹, J. Reichert¹³⁷, D. Reikher¹⁶¹, A. Reiss⁹⁹, A. Rej¹⁵¹, C. Rembser³⁶, M. Renda^{27b}, M. Rescigno^{72a}, S. Resconi^{68a}, E. D. Resseguie¹³⁷, S. Rettie¹⁷⁵, E. Reynolds²¹, O. L. Rezanova^{122a,122b}, P. Reznicek¹⁴³, E. Ricci^{75a,75b}, R. Richter¹¹⁵, S. Richter⁴⁶, E. Richter-Was^{83b}, O. Ricken²⁴, M. Ridet¹³⁶, P. Rieck¹¹⁵, C. J. Riegel¹⁸², O. Rifki⁴⁶, M. Rijssenbeek¹⁵⁵, A. Rimoldi^{70a,70b}, M. Rimoldi⁴⁶, L. Rinaldi^{23b}, G. Ripellino¹⁵⁴, I. Riu¹⁴, J. C. Rivera Vergara¹⁷⁶, F. Rizatdinova¹²⁹, E. Rizvi⁹², C. Rizzi³⁶, R. T. Roberts¹⁰⁰, S. H. Robertson^{103,af}, M. Robin⁴⁶, D. Robinson³², J. E. M. Robinson⁴⁶, C. M. Robles Gajardo^{147b}, A. Robson⁵⁷, A. Rocchi^{73a,73b}, E. Rocco⁹⁹, C. Roda^{71a,71b}, S. Rodriguez Bosca¹⁷⁴, A. Rodriguez Perez¹⁴, D. Rodriguez Rodriguez¹⁷⁴, A. M. Rodriguez Vera^{168b}, S. Roe³⁶, O. Røhne¹³⁴, R. Röhrig¹¹⁵, C. P. A. Roland⁶⁵, J. Roloff⁵⁹, A. Romaniouk¹¹², M. Romano^{23a,23b}, N. Rompotis⁹⁰, M. Ronzani¹²⁴, L. Roos¹³⁶, S. Rosati^{72a}, K. Rosbach⁵², G. Rosin¹⁰², B. J. Rosser¹³⁷, E. Rossi⁴⁶, E. Rossi^{74a,74b}, E. Rossi^{69a,69b}, L. P. Rossi^{55b}, L. Rossini^{68a,68b}, R. Rosten¹⁴, M. Rotaru^{27b}, J. Rothberg¹⁴⁸, D. Rousseau¹³², G. Rovelli^{70a,70b}, A. Roy¹¹, D. Roy^{33c}, A. Rozanov¹⁰¹, Y. Rozen¹⁶⁰, X. Ruan^{33c}, F. Rubbo¹⁵³, F. Rühr⁵², A. Ruiz-Martinez¹⁷⁴, A. Rummeler³⁶, Z. Rurikova⁵², N. A. Rusakovich⁷⁹, H. L. Russell¹⁰³,

L. Rustige^{38,47}, J. P. Rutherford⁷, E. M. Rüttinger¹⁴⁹, M. Rybar³⁹, G. Rybkin¹³², E. B. Rye¹³⁴, A. Ryzhov¹²³, P. Sabatini⁵³, G. Sabato¹²⁰, S. Sacerdoti¹³², H. F.-W. Sadrozinski¹⁴⁶, R. Sadykov⁷⁹, F. Safai Tehrani^{72a}, B. Safarzadeh Samani¹⁵⁶, P. Saha¹²¹, S. Saha¹⁰³, M. Sahinsoy^{61a}, A. Sahu¹⁸², M. Saimpert⁴⁶, M. Saito¹⁶³, T. Saito¹⁶³, H. Sakamoto¹⁶³, A. Sakharov^{124,ap}, D. Salamani⁵⁴, G. Salamanna^{74a,74b}, J. E. Salazar Loyola^{147b}, P. H. Sales De Bruin¹⁷², A. Salnikov¹⁵³, J. Salt¹⁷⁴, D. Salvatore^{41a,41b}, F. Salvatore¹⁵⁶, A. Salvucci^{63a,63b,63c}, A. Salzburger³⁶, J. Samarati³⁶, D. Sammel⁵², D. Sampsonidis¹⁶², D. Sampsonidou¹⁶², J. Sánchez¹⁷⁴, A. Sanchez Pineda^{66a,66c}, H. Sandaker¹³⁴, C. O. Sander⁴⁶, I. G. Sanderswood⁸⁹, M. Sandhoff¹⁸², C. Sandoval²², D. P. C. Sankey¹⁴⁴, M. Sannino^{55a,55b}, Y. Sano¹¹⁷, A. Sansoni⁵¹, C. Santoni³⁸, H. Santos^{140a,140b}, S. N. Santpur¹⁸, A. Santra¹⁷⁴, A. Sapronov⁷⁹, J. G. Saraiva^{140a,140d}, O. Sasaki⁸¹, K. Sato¹⁶⁹, F. Sauerburger⁵², E. Sauvan⁵, P. Savard^{167,az}, N. Savic¹¹⁵, R. Sawada¹⁶³, C. Sawyer¹⁴⁴, L. Sawyer^{95,an}, C. Sbarra^{23b}, A. Sbrizzi^{23a}, T. Scanlon⁹⁴, J. Schaarschmidt¹⁴⁸, P. Schacht¹¹⁵, B. M. Schachtner¹¹⁴, D. Schaefer³⁷, L. Schaefer¹³⁷, J. Schaeffer⁹⁹, S. Schaepe³⁶, U. Schäfer⁹⁹, A. C. Schaffer¹³², D. Schaile¹¹⁴, R. D. Schamberger¹⁵⁵, N. Scharmberg¹⁰⁰, V. A. Schegelsky¹³⁸, D. Scheirich¹⁴³, F. Schenck¹⁹, M. Schernau¹⁷¹, C. Schiavi^{55a,55b}, S. Schier¹⁴⁶, L. K. Schildgen²⁴, Z. M. Schillaci²⁶, E. J. Schioppa³⁶, M. Schioppa^{41a,41b}, K. E. Schleicher⁵², S. Schlenker³⁶, K. R. Schmidt-Sommerfeld¹¹⁵, K. Schmieden³⁶, C. Schmitt⁹⁹, S. Schmitt⁴⁶, S. Schmitz⁹⁹, J. C. Schmoekel⁴⁶, U. Schnoor⁵², L. Schoeffel¹⁴⁵, A. Schoening^{61b}, P. G. Scholer⁵², E. Schopf¹³⁵, M. Schott⁹⁹, J. F. P. Schouwenberg¹¹⁹, J. Schovancova³⁶, S. Schramm⁵⁴, F. Schroeder¹⁸², A. Schulte⁹⁹, H.-C. Schultz-Coulon^{61a}, M. Schumacher⁵², B. A. Schumm¹⁴⁶, Ph. Schune¹⁴⁵, A. Schwartzman¹⁵³, T. A. Schwarz¹⁰⁵, Ph. Schwemling¹⁴⁵, R. Schwienhorst¹⁰⁶, A. Sciandra¹⁴⁶, G. Sciolla²⁶, M. Scodreggio⁴⁶, M. Scornajenghi^{41a,41b}, F. Scuri^{71a}, F. Scutti¹⁰⁴, L. M. Scyboz¹¹⁵, C. D. Sebastiani^{72a,72b}, P. Seema¹⁹, S. C. Seidel¹¹⁸, A. Seiden¹⁴⁶, B. D. Seidlitz²⁹, T. Seiss³⁷, J. M. Seixas^{80b}, G. Sekhniaidze^{69a}, K. Sekhon¹⁰⁵, S. J. Sekula⁴², N. Semprini-Cesari^{23a,23b}, S. Sen⁴⁹, S. Senkin³⁸, C. Serfon⁷⁶, L. Serin¹³², L. Serkin^{66a,66b}, M. Sessa^{60a}, H. Severini¹²⁸, T. Šfiligoj⁹¹, F. Sforza^{55a,55b}, A. Sfyrta⁵⁴, E. Shabalina⁵³, J. D. Shahinian¹⁴⁶, N. W. Shaikh^{45a,45b}, D. Shaked Renous¹⁸⁰, L. Y. Shan^{15a}, R. Shang¹⁷³, J. T. Shank²⁵, M. Shapiro¹⁸, A. Sharma¹³⁵, A. S. Sharma¹, P. B. Shatalov¹¹¹, K. Shaw¹⁵⁶, S. M. Shaw¹⁰⁰, A. Shcherbakova¹³⁸, M. Shehade¹⁸⁰, Y. Shen¹²⁸, N. Sherafati³⁴, A. D. Sherman²⁵, P. Sherwood⁹⁴, L. Shi^{158,av}, S. Shimizu⁸¹, C. O. Shimmin¹⁸³, Y. Shimogama¹⁷⁹, M. Shimojima¹¹⁶, I. P. J. Shipsey¹³⁵, S. Shirabe⁸⁷, M. Shiyakova^{79,ad}, J. Shlomi¹⁸⁰, A. Shmeleva¹¹⁰, M. J. Shochet³⁷, J. Shojaii¹⁰⁴, D. R. Shope¹²⁸, S. Shrestha¹²⁶, E. M. Shrif^{33c}, E. Shulga¹⁸⁰, P. Sicho¹⁴¹, A. M. Sickles¹⁷³, P. E. Sidebo¹⁵⁴, E. Sideras Haddad^{33c}, O. Sidiropoulou³⁶, A. Sidoti^{23a,23b}, F. Siegert⁴⁸, Dj. Sijacki¹⁶, M. Jr. Silva¹⁸¹, M. V. Silva Oliveira^{80a}, S. B. Silverstein^{45a}, S. Simion¹³², E. Simioni⁹⁹, R. Simoniello⁹⁹, S. Simsek^{12b}, P. Sinervo¹⁶⁷, V. Sinetckii^{113,110}, N. B. Sinev¹³¹, M. Sioli^{23a,23b}, I. Siral¹⁰⁵, S. Yu. Sivoklokov¹¹³, J. Sjölin^{45a,45b}, E. Skorda⁹⁶, P. Skubic¹²⁸, M. Slawinska⁸⁴, K. Sliwa¹⁷⁰, R. Slovak¹⁴³, V. Smakhtin¹⁸⁰, B. H. Smart¹⁴⁴, J. Smiesko^{28a}, N. Smirnov¹¹², S. Yu. Smirnov¹¹², Y. Smirnov¹¹², L. N. Smirnova^{113,w}, O. Smirnova⁹⁶, J. W. Smith⁵³, M. Smizanska⁸⁹, K. Smolek¹⁴², A. Smykiewicz⁸⁴, A. A. Snesarev¹¹⁰, H. L. Snoek¹²⁰, I. M. Snyder¹³¹, S. Snyder²⁹, R. Sobie^{176,af}, A. Soffer¹⁶¹, A. Sogaard⁵⁰, F. Sohns⁵³, C. A. Solans Sanchez³⁶, E. Yu. Soldatov¹¹², U. Soldevila¹⁷⁴, A. A. Solodkov¹²³, A. Soloshenko⁷⁹, O. V. Solovyanov¹²³, V. Solovyev¹³⁸, P. Sommer¹⁴⁹, H. Son¹⁷⁰, W. Song¹⁴⁴, W. Y. Song^{168b}, A. Sopczak¹⁴², F. Sopkova^{28b}, C. L. Sotiropoulou^{71a,71b}, S. Sottocornola^{70a,70b}, R. Soualah^{66a,66c,g}, A. M. Soukharev^{122a,122b}, D. South⁴⁶, S. Spagnolo^{67a,67b}, M. Spalla¹¹⁵, M. Spangenberg¹⁷⁸, F. Spanò⁹³, D. Sperlich⁵², T. M. Spieker^{61a}, R. Spighi^{23b}, G. Spigo³⁶, M. Spina¹⁵⁶, D. P. Spiteri⁵⁷, M. Spousta¹⁴³, A. Stabile^{68a,68b}, B. L. Stamas¹²¹, R. Stamen^{61a}, M. Stamenkovic¹²⁰, E. Stanecka⁸⁴, B. Stanislaus¹³⁵, M. M. Stanitzki⁴⁶, M. Stankaityte¹³⁵, B. Stapf¹²⁰, E. A. Starchenko¹²³, G. H. Stark¹⁴⁶, J. Stark⁵⁸, S. H. Stark⁴⁰, P. Staroba¹⁴¹, P. Starovoitov^{61a}, S. Stärz¹⁰³, R. Staszewski⁸⁴, G. Stavropoulos⁴⁴, M. Stegler⁴⁶, P. Steinberg²⁹, A. L. Steinhebel¹³¹, B. Stelzer¹⁵², H. J. Stelzer¹³⁹, O. Stelzer-Chilton^{168a}, H. Stenzel⁵⁶, T. J. Stevenson¹⁵⁶, G. A. Stewart³⁶, M. C. Stockton³⁶, G. Stoica^{27b}, M. Stolarski^{140a}, S. Stonjek¹¹⁵, A. Straessner⁴⁸, J. Strandberg¹⁵⁴, S. Strandberg^{45a,45b}, M. Strauss¹²⁸, P. Strizenc^{28b}, R. Ströhmer¹⁷⁷, D. M. Strom¹³¹, R. Stroynowski⁴², A. Strubig⁵⁰, S. A. Stucci²⁹, B. Stugu¹⁷, J. Stupak¹²⁸, N. A. Styles⁴⁶, D. Su¹⁵³, S. Suchek^{61a}, V. V. Sulin¹¹⁰, M. J. Sullivan⁹⁰, D. M. S. Sultan⁵⁴, S. Sultansoy^{4c}, T. Sumida⁸⁵, S. Sun¹⁰⁵, X. Sun³, K. Suruliz¹⁵⁶, C. J. E. Suster¹⁵⁷, M. R. Sutton¹⁵⁶, S. Suzuki⁸¹, M. Svatos¹⁴¹, M. Swiatlowski³⁷, S. P. Swift², T. Swirski¹⁷⁷, A. Sydorenko⁹⁹, I. Sykora^{28a}, M. Sykora¹⁴³, T. Sykora¹⁴³, D. Ta⁹⁹, K. Tackmann^{46,ab}, J. Taenzer¹⁶¹, A. Taffard¹⁷¹, R. Tahirout^{168a}, H. Takai²⁹, R. Takashima⁸⁶, K. Takeda⁸², T. Takeshita¹⁵⁰, E. P. Takeva⁵⁰, Y. Takubo⁸¹, M. Talby¹⁰¹, A. A. Talyshev^{122a,122b}, N. M. Tamir¹⁶¹, J. Tanaka¹⁶³, M. Tanaka¹⁶⁵, R. Tanaka¹³², S. Tapia Araya¹⁷³, S. Tapprogge⁹⁹, A. Tarek Abouelfadl Mohamed¹³⁶, S. Tarem¹⁶⁰, K. Tariq^{60b}, G. Tarna^{27b,c}, G. F. Tartarelli^{68a}, P. Tas¹⁴³, M. Tasevsky¹⁴¹, T. Tashiro⁸⁵, E. Tassi^{41a,41b}, A. Tavares Delgado^{140a,140b}, Y. Tayalati^{35e}, A. J. Taylor⁵⁰, G. N. Taylor¹⁰⁴, W. Taylor^{168b}, A. S. Tee⁸⁹, R. Teixeira De Lima¹⁵³, P. Teixeira-Dias⁹³, H. Ten Kate³⁶, J. J. Teoh¹²⁰, S. Terada⁸¹, K. Terashi¹⁶³, J. Terron⁹⁸, S. Terzo¹⁴, M. Testa⁵¹, R. J. Teuscher^{167,af}, S. J. Thais¹⁸³, T. Theveneaux-Pelzer⁴⁶, F. Thiele⁴⁰, D. W. Thomas⁹³, J. O. Thomas⁴², J. P. Thomas²¹, A. S. Thompson⁵⁷, P. D. Thompson²¹, L. A. Thomsen¹⁸³, E. Thomson¹³⁷, E. J. Thorpe⁹², Y. Tian³⁹, R. E. Ticse Torres⁵³, V. O. Tikhomirov^{110,ar}, Yu. A. Tikhonov^{122a,122b}, S. Timoshenko¹¹²,

P. Tipton¹⁸³, S. Tisserant¹⁰¹, K. Todome^{23a,23b}, S. Todorova-Nova⁵, S. Todt⁴⁸, J. Tojo⁸⁷, S. Tokár^{28a}, K. Tokushuku⁸¹, E. Tolley¹²⁶, K. G. Tomiwa^{33c}, M. Tomoto¹¹⁷, L. Tompkins^{153,q}, B. Tong⁵⁹, P. Tornambe¹⁰², E. Torrence¹³¹, H. Torres⁴⁸, E. Torró Pastor¹⁴⁸, C. Tosci¹³⁵, J. Toth^{101,ac}, D. R. Tovey¹⁴⁹, A. Traeet¹⁷, C. J. Treado¹²⁴, T. Trefzger¹⁷⁷, F. Tresoldi¹⁵⁶, A. Tricoli²⁹, I. M. Trigger^{168a}, S. Trincaz-Duvoid¹³⁶, W. Trischuk¹⁶⁷, B. Trocmé⁵⁸, A. Trofymov¹⁴⁵, C. Troncon^{68a}, M. Trovatelli¹⁷⁶, F. Trovato¹⁵⁶, L. Truong^{33b}, M. Trzebinski⁸⁴, A. Trzupek⁸⁴, F. Tsai⁴⁶, J. C.-L. Tseng¹³⁵, P. V. Tsiarshka^{107,al}, A. Tsigotidis¹⁶², N. Tsirintanis⁹, V. Tsiskaridze¹⁵⁵, E. G. Tskhadadze^{159a}, M. Tsopoulou¹⁶², I. I. Tsukerman¹¹¹, V. Tsulaia¹⁸, S. Tsuno⁸¹, D. Tsybychev¹⁵⁵, Y. Tu^{63b}, A. Tudorache^{27b}, V. Tudorache^{27b}, T. T. Tulbure^{27a}, A. N. Tuna⁵⁹, S. Turchikhin⁷⁹, D. Turgeman¹⁸⁰, I. Turk Cakir^{4b,x}, R. J. Turner²¹, R. T. Turra^{68a}, P. M. Tuts³⁹, S. Tzamarias¹⁶², E. Tzovara⁹⁹, G. Uccielli⁴⁷, K. Uchida¹⁶³, I. Ueda⁸¹, M. Ughetto^{45a,45b}, F. Ukegawa¹⁶⁹, G. Unal³⁶, A. Undrus²⁹, G. Unel¹⁷¹, F. C. Ungaro¹⁰⁴, Y. Unno⁸¹, K. Uno¹⁶³, J. Urban^{28b}, P. Urquijo¹⁰⁴, G. Usai⁸, Z. Uysal^{12d}, L. Vacavant¹⁰¹, V. Vacek¹⁴², B. Vachon¹⁰³, K. O. H. Vadla¹³⁴, A. Vaidya⁹⁴, C. Valderanis¹¹⁴, E. Valdes Santurio^{45a,45b}, M. Valente⁵⁴, S. Valentini^{23a,23b}, A. Valero¹⁷⁴, L. Valéry⁴⁶, R. A. Vallance²¹, A. Vallier³⁶, J. A. Valls Ferrer¹⁷⁴, T. R. Van Daalen¹⁴, P. Van Gemmeren⁶, I. Van Vulpen¹²⁰, M. Vanadia^{73a,73b}, W. Vandelli³⁶, A. Vaniachine¹⁶⁶, D. Vannicola^{72a,72b}, R. Vari^{72a}, E. W. Varnes⁷, C. Varni^{55a,55b}, T. Varol¹⁵⁸, D. Varouchas¹³², K. E. Varvell¹⁵⁷, M. E. Vasile^{27b}, G. A. Vasquez¹⁷⁶, J. G. Vasquez¹⁸³, F. Vazeille³⁸, D. Vazquez Furelos¹⁴, T. Vazquez Schroeder³⁶, J. Veatch⁵³, V. Vecchio^{74a,74b}, M. J. Veen¹²⁰, L. M. Veloce¹⁶⁷, F. Veloso^{140a,140c}, S. Veneziano^{72a}, A. Ventura^{67a,67b}, N. Venturi³⁶, A. Verbytskyi¹¹⁵, V. Vercesi^{70a}, M. Verducci^{71a,71b}, C. M. Vergel Infante⁷⁸, C. Vergis²⁴, W. Verkerke¹²⁰, A. T. Vermeulen¹²⁰, J. C. Vermeulen¹²⁰, M. C. Vetterli^{152,az}, N. Viaux Maira^{147b}, M. Vicente Barreto Pinto⁵⁴, T. Vickey¹⁴⁹, O. E. Vickey Boeriu¹⁴⁹, G. H. A. Viehhauser¹³⁵, L. Vigani^{61b}, M. Villa^{23a,23b}, M. Villaplana Perez^{68a,68b}, E. Vilucchi⁵¹, M. G. Vincker³⁴, G. S. Virdee²¹, A. Vishwakarma⁴⁶, C. Vittori^{23a,23b}, I. Vivarelli¹⁵⁶, M. Vogel¹⁸², P. Vokac¹⁴², S. E. von Buddenbrock^{33c}, E. Von Toerne²⁴, V. Vorobel¹⁴³, K. Vorobev¹¹², M. Vos¹⁷⁴, J. H. Vossebeld⁹⁰, M. Vozak¹⁰⁰, N. Vranjes¹⁶, M. Vranjes Milosavljevic¹⁶, V. Vrba¹⁴², M. Vreeswijk¹²⁰, R. Vuillermet³⁶, I. Vukotic³⁷, P. Wagner²⁴, W. Wagner¹⁸², J. Wagner-Kuhr¹¹⁴, S. Wahdan¹⁸², H. Wahlberg⁸⁸, V. M. Walbrecht¹¹⁵, J. Walder⁸⁹, R. Walker¹¹⁴, S. D. Walker⁹³, W. Walkowiak¹⁵¹, V. Wallangen^{45a,45b}, A. M. Wang⁵⁹, C. Wang^{60c}, C. Wang^{60b}, F. Wang¹⁸¹, H. Wang¹⁸, H. Wang³, J. Wang¹⁵⁷, J. Wang^{61b}, P. Wang⁴², Q. Wang¹²⁸, R.-J. Wang⁹⁹, R. Wang^{60a}, R. Wang⁶, S. M. Wang¹⁵⁸, W. T. Wang^{60a}, W. Wang^{15c,ag}, W. X. Wang^{60a,ag}, Y. Wang^{60a,ao}, Z. Wang^{60c}, C. Wanotayaroj⁴⁶, A. Warburton¹⁰³, C. P. Ward³², D. R. Wardrope⁹⁴, N. Warrack⁵⁷, A. Washbrook⁵⁰, A. T. Watson²¹, M. F. Watson²¹, G. Watts¹⁴⁸, B. M. Waugh⁹⁴, A. F. Webb¹¹, S. Webb⁹⁹, C. Weber¹⁸³, M. S. Weber²⁰, S. A. Weber³⁴, S. M. Weber^{61a}, A. R. Weidberg¹³⁵, J. Weingarten⁴⁷, M. Weirich⁹⁹, C. Weiser⁵², P. S. Wells³⁶, T. Wenaus²⁹, T. Wengler³⁶, S. Wenig³⁶, N. Wermes²⁴, M. D. Werner⁷⁸, M. Wessels^{61a}, T. D. Weston²⁰, K. Whalen¹³¹, N. L. Whallon¹⁴⁸, A. M. Wharton⁸⁹, A. S. White¹⁰⁵, A. White⁸, M. J. White¹, D. Whiteson¹⁷¹, B. W. Whitmore⁸⁹, W. Wiedenmann¹⁸¹, M. Wielers¹⁴⁴, N. Wieseotte⁹⁹, C. Wiglesworth⁴⁰, L. A. M. Wiik-Fuchs⁵², F. Wilk¹⁰⁰, H. G. Wilkens³⁶, L. J. Wilkins⁹³, H. H. Williams¹³⁷, S. Williams³², C. Willis¹⁰⁶, S. Willocq¹⁰², J. A. Wilson²¹, I. Wingerter-Seez⁵, E. Winkels¹⁵⁶, F. Winklmeier¹³¹, O. J. Winston¹⁵⁶, B. T. Winter⁵², M. Wittgen¹⁵³, M. Wobisch⁹⁵, A. Wolf⁹⁹, T. M. H. Wolf¹²⁰, R. Wolff¹⁰¹, R. W. Wölker¹³⁵, J. Wollrath⁵², M. W. Wolter⁸⁴, H. Wolters^{140a,140c}, V. W. S. Wong¹⁷⁵, N. L. Woods¹⁴⁶, S. D. Worm²¹, B. K. Wosiek⁸⁴, K. W. Woźniak⁸⁴, K. Wraight⁵⁷, S. L. Wu¹⁸¹, X. Wu⁵⁴, Y. Wu^{60a}, T. R. Wyatt¹⁰⁰, B. M. Wynne⁵⁰, S. Xella⁴⁰, Z. Xi¹⁰⁵, L. Xia¹⁷⁸, X. Xiao¹⁰⁵, I. Xiolidis¹⁵⁶, D. Xu^{15a}, H. Xu^{60a,c}, L. Xu²⁹, T. Xu¹⁴⁵, W. Xu¹⁰⁵, Z. Xu^{60b}, Z. Xu¹⁵³, B. Yabsley¹⁵⁷, S. Yacoub^{33a}, K. Yajima¹³³, D. P. Yallup⁹⁴, D. Yamaguchi¹⁶⁵, Y. Yamaguchi¹⁶⁵, A. Yamamoto⁸¹, M. Yamatani¹⁶³, T. Yamazaki¹⁶³, Y. Yamazaki⁸², Z. Yan²⁵, H. J. Yang^{60c,60d}, H. T. Yang¹⁸, S. Yang⁷⁷, X. Yang^{58,60b}, Y. Yang¹⁶³, W.-M. Yao¹⁸, Y. C. Yap⁴⁶, Y. Yasu⁸¹, E. Yatsenko^{60c,60d}, J. Ye⁴², S. Ye²⁹, I. Yeletsikh⁷⁹, M. R. Yexley⁸⁹, E. Yigitbasi²⁵, K. Yorita¹⁷⁹, K. Yoshihara¹³⁷, C. J. S. Young³⁶, C. Young¹⁵³, J. Yu⁷⁸, R. Yuan^{60b,i}, X. Yue^{61a}, S. P. Y. Yuen²⁴, M. Zaazoua^{35e}, B. Zabinski⁸⁴, G. Zacharis¹⁰, E. Zaffaroni⁵⁴, J. Zahreddine¹³⁶, A. M. Zaitsev^{123,aq}, T. Zakareishvili^{159b}, N. Zakharchuk³⁴, S. Zambito⁵⁹, D. Zanzi³⁶, D. R. Zaripovas⁵⁷, S. V. Zeißner⁴⁷, C. Zeitnitz¹⁸², G. Zemaityte¹³⁵, J. C. Zeng¹⁷³, O. Zenin¹²³, T. Ženiš^{28a}, D. Zerwas¹³², M. Zgubić¹³⁵, D. F. Zhang^{15b}, G. Zhang^{15b}, H. Zhang^{15c}, J. Zhang⁶, L. Zhang^{15c}, L. Zhang^{60a}, M. Zhang¹⁷³, R. Zhang²⁴, X. Zhang^{60b}, Y. Zhang^{15a,15d}, Z. Zhang^{63a}, Z. Zhang¹³², P. Zhao⁴⁹, Y. Zhao^{60b}, Z. Zhao^{60a}, A. Zhemchugov⁷⁹, Z. Zheng¹⁰⁵, D. Zhong¹⁷³, B. Zhou¹⁰⁵, C. Zhou¹⁸¹, M. S. Zhou^{15a,15d}, M. Zhou¹⁵⁵, N. Zhou^{60c}, Y. Zhou⁷, C. G. Zhu^{60b}, H. L. Zhu^{60a}, H. Zhu^{15a}, J. Zhu¹⁰⁵, Y. Zhu^{60a}, X. Zhuang^{15a}, K. Zhukov¹¹⁰, V. Zhulanov^{122a,122b}, D. Zieminska⁶⁵, N. I. Zimine⁷⁹, S. Zimmermann⁵², Z. Zinonos¹¹⁵, M. Ziolkowski¹⁵¹, L. Živković¹⁶, G. Zobernig¹⁸¹, A. Zoccoli^{23a,23b}, K. Zoch⁵³, T. G. Zorbas¹⁴⁹, R. Zou³⁷, L. Zwalinski³⁶

¹ Department of Physics, University of Adelaide, Adelaide, Australia

² Physics Department, SUNY Albany, Albany, NY, USA

³ Department of Physics, University of Alberta, Edmonton, AB, Canada

- ⁴ (a)Department of Physics, Ankara University, Ankara, Turkey; (b)Istanbul Aydin University, Istanbul, Turkey; (c)Division of Physics, TOBB University of Economics and Technology, Ankara, Turkey
- ⁵ LAPP, Université Grenoble Alpes, Université Savoie Mont Blanc, CNRS/IN2P3, Annecy, France
- ⁶ High Energy Physics Division, Argonne National Laboratory, Argonne, IL, USA
- ⁷ Department of Physics, University of Arizona, Tucson, AZ, USA
- ⁸ Department of Physics, University of Texas at Arlington, Arlington, TX, USA
- ⁹ Physics Department, National and Kapodistrian University of Athens, Athens, Greece
- ¹⁰ Physics Department, National Technical University of Athens, Zografou, Greece
- ¹¹ Department of Physics, University of Texas at Austin, Austin, TX, USA
- ¹² (a)Faculty of Engineering and Natural Sciences, Bahcesehir University, Istanbul, Turkey; (b)Faculty of Engineering and Natural Sciences, Istanbul Bilgi University, Istanbul, Turkey; (c)Department of Physics, Bogazici University, Istanbul, Turkey; (d)Department of Physics Engineering, Gaziantep University, Gaziantep, Turkey
- ¹³ Institute of Physics, Azerbaijan Academy of Sciences, Baku, Azerbaijan
- ¹⁴ Institut de Física d'Altes Energies (IFAE), Barcelona Institute of Science and Technology, Barcelona, Spain
- ¹⁵ (a)Institute of High Energy Physics, Chinese Academy of Sciences, Beijing, China; (b)Physics Department, Tsinghua University, Beijing, China; (c)Department of Physics, Nanjing University, Nanjing, China; (d)University of Chinese Academy of Science (UCAS), Beijing, China
- ¹⁶ Institute of Physics, University of Belgrade, Belgrade, Serbia
- ¹⁷ Department for Physics and Technology, University of Bergen, Bergen, Norway
- ¹⁸ Physics Division, Lawrence Berkeley National Laboratory and University of California, Berkeley, CA, USA
- ¹⁹ Institut für Physik, Humboldt Universität zu Berlin, Berlin, Germany
- ²⁰ Albert Einstein Center for Fundamental Physics and Laboratory for High Energy Physics, University of Bern, Bern, Switzerland
- ²¹ School of Physics and Astronomy, University of Birmingham, Birmingham, UK
- ²² Facultad de Ciencias y Centro de Investigaciones, Universidad Antonio Nariño, Bogota, Colombia
- ²³ (a)Dipartimento di Fisica, INFN Bologna and Università di Bologna, Bologna, Italy; (b)INFN Sezione di Bologna, Bologna, Italy
- ²⁴ Physikalisches Institut, Universität Bonn, Bonn, Germany
- ²⁵ Department of Physics, Boston University, Boston, MA, USA
- ²⁶ Department of Physics, Brandeis University, Waltham, MA, USA
- ²⁷ (a)Transilvania University of Brasov, Brasov, Romania; (b)Horia Hulubei National Institute of Physics and Nuclear Engineering, Bucharest, Romania; (c)Department of Physics, Alexandru Ioan Cuza University of Iasi, Iasi, Romania; (d)Physics Department, National Institute for Research and Development of Isotopic and Molecular Technologies, Cluj-Napoca, Romania; (e)University Politehnica Bucharest, Bucharest, Romania; (f)West University in Timisoara, Timisoara, Romania
- ²⁸ (a)Faculty of Mathematics, Physics and Informatics, Comenius University, Bratislava, Slovakia; (b)Department of Subnuclear Physics, Institute of Experimental Physics of the Slovak Academy of Sciences, Kosice, Slovak Republic
- ²⁹ Physics Department, Brookhaven National Laboratory, Upton, NY, USA
- ³⁰ Departamento de Física, Universidad de Buenos Aires, Buenos Aires, Argentina
- ³¹ California State University, Long Beach, CA, USA
- ³² Cavendish Laboratory, University of Cambridge, Cambridge, UK
- ³³ (a)Department of Physics, University of Cape Town, Cape Town, South Africa; (b)Department of Mechanical Engineering Science, University of Johannesburg, Johannesburg, South Africa; (c)School of Physics, University of the Witwatersrand, Johannesburg, South Africa
- ³⁴ Department of Physics, Carleton University, Ottawa, ON, Canada
- ³⁵ (a)Faculté des Sciences Ain Chock, Réseau Universitaire de Physique des Hautes Energies-Université Hassan II, Casablanca, Morocco; (b)Faculté des Sciences, Université Ibn-Tofail, Kénitra, Morocco; (c)Faculté des Sciences Semlalia, Université Cadi Ayyad, LPHEA-Marrakech, Marrakech, Morocco; (d)Faculté des Sciences, Université Mohamed Premier and LTPM, Oujda, Morocco; (e)Faculté des sciences, Université Mohammed V, Rabat, Morocco
- ³⁶ CERN, Geneva, Switzerland
- ³⁷ Enrico Fermi Institute, University of Chicago, Chicago, IL, USA
- ³⁸ LPC, Université Clermont Auvergne, CNRS/IN2P3, Clermont-Ferrand, France
- ³⁹ Nevis Laboratory, Columbia University, Irvington, NY, USA

- 40 Niels Bohr Institute, University of Copenhagen, Copenhagen, Denmark
- 41 (a)Dipartimento di Fisica, Università della Calabria, Rende, Italy; (b)INFN Gruppo Collegato di Cosenza, Laboratori Nazionali di Frascati, Frascati, Italy
- 42 Physics Department, Southern Methodist University, Dallas, TX, USA
- 43 Physics Department, University of Texas at Dallas, Richardson, TX, USA
- 44 National Centre for Scientific Research “Demokritos”, Agia Paraskevi, Greece
- 45 (a)Department of Physics, Stockholm University, Stockholm, Sweden; (b)Oskar Klein Centre, Stockholm, Sweden
- 46 Deutsches Elektronen-Synchrotron DESY, Hamburg and Zeuthen, Germany
- 47 Lehrstuhl für Experimentelle Physik IV, Technische Universität Dortmund, Dortmund, Germany
- 48 Institut für Kern- und Teilchenphysik, Technische Universität Dresden, Dresden, Germany
- 49 Department of Physics, Duke University, Durham, NC, USA
- 50 SUPA-School of Physics and Astronomy, University of Edinburgh, Edinburgh, UK
- 51 INFN e Laboratori Nazionali di Frascati, Frascati, Italy
- 52 Physikalisches Institut, Albert-Ludwigs-Universität Freiburg, Freiburg, Germany
- 53 II. Physikalisches Institut, Georg-August-Universität Göttingen, Göttingen, Germany
- 54 Département de Physique Nucléaire et Corpusculaire, Université de Genève, Geneva, Switzerland
- 55 (a)Dipartimento di Fisica, Università di Genova, Genoa, Italy; (b)INFN Sezione di Genova, Genoa, Italy
- 56 II. Physikalisches Institut, Justus-Liebig-Universität Giessen, Giessen, Germany
- 57 SUPA-School of Physics and Astronomy, University of Glasgow, Glasgow, UK
- 58 LPSC, Université Grenoble Alpes, CNRS/IN2P3, Grenoble INP, Grenoble, France
- 59 Laboratory for Particle Physics and Cosmology, Harvard University, Cambridge, MA, USA
- 60 (a)Department of Modern Physics and State Key Laboratory of Particle Detection and Electronics, University of Science and Technology of China, Hefei, China; (b)Institute of Frontier and Interdisciplinary Science and Key Laboratory of Particle Physics and Particle Irradiation (MOE), Shandong University, Qingdao, China; (c)School of Physics and Astronomy, Shanghai Jiao Tong University, KLPPAC-MoE, SKLPPC, Shanghai, China; (d)Tsung-Dao Lee Institute, Shanghai, China
- 61 (a)Kirchhoff-Institut für Physik, Ruprecht-Karls-Universität Heidelberg, Heidelberg, Germany; (b)Physikalisches Institut, Ruprecht-Karls-Universität Heidelberg, Heidelberg, Germany
- 62 Faculty of Applied Information Science, Hiroshima Institute of Technology, Hiroshima, Japan
- 63 (a)Department of Physics, Chinese University of Hong Kong, Shatin, N.T., Hong Kong; (b)Department of Physics, University of Hong Kong, Pok Fu Lam, Hong Kong; (c)Department of Physics and Institute for Advanced Study, Hong Kong University of Science and Technology, Clear Water Bay, Kowloon, Hong Kong, China
- 64 Department of Physics, National Tsing Hua University, Hsinchu, Taiwan
- 65 Department of Physics, Indiana University, Bloomington, IN, USA
- 66 (a)INFN Gruppo Collegato di Udine, Sezione di Trieste, Udine, Italy; (b)ICTP, Trieste, Italy; (c)Dipartimento Politecnico di Ingegneria e Architettura, Università di Udine, Udine, Italy
- 67 (a)INFN Sezione di Lecce, Lecce, Italy; (b)Dipartimento di Matematica e Fisica, Università del Salento, Lecce, Italy
- 68 (a)INFN Sezione di Milano, Milan, Italy; (b)Dipartimento di Fisica, Università di Milano, Milan, Italy
- 69 (a)INFN Sezione di Napoli, Naples, Italy; (b)Dipartimento di Fisica, Università di Napoli, Naples, Italy
- 70 (a)INFN Sezione di Pavia, Pavia, Italy; (b)Dipartimento di Fisica, Università di Pavia, Pavia, Italy
- 71 (a)INFN Sezione di Pisa, Pisa, Italy; (b)Dipartimento di Fisica E. Fermi, Università di Pisa, Pisa, Italy
- 72 (a)INFN Sezione di Roma, Rome, Italy; (b)Dipartimento di Fisica, Sapienza Università di Roma, Rome, Italy
- 73 (a)INFN Sezione di Roma Tor Vergata, Rome, Italy; (b)Dipartimento di Fisica, Università di Roma Tor Vergata, Rome, Italy
- 74 (a)INFN Sezione di Roma Tre, Rome, Italy; (b)Dipartimento di Matematica e Fisica, Università Roma Tre, Rome, Italy
- 75 (a)INFN-TIFPA, Povo, Italy; (b)Università degli Studi di Trento, Trento, Italy
- 76 Institut für Astro- und Teilchenphysik, Leopold-Franzens-Universität, Innsbruck, Austria
- 77 University of Iowa, Iowa City, IA, USA
- 78 Department of Physics and Astronomy, Iowa State University, Ames, IA, USA
- 79 Joint Institute for Nuclear Research, Dubna, Russia
- 80 (a)Departamento de Engenharia Elétrica, Universidade Federal de Juiz de Fora (UFJF), Juiz de Fora, Brazil; (b)Universidade Federal do Rio de Janeiro COPPE/EE/IF, Rio de Janeiro, Brazil; (c)Universidade Federal de São João del Rei (UFSJ), São João del Rei, Brazil; (d)Instituto de Física, Universidade de São Paulo, Sao Paulo, Brazil

- 81 KEK, High Energy Accelerator Research Organization, Tsukuba, Japan
- 82 Graduate School of Science, Kobe University, Kobe, Japan
- 83 (a) AGH University of Science and Technology, Faculty of Physics and Applied Computer Science, Kraków, Poland; (b) Marian Smoluchowski Institute of Physics, Jagiellonian University, Kraków, Poland
- 84 Institute of Nuclear Physics Polish Academy of Sciences, Kraków, Poland
- 85 Faculty of Science, Kyoto University, Kyoto, Japan
- 86 Kyoto University of Education, Kyoto, Japan
- 87 Research Center for Advanced Particle Physics and Department of Physics, Kyushu University, Fukuoka, Japan
- 88 Instituto de Física La Plata, Universidad Nacional de La Plata and CONICET, La Plata, Argentina
- 89 Physics Department, Lancaster University, Lancaster, UK
- 90 Oliver Lodge Laboratory, University of Liverpool, Liverpool, UK
- 91 Department of Experimental Particle Physics, Jožef Stefan Institute and Department of Physics, University of Ljubljana, Ljubljana, Slovenia
- 92 School of Physics and Astronomy, Queen Mary University of London, London, UK
- 93 Department of Physics, Royal Holloway University of London, Egham, UK
- 94 Department of Physics and Astronomy, University College London, London, UK
- 95 Louisiana Tech University, Ruston, LA, USA
- 96 Fysiska institutionen, Lunds universitet, Lund, Sweden
- 97 Centre de Calcul de l'Institut National de Physique Nucléaire et de Physique des Particules (IN2P3), Villeurbanne, France
- 98 Departamento de Física Teórica C-15 and CIAFF, Universidad Autónoma de Madrid, Madrid, Spain
- 99 Institut für Physik, Universität Mainz, Mainz, Germany
- 100 School of Physics and Astronomy, University of Manchester, Manchester, UK
- 101 CPPM, Aix-Marseille Université, CNRS/IN2P3, Marseille, France
- 102 Department of Physics, University of Massachusetts, Amherst, MA, USA
- 103 Department of Physics, McGill University, Montreal, QC, Canada
- 104 School of Physics, University of Melbourne, Melbourne, VIC, Australia
- 105 Department of Physics, University of Michigan, Ann Arbor, MI, USA
- 106 Department of Physics and Astronomy, Michigan State University, East Lansing, MI, USA
- 107 B.I. Stepanov Institute of Physics, National Academy of Sciences of Belarus, Minsk, Belarus
- 108 Research Institute for Nuclear Problems of Byelorussian State University, Minsk, Belarus
- 109 Group of Particle Physics, University of Montreal, Montreal, QC, Canada
- 110 P.N. Lebedev Physical Institute of the Russian Academy of Sciences, Moscow, Russia
- 111 Institute for Theoretical and Experimental Physics of the National Research Centre Kurchatov Institute, Moscow, Russia
- 112 National Research Nuclear University MEPhI, Moscow, Russia
- 113 D.V. Skobeltsyn Institute of Nuclear Physics, M.V. Lomonosov Moscow State University, Moscow, Russia
- 114 Fakultät für Physik, Ludwig-Maximilians-Universität München, Munich, Germany
- 115 Max-Planck-Institut für Physik (Werner-Heisenberg-Institut), Munich, Germany
- 116 Nagasaki Institute of Applied Science, Nagasaki, Japan
- 117 Graduate School of Science and Kobayashi-Maskawa Institute, Nagoya University, Nagoya, Japan
- 118 Department of Physics and Astronomy, University of New Mexico, Albuquerque, NM, USA
- 119 Institute for Mathematics, Astrophysics and Particle Physics, Radboud University Nijmegen/Nikhef, Nijmegen, The Netherlands
- 120 Nikhef National Institute for Subatomic Physics and University of Amsterdam, Amsterdam, The Netherlands
- 121 Department of Physics, Northern Illinois University, DeKalb, IL, USA
- 122 (a) Budker Institute of Nuclear Physics and NSU, SB RAS, Novosibirsk, Siberia, Russia; (b) Novosibirsk State University, Novosibirsk, Russia
- 123 Institute for High Energy Physics of the National Research Centre, Kurchatov Institute, Protvino, Russia
- 124 Department of Physics, New York University, New York, NY, USA
- 125 Ochanomizu University, Otsuka, Bunkyo-ku, Tokyo, Japan
- 126 Ohio State University, Columbus, OH, USA
- 127 Faculty of Science, Okayama University, Okayama, Japan
- 128 Homer L. Dodge Department of Physics and Astronomy, University of Oklahoma, Norman, OK, USA

- ¹²⁹ Department of Physics, Oklahoma State University, Stillwater, OK, USA
- ¹³⁰ Palacký University, RCPTM, Joint Laboratory of Optics, Olomouc, Czech Republic
- ¹³¹ Center for High Energy Physics, University of Oregon, Eugene, OR, USA
- ¹³² LAL, Université Paris-Sud, CNRS/IN2P3, Université Paris-Saclay, Orsay, France
- ¹³³ Graduate School of Science, Osaka University, Osaka, Japan
- ¹³⁴ Department of Physics, University of Oslo, Oslo, Norway
- ¹³⁵ Department of Physics, Oxford University, Oxford, UK
- ¹³⁶ LPNHE, Sorbonne Université, Université de Paris, CNRS/IN2P3, Paris, France
- ¹³⁷ Department of Physics, University of Pennsylvania, Philadelphia, PA, USA
- ¹³⁸ Konstantinov Nuclear Physics Institute of National Research Centre “Kurchatov Institute”, PNPI, St. Petersburg, Russia
- ¹³⁹ Department of Physics and Astronomy, University of Pittsburgh, Pittsburgh, PA, USA
- ¹⁴⁰ (a) Laboratório de Instrumentação e Física Experimental de Partículas - LIP, Lisbon, Portugal; (b) Departamento de Física, Faculdade de Ciências, Universidade de Lisboa, Lisbon, Portugal; (c) Departamento de Física, Universidade de Coimbra, Coimbra, Portugal; (d) Centro de Física Nuclear da Universidade de Lisboa, Lisbon, Portugal; (e) Departamento de Física, Universidade do Minho, Braga, Portugal; (f) Universidad de Granada, Granada, Spain; (g) Dep Física and CEFITEC of Faculdade de Ciências e Tecnologia, Universidade Nova de Lisboa, Caparica, Portugal; (h) Av. Rovisco Pais, 1, 1049-001 Lisbon, Portugal
- ¹⁴¹ Institute of Physics of the Czech Academy of Sciences, Prague, Czech Republic
- ¹⁴² Czech Technical University in Prague, Prague, Czech Republic
- ¹⁴³ Charles University, Faculty of Mathematics and Physics, Prague, Czech Republic
- ¹⁴⁴ Particle Physics Department, Rutherford Appleton Laboratory, Didcot, UK
- ¹⁴⁵ IRFU, CEA, Université Paris-Saclay, Gif-sur-Yvette, France
- ¹⁴⁶ Santa Cruz Institute for Particle Physics, University of California Santa Cruz, Santa Cruz, CA, USA
- ¹⁴⁷ (a) Departamento de Física, Pontificia Universidad Católica de Chile, Santiago, Chile; (b) Departamento de Física, Universidad Técnica Federico Santa María, Valparaíso, Chile
- ¹⁴⁸ Department of Physics, University of Washington, Seattle, WA, USA
- ¹⁴⁹ Department of Physics and Astronomy, University of Sheffield, Sheffield, UK
- ¹⁵⁰ Department of Physics, Shinshu University, Nagano, Japan
- ¹⁵¹ Department Physik, Universität Siegen, Siegen, Germany
- ¹⁵² Department of Physics, Simon Fraser University, Burnaby, BC, Canada
- ¹⁵³ SLAC National Accelerator Laboratory, Stanford, CA, USA
- ¹⁵⁴ Physics Department, Royal Institute of Technology, Stockholm, Sweden
- ¹⁵⁵ Departments of Physics and Astronomy, Stony Brook University, Stony Brook, NY, USA
- ¹⁵⁶ Department of Physics and Astronomy, University of Sussex, Brighton, UK
- ¹⁵⁷ School of Physics, University of Sydney, Sydney, Australia
- ¹⁵⁸ Institute of Physics, Academia Sinica, Taipei, Taiwan
- ¹⁵⁹ (a) E. Andronikashvili Institute of Physics, Iv. Javakhishvili Tbilisi State University, Tbilisi, Georgia; (b) High Energy Physics Institute, Tbilisi State University, Tbilisi, Georgia
- ¹⁶⁰ Department of Physics, Technion, Israel Institute of Technology, Haifa, Israel
- ¹⁶¹ Raymond and Beverly Sackler School of Physics and Astronomy, Tel Aviv University, Tel Aviv, Israel
- ¹⁶² Department of Physics, Aristotle University of Thessaloniki, Thessaloniki, Greece
- ¹⁶³ International Center for Elementary Particle Physics and Department of Physics, University of Tokyo, Tokyo, Japan
- ¹⁶⁴ Graduate School of Science and Technology, Tokyo Metropolitan University, Tokyo, Japan
- ¹⁶⁵ Department of Physics, Tokyo Institute of Technology, Tokyo, Japan
- ¹⁶⁶ Tomsk State University, Tomsk, Russia
- ¹⁶⁷ Department of Physics, University of Toronto, Toronto, ON, Canada
- ¹⁶⁸ (a) TRIUMF, Vancouver, BC, Canada; (b) Department of Physics and Astronomy, York University, Toronto, ON, Canada
- ¹⁶⁹ Division of Physics and Tomonaga Center for the History of the Universe, Faculty of Pure and Applied Sciences, University of Tsukuba, Tsukuba, Japan
- ¹⁷⁰ Department of Physics and Astronomy, Tufts University, Medford, MA, USA
- ¹⁷¹ Department of Physics and Astronomy, University of California Irvine, Irvine, CA, USA
- ¹⁷² Department of Physics and Astronomy, University of Uppsala, Uppsala, Sweden
- ¹⁷³ Department of Physics, University of Illinois, Urbana, IL, USA

- 174 Instituto de Física Corpuscular (IFIC), Centro Mixto Universidad de Valencia - CSIC, Valencia, Spain
- 175 Department of Physics, University of British Columbia, Vancouver, BC, Canada
- 176 Department of Physics and Astronomy, University of Victoria, Victoria, BC, Canada
- 177 Fakultät für Physik und Astronomie, Julius-Maximilians-Universität Würzburg, Würzburg, Germany
- 178 Department of Physics, University of Warwick, Coventry, UK
- 179 Waseda University, Tokyo, Japan
- 180 Department of Particle Physics, Weizmann Institute of Science, Rehovot, Israel
- 181 Department of Physics, University of Wisconsin, Madison, WI, USA
- 182 Fakultät für Mathematik und Naturwissenschaften, Fachgruppe Physik, Bergische Universität Wuppertal, Wuppertal, Germany
- 183 Department of Physics, Yale University, New Haven, CT, USA
- 184 Yerevan Physics Institute, Yerevan, Armenia
- ^a Also at Borough of Manhattan Community College, City University of New York, New York, NY, USA
- ^b Also at CERN, Geneva, Switzerland
- ^c Also at CPPM, Aix-Marseille Université, CNRS/IN2P3, Marseille, France
- ^d Also at Département de Physique Nucléaire et Corpusculaire, Université de Genève, Geneva, Switzerland
- ^e Also at Departament de Física de la Universitat Autònoma de Barcelona, Barcelona, Spain
- ^f Also at Departamento de Física, Instituto Superior Técnico, Universidade de Lisboa, Lisbon, Portugal
- ^g Also at Department of Applied Physics and Astronomy, University of Sharjah, Sharjah, United Arab Emirates
- ^h Also at Department of Financial and Management Engineering, University of the Aegean, Chios, Greece
- ⁱ Also at Department of Physics and Astronomy, Michigan State University, East Lansing, MI, USA
- ^j Also at Department of Physics and Astronomy, University of Louisville, Louisville, KY, USA
- ^k Also at Department of Physics, Ben Gurion University of the Negev, Beer Sheva, Israel
- ^l Also at Department of Physics, California State University, East Bay, USA
- ^m Also at Department of Physics, California State University, Fresno, USA
- ⁿ Also at Department of Physics, California State University, Sacramento, USA
- ^o Also at Department of Physics, King's College London, London, UK
- ^p Also at Department of Physics, St. Petersburg State Polytechnical University, St. Petersburg, Russia
- ^q Also at Department of Physics, Stanford University, Stanford, CA, USA
- ^r Also at Department of Physics, University of Adelaide, Adelaide, Australia
- ^s Also at Department of Physics, University of Fribourg, Fribourg, Switzerland
- ^t Also at Department of Physics, University of Michigan, Ann Arbor, MI, USA
- ^u Also at Department of Physics, University of Toronto, Toronto, ON, Canada
- ^v Also at Dipartimento di Matematica, Informatica e Fisica, Università di Udine, Udine, Italy
- ^w Also at Faculty of Physics, M.V. Lomonosov Moscow State University, Moscow, Russia
- ^x Also at Giresun University, Faculty of Engineering, Giresun, Turkey
- ^y Also at Graduate School of Science, Osaka University, Osaka, Japan
- ^z Also at Hellenic Open University, Patras, Greece
- ^{aa} Also at Institutio Catalana de Recerca i Estudis Avancats, ICREA, Barcelona, Spain
- ^{ab} Also at Institut für Experimentalphysik, Universität Hamburg, Hamburg, Germany
- ^{ac} Also at Institute for Mathematics, Astrophysics and Particle Physics, Radboud University Nijmegen/Nikhef, Nijmegen, The Netherlands
- ^{ad} Also at Institute for Nuclear Research and Nuclear Energy (INRNE) of the Bulgarian Academy of Sciences, Sofia, Bulgaria
- ^{ae} Also at Institute for Particle and Nuclear Physics, Wigner Research Centre for Physics, Budapest, Hungary
- ^{af} Also at Institute of Particle Physics (IPP), Vancouver, Canada
- ^{ag} Also at Institute of Physics, Academia Sinica, Taipei, Taiwan
- ^{ah} Also at Institute of Physics, Azerbaijan Academy of Sciences, Baku, Azerbaijan
- ^{ai} Also at Institute of Theoretical Physics, Ilia State University, Tbilisi, Georgia
- ^{aj} Also at Instituto de Física Teórica, IFT-UAM/CSIC, Madrid, Spain
- ^{ak} Also at Department of Physics, Istanbul University, Istanbul, Turkey
- ^{al} Also at Joint Institute for Nuclear Research, Dubna, Russia

- ^{am} Also at LAL, Université Paris-Sud, CNRS/IN2P3, Université Paris-Saclay, Orsay, France
- ^{an} Also at Louisiana Tech University, Ruston, LA, USA
- ^{ao} Also at LPNHE, Sorbonne Université, Université de Paris, CNRS/IN2P3, Paris, France
- ^{ap} Also at Manhattan College, New York, NY, USA
- ^{aq} Also at Moscow Institute of Physics and Technology State University, Dolgoprudny, Russia
- ^{ar} Also at National Research Nuclear University MEPhI, Moscow, Russia
- ^{as} Also at Physics Department, An-Najah National University, Nablus, Palestine
- ^{at} Also at Physics Dept, University of South Africa, Pretoria, South Africa
- ^{au} Also at Physikalisches Institut, Albert-Ludwigs-Universität Freiburg, Freiburg, Germany
- ^{av} Also at School of Physics, Sun Yat-sen University, Guangzhou, China
- ^{aw} Also at The City College of New York, New York, NY, USA
- ^{ax} Also at The Collaborative Innovation Center of Quantum Matter (CICQM), Beijing, China
- ^{ay} Also at Tomsk State University, Tomsk, and Moscow Institute of Physics and Technology State University, Dolgoprudny, Russia
- ^{az} Also at TRIUMF, Vancouver, BC, Canada
- ^{aaa} Also at Università di Napoli Parthenope, Naples, Italy
- *Deceased